INTEGRATED RESERVOIR CHARACTERIZATION:

OFFSHORE LOUISIANA, GRAND ISLE BLOCKS 32 & 33

A Thesis

by

MICHAEL CHASE CASEY

Submitted to the Office of Graduate Studies of
Texas A&M University
in partial fulfillment of the requirements for the degree of

MASTER OF SCIENCE

May 2011

Major Subject: Geology

Integrated Reservoir Characterization: Offshore Louisiana, Grand Isle Blocks 32 & 33

INTEGRATED RESERVOIR CHARACTERIZATION:

OFFSHORE LOUISIANA, GRAND ISLE BLOCKS 32 & 33

A Thesis

by

MICHAEL CHASE CASEY

Submitted to the Office of Graduate Studies of
Texas A&M University
in partial fulfillment of the requirements for the degree of

MASTER OF SCIENCE

Approved by:

Chair of Committee,	Yuefeng Sun
Committee Members,	Michael Pope
	Walter Ayers
Head of Department,	Andreas Kronenberg

May 2011

Major Subject: Geology

ABSTRACT

Integrated Reservoir Characterization: Offshore Louisiana, Grand Isle Blocks 32 & 33.

(May 2011)

Michael Chase Casey, B.S., Texas A&M University

Chair of Advisory Committee: Dr. Yuefeng Sun

This thesis integrated geology, geophysics, and petroleum engineering data to build a detailed reservoir characterization model for three gas pay sands in the Grand Isle 33 and 43 fields, offshore Louisiana. The reservoirs are Late Miocene in age and include the upper (PM), middle (QH), and lower (RD) sands. The reservoir models address the stratigraphy of the upper (PM) sand and help delineate the lower (RD) reservoir. In addition, this research addresses the partially depleted QH-2 reservoir compartment. The detailed models were constructed by integrating seismic, well log, and production data. These detailed models can help locate recoverable oil and gas that has been left behind.

The upper PM model further delineated that the PM sand has several areas that are shaled-out effectively creating a flow barrier within reservoir compartments. Due to the barrier in the PM-1 reservoir compartment, an area of potentially recoverable hydrocarbons remains. In Grand Isle 33, the middle QH sand was partially depleted in the QH-2 reservoir compartment by a series of development wells. Bottom hole pressure data from wells in Grand Isle 32 and 33 reveal that the two QH fault compartments are

in communication across a leaking fault. Production wells in the QH-1 compartment produced reserves from the QH-2 compartment. The lower RD sand model helped further delineate the reservoir in the RD-2 compartment and show that this compartment has been depleted. The RD model also shows the possible presence of remaining recoverable hydrocarbons in the RD-1 compartment. It is estimated that about 6.7 billion cubic feet of gas might remain within this reservoir waiting to be recovered. A seismic amplitude anomaly response from the QH and RD sands is interpreted to be a lithologic indicator rather than the presence of hydrocarbons. Amplitude response from the PM level appears to be below the resolution of the seismic data. A synthetic seismogram model was generated to represent the PM and surrounding sands. This model shows that by increasing the frequency of the seismic data from 20 Hz to a dominant frequency of 30 Hz that the PM and surrounding sands could be seismically resolvable. Also the PM-1 compartment has possible recoverable hydrocarbons of 1.5 billion cubic feet of gas remaining.

DEDICATION

This thesis is dedicated to my family and friends. Without their support and love I would not be where I am today.

ACKNOWLEDGEMENTS

I would like to thank my committee chair, Dr. Sun, and my committee members, Dr. Pope, and Dr. Ayers, for their guidance and support throughout this research.

Thanks also to my friends and the Department of Geology and Geophysics at Texas A&M University. I also want to extend my gratitude to Apache Corporation, which provided financial support, data, and mentorship during the research. Specifically, I would like to thank everyone in the Gulf Coast Exploitation group at Apache Corp. that helped me along the way. I would also like to thank Seismic Exchange, Inc. (SEI) for providing the seismic data for use in this research.

Finally, thanks to my family for their continued support.

NOMENCLATURE

BOE	Barrels of Oil Equivalent
TCF	Trillion Cubic Feet
BCFG	Billion Cubic Feet of Gas
GOM	Gulf of Mexico
DHI's	Direct Hydrocarbon Indicators
SEI	Seismic Exchange, Inc.
AVO	Amplitude vs Offset
GI	Grand Isle
GOR	Gas Oil Ratio
BHP	Bottom Hole Pressure
Ac.	Acre
FTP	Flowing Tubing Pressure
Bbl	Barrels
Hz	Hertz
BCF	Billion Cubic Feet
MMBO	Million Barrels of Oil
MBO	Thousand Barrels of Oil
MBW	Thousand Barrels of Water

TABLE OF CONTENTS

CHAPTER Page

LIST OF FIGURES

FIGURE Page

FIGURE Page

FIGURE Page

LIST OF TABLES

CHAPTER I

INTRODUCTION

World population has doubled in the past fifty years, and so, the need for energy has increased dramatically. Integration of seismic data with other forms of subsurface information such as geological and engineering data is increasingly used worldwide for exploration of new hydrocarbon fields and for enhanced hydrocarbon recovery methods of mature fields, in order to help meet world energy needs. This study focuses on the integration of geological, geophysical, and reservoir engineering data to more accurately characterize the sandstone reservoirs of a field in the Gulf of Mexico, offshore Louisiana, USA.

Annual production from the Gulf of Mexico (GOM) is about 580 million barrels of oil (MMBO) and 2.7 trillion cubic feet of gas (TCF), which is about 30% of domestic oil and about 13% of domestic gas production (USEIA 2010). Two thirds of the oil and gas production comes from deepwater fields, these discoveries have helped production keep pace with the overall natural oil and gas decline of the region. The remaining third of oil and gas production comes from mature fields on the shelf. With its established infrastructure and bountiful supply of data, the shelf represents an excellent area to develop new techniques to locate and exploit bypassed and previously unrecognized reservoirs. These techniques demand a thorough review, interpretation, and integration of all available data.

This thesis follows the style of American Association of Petroleum Geologists Bulletin.

Offshore exploration in the Gulf of Mexico has occurred for more than sixty years. During this time, there were substantial advancements in exploration technologies. Many of these new technologies have produced a better understanding of the geological processes that created these hydrocarbon deposits. Understanding the subsurface geology of oil and gas fields is imperative for field development. Geological, geophysical, and petroleum engineering data are used to understand oil and gas occurrence and producibility.

Seismic technology, the primary exploration tool in the Gulf of Mexico for decades, has seen significant improvements in acquisition, processing, and interpretation in the past twenty years. Seismic data interpretation has transitioned from historical 2-D paper-line interpretations to the high-resolution 3-D data cubes interpreted on computer workstations. Seismic data can be used to detect large-scale features in sedimentary basins such as faults, anticlines, synclines, and salt diapirs, but these features only provide a framework for trapping oil and gas. Many areas are under-explored and under-exploited for stratigraphic traps. Integrating seismic data with other forms of information can be useful in recognizing the finer stratigraphic characteristics of reservoirs.

While seismic data provides good lateral resolution in most instances, vertical resolution is often wanting. Thicknesses of single mappable units are commonly less than the resolution of a single wavelet in the seismic data. By integrating well data from logs and other engineering tools, vertical resolution can be enhanced. Reservoir characterization models are created by integration of all available data, including core, log, seismic and engineering data. These models aid in understanding reservoirs

properties, such as geometry and connectivity of producing beds. Models have the potential to expose areas of bypassed hydrocarbons, thereby increasing the life of mature fields.

The study area of this investigation (Figure 1), contains several mature oil and gas fields that were discovered and developed in the late 1960's, 70's and early 80's (OWL 2010). Cumulative production from the Grand Isle 33 & 43 fields to date is 27 million barrels of oil (MMBO), 343 billion cubic feet of gas (BCFG), and 57 million barrels of water (MMBW) (OWL 2010). Several identified structural traps are responsible for the oil and gas accumulations. This research will focus on locating potential stratigraphic traps on the basis of the subtleties of the reservoirs, using reservoir characterization techniques involving the integration of seismic, well logs, and engineering data.

Figure 1: Index map of a portion of offshore Louisiana, showing the location of the Grand Isle study area.

Previous Work

This research focuses on the Grand Isle 33 & 43 field's offshore Louisiana, where water depths range from 70-100 ft. Previous researchers have concluded that the reservoirs, which range from -10,500 to -13,500 ft deep, were deposited in deltaic and marine environments (Everson 1989). These producing reservoirs are Late Miocene in age, and include the upper (PM), middle (QH), and lower (RD) sands which will be studied in this investigation. Structurally, there are a series of east-west trending normal down-to-the-basin growth faults, these faults are associated with a large salt complex to the north (Everson 1989). Seismic amplitude anomalies are regarding as one group of Direct Hydrocarbon Indicators in the GOM shallow unconsolidated sediments (Forrest et al. 2010). Extensive work was done using seismic amplitude anomalies to de-risk drilling prospects. Although amplitude anomalies can also indicate low saturations of hydrocarbons in sands as well (O'Brien 2004). However, there have been no seismic amplitude anomaly studies conducted in the Grand Isle 33 & 43 fields.

Statement of Problems

The proposed research is designed to address some of the problems observed throughout the Grand Isle 33 & 43 fields. This research will focus on trying to resolve the stratigraphic nature of the upper (PM) and lower (RD) sand to delineate the reservoir. Also this research will address why the middle (QH)-1 compartment was found to be under pressured by the A wells. Another goal will be to address the potential of bypassed hydrocarbons within the three identified reservoirs. This research will integrate historical well production data, well logs, and seismic data volumes to create a comprehensive

reservoir characterization model for numerous pays sands in the fields. This model will provide a framework to help solve some of the field specific problems identified.

Objectives

This research attempts to produce a more accurate way to define reservoir geometries and volumes from the integration of data from multiple disciplines. The first objective is to characterize the structure and stratigraphy of the field, best achieved through literature review, and a baseline interpretation of the available data, well logs, seismic, and field production. The second objective is to apply the results of the integrated data to the problems observed throughout the fields. A third objective is to use seismic amplitude anomalies to further delineate the reservoirs.

Methods

This reservoir characterization research will be conducted, will integrate geology, geophysics, and petroleum engineering data, as described in the following steps.

I. Multiple mappable reservoir sands will be identified from log data and physical properties such as water saturation ($S_{w)}$, hydrocarbon saturation ($S_{h),}$ resistivity, shale content (Vsh), porosity, sonic (ΔT), net/gross sand, and net/gross pay.

II. Synthetic seismograms will be derived and compared to conventional seismic to identify key seismic horizons and to convert time to depth; velocity surveys will be compared with the synthetic seismograms.

III. Interpretation of seismic cubes will be performed to define the field structure and stratigraphy.

IV. Seismic amplitude extractions will be made from original interpreted volumes to determine reservoir geometries and to estimate reservoir heterogeneity.

V. Pay maps will be generated from the seismic amplitude maps and well log data.

VI. The pay maps will be compared to production data to check for validity.

VII. A detailed analysis will be conducted from the integration of the data to solve the research problems presented.

The reservoir characterization model will be made for several sands in the Grand Isle 33 and 43 fields offshore Louisiana. Well log data will be analyzed to identify the reservoir zones within the field. Physical properties will be calculated for later use in the integrated maps. The primary objective of this research is to create detailed reservoir models of the defined reservoirs. Seismic amplitude extractions will be used to better understand reservoir geometries and connectivity.

A number of different seismic amplitude maps will be created, including Root Mean Square (RMS) Amplitude, Maximum Trough Amplitude, and Absolute Amplitude. The seismic maps will be interpreted looking for properties that exist in multiple maps that can be related to physical rock properties measured from the well logs and cores. These amplitude maps should provide a more detailed understanding of the reservoir(s) stratigraphically and structurally, rather than just conventional seismic contour maps. The amplitude maps will be integrated with the well log information to create pay maps that define the reservoir geometries and connectivity. These maps will then be compared with the available production data to see how they compared to the original maps of the field. The volumetric calculations will be from the physical

properties of the well logs and the integrated pay maps. This step will help validate existing maps. However, some of the maps might identify new locations where there are no production wells. Detailed analysis of the data in these areas may suggest bypassed hydrocarbons or potential for infill well prospects.

Dataset

A digital seismic full stack 3-D seismic cube was provided to Apache Corporation (Apache) by Seismic Exchange, Inc. (SEI). Apache licensed this data in order to assess the structure and stratigraphy of about 18 federal lease blocks in the Grand Isle/West Delta offshore Louisiana area, for the potential accumulation of hydrocarbons. Apache provided access to this dataset for the purpose of this research. The digital seismic data was provided in a SEGY format, which was loaded into Landmarks Seisworks 2003 interpretation software. The seismic data was sampled to a depth of 6.5 seconds with data sampled every 4 milliseconds. The inline and crossline spacing for the data is 82 feet. There are over 300 wells within the seismic data coverage but only about 30-40 wells will be analyzed. These wells have wireline logs generally consisting of Gamma Ray, Resistivity, Neutron porosity, Density, and Sonic logs. Additionally, production data is available for the wells in the study area. Core data was rarely available and independently interpreted when available. The log, production, and core data were obtained from the Owl data base system which Apache.

Field Background

The Grand Isle 33 & 43 fields are located 15 miles offshore of Grand Isle, Louisiana in the Gulf of Mexico. Average water depth throughout the two fields is about 100 feet. The first wells in the Grand Isle 33 and 43 fields were drilled in 1965 and 1967, targeting the Late Miocene middle QH sand. This sand was the main exploration target for the two companies drilling in the area during this time, Catco and Conoco (Everson 1989). Although initial drilling occurred during the 1960's it was not until 1972 in the Grand Isle 32 W-1 well that commercial quantities of hydrocarbons were discovered. The W-1 well encountered hydrocarbons in six different reservoir zones including the PM, QH, and RD sands (OWL 2010). After this discovery, a series of development wells were drilled in the Grand Isle 32 block until the early 1980's. The discovery in Grand Isle 32 also led to the 1982 discovery in Grand Isle 33. The GI-33 A-1 well discovered many of the same productive reservoirs as the GI-32 W-1 well. Again, the main target of the Grand Isle 33 field was the QH reservoir. A series of development wells were drilled in the Grand Isle 33 block until 2001. Currently there are two active producing platforms with 3 wells still producing hydrocarbons.

CHAPTER II

GEOLOGIC BACKGROUND

Basin Evolution

The Gulf of Mexico (GOM) began forming in the Early Mesozoic (~245M.Y.A.), during the breakup of the Pangea supercontinent. Triassic rifting of the North American plate away from the South American and African plates was the first stage of the basin's creation. During the Middle Jurassic, continental stretching and thinning between the North American and South American plate occurred. As a result of this thinning process, marine deposition took place in an embayment within the paleo-Pacific Ocean. This marine embayment experienced poor circulations which led to the development of hyper-saline water during semi-arid to arid climate conditions. Evaporation exceeded the inflow of water, leading to the formation of the thick Louann evaporite deposits estimated to be 2000-3000 meters thick (Salvador 1991). Later, during the Middle to Late Jurassic, the Yucatan plate began to separate from the North American plate, and the first stage of new oceanic crust formed. Cooling and subsequent subsidence of the newly formed oceanic crust created the modern basin seen today (Salvador 1991). By the Late Jurassic to Early Cretaceous the rifting ended and the GOM transitioned from an active rift margin to a passive margin (Bird et al., 2005).

Deposition in the GOM can be characterized by two major events in different eras: the Late Mesozoic and the Cenozoic. During the Late Jurassic and Early Cretaceous terrigenous clastics were the main sediments. These terrigenous clastic sediments were the product of denudation of the Ouachita and Appalachian mountain

belts. Sediments were deposited from the northwest, north, and northeast. During this influx of terrigenous clastic sediments, deposition rates were high, and a shallow shelf margin began to form. Toward the end of the Early Cretaceous sedimentation rates of the terrigenous clastics had slowed considerably, and the shelf became the site of widespread carbonate deposition (Salvador 1991). The Late Cretaceous was characterized by terrigenous clastics sourced from the north, northwest, and west. Deposition of these sediments was the ultimate product of the Laramide orogeny. The influx of terrigenous clastics in the Cenozoic from the north and northwest significantly increased during periods of the Laramide orogeny. Sediment influx was associated with the uplift and orogenic deformation of the Cordilleran front and was characterized by terrigenous clastics prograding basinward over the Cretaceous carbonates, which migrated shorelines and the shelf farther basinward (Salvador 1991).

Depositional Setting

During the Late Miocene, shallow marine deltaic systems dominated the depositional setting in the Grand Isle-West Delta area. The paleo-markers *Cyclammina 3, Discorbis 12, and Textularia L.*, all occur in the GI-33 A-1 well. These biomarkers indicate that the sands range in age from 7.94 to 9.56 million years (Figure 2). The paleoenvironment for these markers vary from inner neritic, middle neritic, outer neritic, and upper bathyal (Figure 3). The paleo-Mississippi River was the dominant sediment source in the Grand Isle-West Delta area during the Late Miocene (Wu & Galloway 2002). Distributary Mouth Bar (DMB) and Distal Bar are the two main delta front sub environments that the PM and QH sands are interpreted to be respectively. The lower

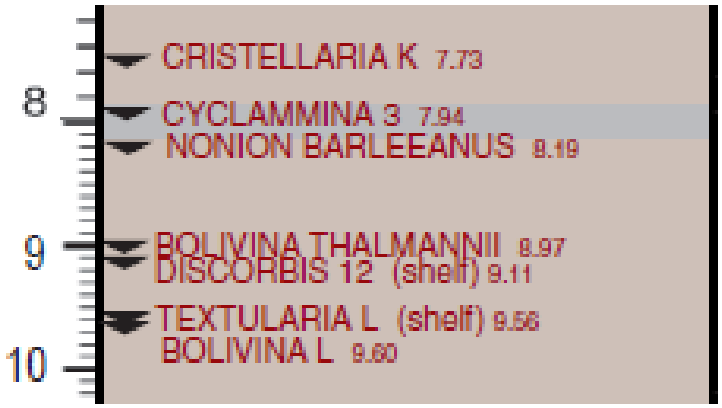

Figure 2: Biostratigraphic Neogene chart of the Gulf of Mexico. (Modified from Paleo-data 2010).

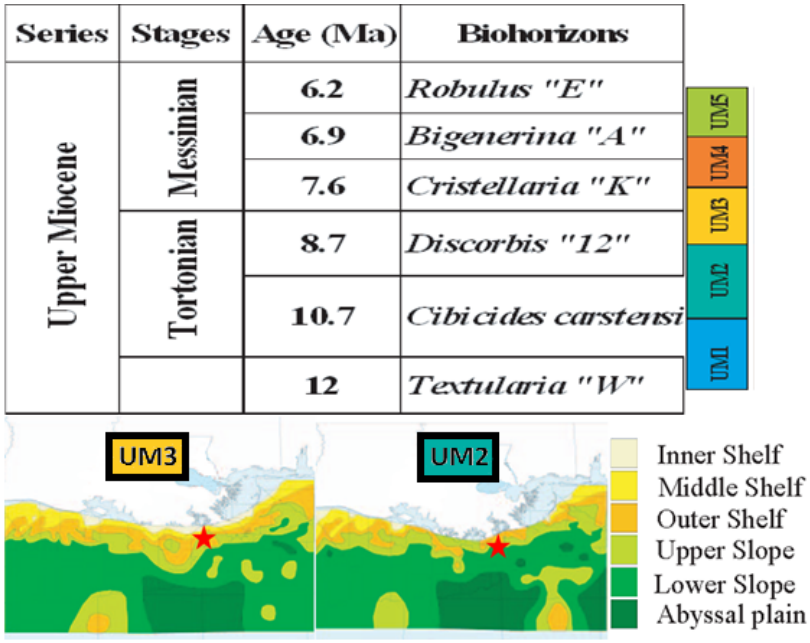

Figure 3: Upper Miocene stratigraphic and biostratigraphic correlation. Paleo-bathymetry for the Upper Miocene 2 & 3. The study field shown with a red star. (Modified from Wu & Galloway 2002).

RD sand is interpreted as a subaqueous outer shelf to upper bathyal channel sand.

Regional Structure

The regional structure of the Grand Isle-West Delta area is influenced by a series of normal, down-to-the-basin, growth faults (Figure 4). These faults are sub-parallel and trend east-west. Throw across the faults varies from about 150 ft to over 1000 ft. Many small post depositional relief faults are observed throughout the area associated with the development of the regional growth faults. A large down-to-the west normal fault is associated with salt evacuation from the Terrebonne Trough and subsequent Bay Marchand salt ridge system to the south (Figure 5). The Terrebonne Trough is the result of the paleo-Mississippi river depositing immense amounts of sediment into the region. Sediment influx resulted in the evacuation of the underlying salt, which created the Bay Marchand salt ridge system. Deposition was greater than subsidence in this portion of the Grand Isle-West Delta area (Figures 6 & 7). When viewing the seismic cross section there is clearly thickening of the red to yellow interval across the faults toward the basin. Also, progressively younger intervals thicken down-thrown to the more basinward faults.

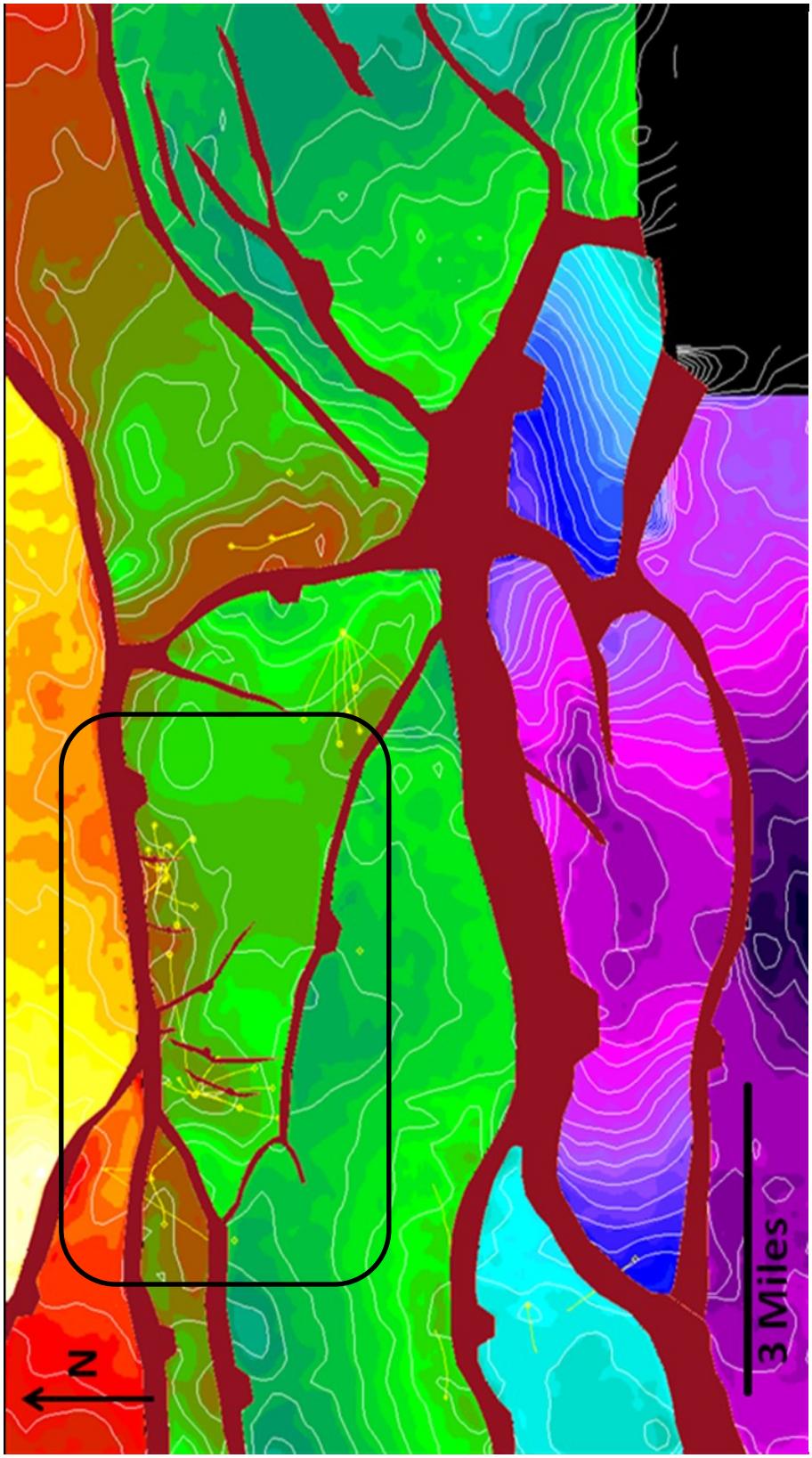

Figure 4: Regional QH sand structure map. Structural highs in reds and oranges and lows in blues and purples.

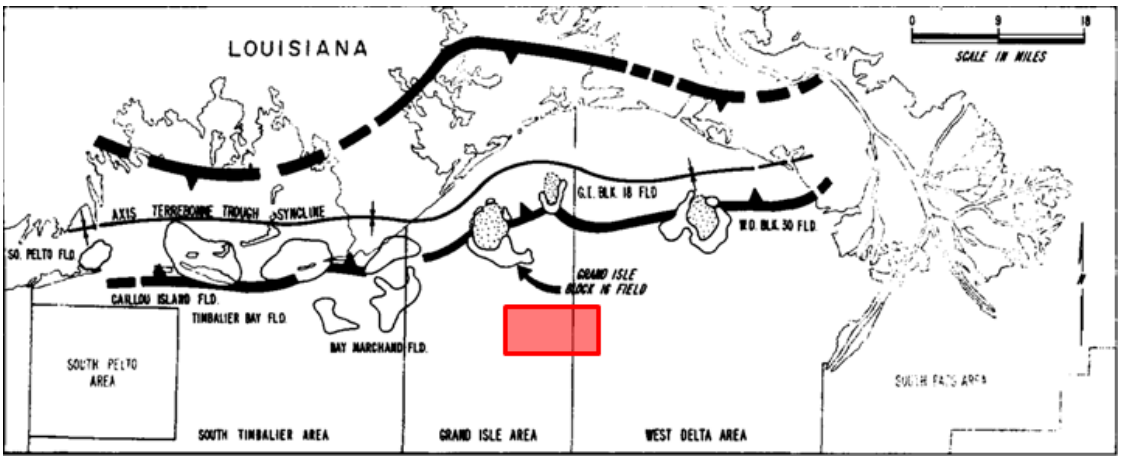

Figure 5: Regional map showing the Terreboone Trough and Bay Marchand salt ridge. The salt ridge system lines the southern boundary of the trough. The red box is the field of study (Modified from Steiner 1974).

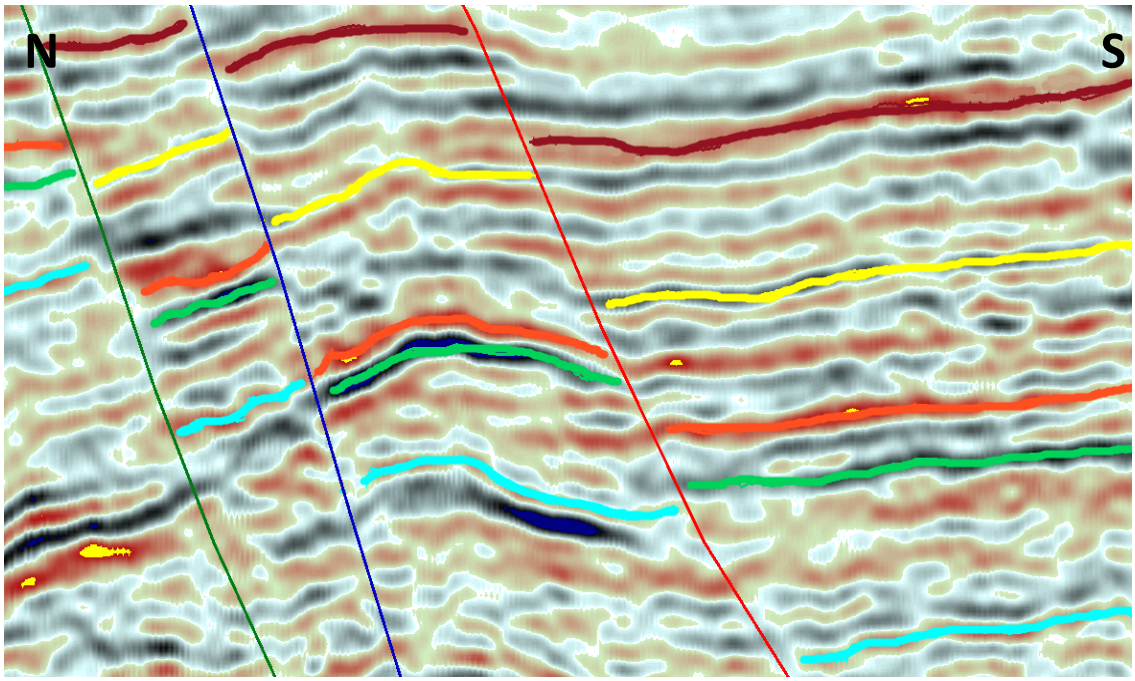

Figure 6: North-south trending seismic line showing the normal growth faulting seen within the study area. The seismic intervals thicken down-thrown as well as progressively younger sediments thicken down-thrown. Seismic data owned or controlled by Seismic Exchange, Inc.

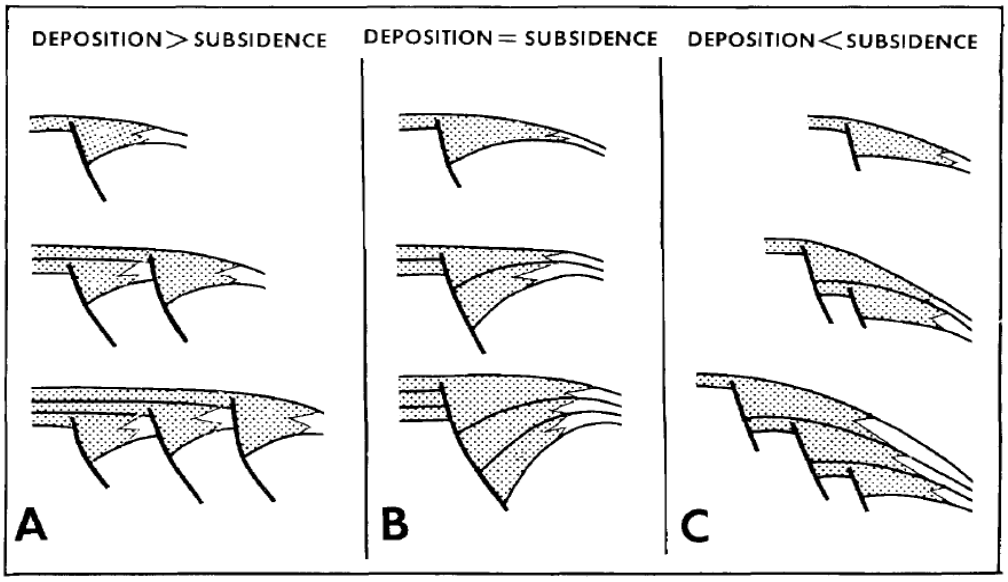

Figure 7: Illustration showing the different types of sediment faulting relationship depending on sedimentation rates (Bruce 1973).

CHAPTER III

RESERVOIR CHARACTERIZATION METHODOLOGY

Introduction

This chapter will outline the methodology that was used to integrate the geologic history, well information, and seismic, and production data in order to achieve detailed reservoir models. This methodology can prove useful in understanding the finer structural and stratigraphic characteristics of under-exploited complex reservoirs. With a better understanding of these complex reservoirs, bypassed hydrocarbon zones can be identified with greater confidence.

Geologic History

The first step to developing detailed reservoir models was to understand the fields depositional history. By analyzing paleontological data, wire line logs, and background literature review. Paleo-data provided approximate ages of the sediments and a general paleo-environment in which they were deposited. Wire line log signatures combined with analog models provided a basic depositional model. Interpretation of the regional seismic data set revealed the regional structuring. The regional structural understanding and depositional history help to determine the relationship between deposition and tectonic events. Once the regional structural interpretation was complete a more detailed field interpretation was conducted in the Grand Isle 33 & 43 fields.

Petrophysical Analysis

A variety of well logs were analyzed to understand the petrophysical properties of the reservoirs in the study area. A detailed petrophysical analysis helped to define the reservoir units in the study area. Once the reservoir units were defined, detailed field seismic interpretation began. Water saturation (S_w), hydrocarbon saturation (S_h), formation resistivity (R_t), shale volume (V_{sh}), and density porosity, were all calculated using the following equations (Asquith and Krygowski 2004).

$$S_w = \left(\frac{a \times R_W}{R_t \times \emptyset^m}\right)^{\left(\frac{1}{n}\right)}$$

$$S_h = (1 - S_w)$$

$$V_{Sh} = \frac{GR_{log} - GR_{min}}{GR_{max} - GR_{min}}$$

$$\emptyset_D = \frac{\rho_{ma} - \rho_b}{\rho_{ma} - \rho_{fl}}$$

$$\emptyset_{NDgas} = \sqrt{\frac{\emptyset^2{}_N + \emptyset^2{}_D}{2}}$$

Water saturation (S_w) and hydrocarbon saturation (S_h) calculate the percentage of fluid type occupying the pore space of the rocks. Shale volume (V_{sh}) is calculated as a percentage of shale within the reservoir; shale volume is important as shale is considered a flow barrier because of its low porosity and permeability characteristics. Porosity ($\emptyset_D$) and ($\emptyset_{NDgas}$) were calculated two different ways depending on the available log information. The first porosity calculation uses just the bulk density log, while the

second calculation considers both bulk density and neutron porosity. When a gas bearing interval is logged by the neutron porosity tool it gives an abnormally low porosity reading. This is because the neutron tool reads the concentration of hydrogen in the formation, and gas has a lower hydrogen concentration than water and oil (Asquith and Krygowski 2004). When displayed on a well log, the density porosity and neutron porosity logs commonly cross when logging a gas bearing zone; this is known as the gas effect (Figure 8). All of the previous reservoir parameters are used to define reservoir intervals that contain commercial quantities of hydrocarbons. The cut-off parameters used to define pay in this study were hydrocarbon saturation greater than 60%, shale volume less than 30%, and porosity greater than 20%.

The petrophysical calculations were performed using Dual Water Shaly Analysis Model commercial software, this program follows John Dewans Modern Open hole Log Interpretation 1983. The software follows many of the equations defined previously as well as some more equations and parameters. A simple water saturation calculation was performed on the top ten feet the CC-1 well (Figure 8) to show some differences between the Archie's equation and how the software calculates water saturation. The Archie's equation yields a water saturation of 15.6% while the software calculates 16.7%, a small difference.. However that calculation was performed where the sand was the cleanest and contains less than 2% shale volume. Another calculation was performed on the bottom pay interval to show how shale content can affect the saturation. Archie's yields a 32.4% water saturation while the software gave a 20.1% water saturation. In this case there is a significant difference in the two methods. This is

because the Archie's method does not account for shale volume, effective porosity, and effective saturation. The software can make multiple calculations that accounts for the volume of shale that occupies the rock as well as the clay bound immoveable water, and a neutron density correction.

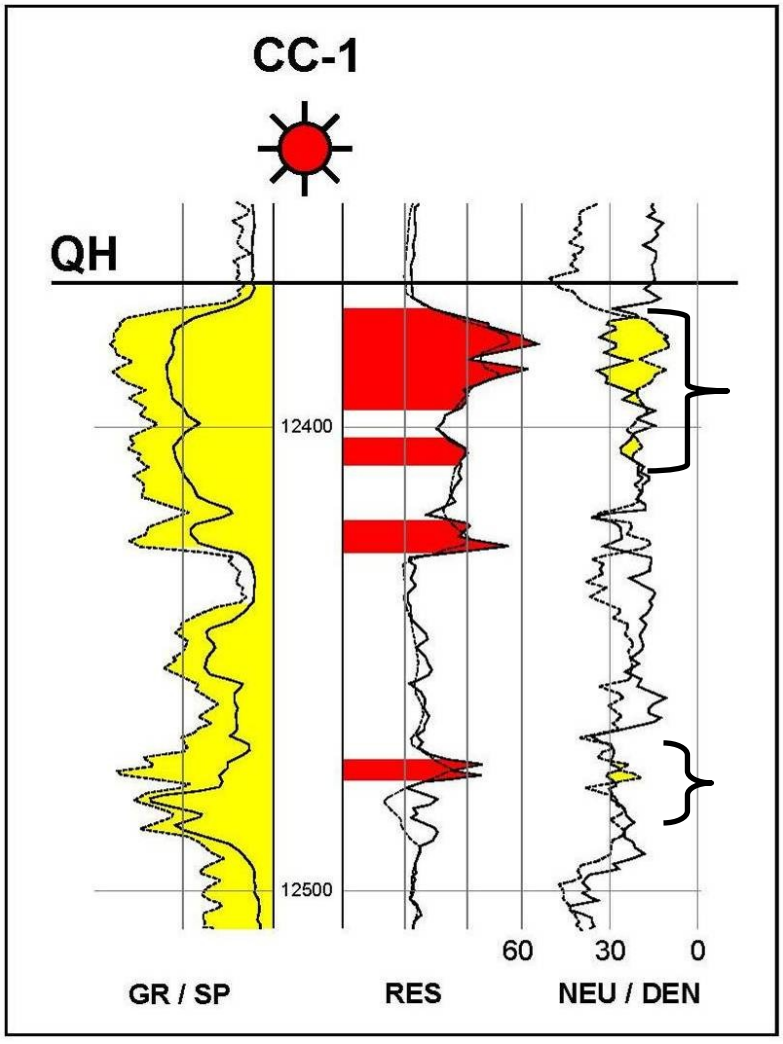

Figure 8: Gamma ray, resistivity, and neutron density log (Triple combo log) displaying the gas effect observed in the QH in the CC-1 wellbore. The gas effect is when the neutron and density curves cross each other, indicating the dominant hydrocarbon type as gas.

Synthetic Seismogram Tie

Once the reservoir zones have been identified a good synthetic seismogram tie is critical to ensure that the well data is properly tied to the seismic data. A synthetic seismogram tie generates time-depth conversions, conveys seismic resolutions, and matches lithologic intervals of interest to seismic reflectors. Synthetic seismograms are generated by convolving the reflection coefficient (R) with the extracted source wavelet (Figure 9) (Keary et al. 2002). The acoustic impedance (Z) is a function of density and velocity and is calculated using rock properties from the sonic and density logs. The reflection coefficient (R) is a ratio of the amplitude of the reflected ray to the incident ray (Keary et al. 2002).

$$Z = \rho v$$

$$R = \frac{\rho_2 v_2 - \rho_1 v_1}{\rho_2 v_2 + \rho_1 v_1} = \frac{Z_2 - Z_1}{Z_2 + Z_1} = \frac{A_1}{A_0}$$

$$Synthetic\ Seismogram = R \times wavelet$$

Once the synthetic seismogram is generated it is matched to extracted seismic traces as closely as possible (Figure 9). The matching of synthetic seismogram to seismic traces creates the time depth conversion and enables the matching of certain reservoirs with mappable seismic reflectors.

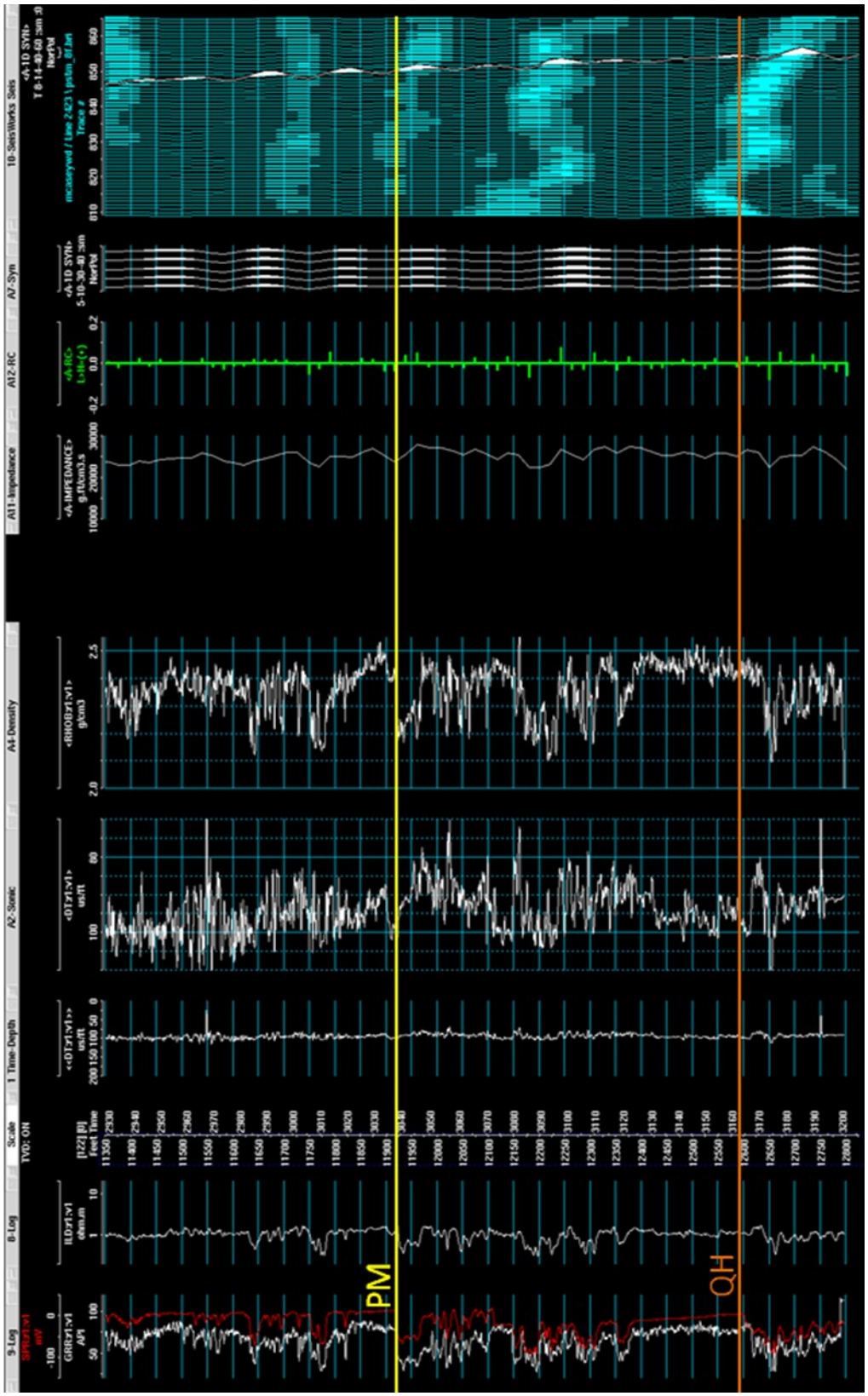

Figure 9: Synthetic seismogram analysis from the GI-33 A-3 wellbore. The synthetic shows both the PM and QH sands as troughs. Seismic data owned or controlled by Seismic Exchange, Inc.

From the synthetic seismogram is it apparent that the QH sand has a difussed trough and subsequent peak which can be compared to Figure 10,a model study of the seismic response to several different sand thicknesses with gradational contacts. A clean blocky sand encased top and bottom by thick shale yields a strong trough and strong peak relationship. In the case of a thick sand interval in which the grain size decreases with depth, the seismic effect is a broadened wavelet with diminished amplitude. To show what an ideal synthetic would look like, a model synthetic was created to show the difference between clean blocky wet sands and sands filled with pay (Figure 11).

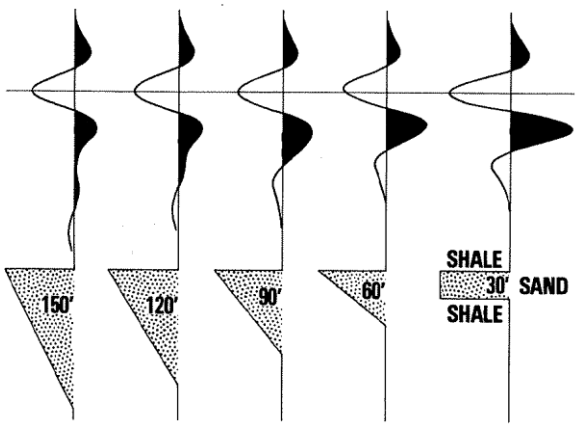

Figure 10: Synthetic seismogram model defending on sand shale thickness relationship and its effect on the synthetic wavelet (Neidell and Poggiagliolmi 1977).

From Figure 11 the model synthetic, the blocky sand filled with pay has a very strong trough marking the top, while the blocky clean wet sand has a very weak trough. This is due to the affect of gas on a rock's velocity and density. At the top of the model a fining downward pay sand is shown and it is represented by a strong trough followed by a strong peak.

Figure 11: Generalized synthetic model for blocky wet seen in the PM and QH sands. Both sands are troughs in the synthetic.

The source wavelet was extracted from the synthetic seismogram indicating that the data is zero phase (Figure 12). From the rock velocity (*V*) and the frequency (*f*) of the seismic data we can calculate the wavelength (λ). From the wavelength we can determine the resolution of the seismic data (Widess 1973).

$$\lambda = \frac{V}{f}$$

$$\text{Separable Beds} = \frac{\lambda}{4}$$

$$\text{Visible Beds} = \frac{\lambda}{8}$$

Separable beds are defined as intervals thick enough to permit identification of the top and base. Visible beds are defined as a bed composed of a single reflector (Widess 1973). The amplitude spectrum was extracted from the seismic data and a dominant frequency of 20 Hz. was observed. An average velocity of 10,000 ft/sec taken from a sonic log in the A-3 well-bore (Figure 9) was used for the resolution calculations. Using the Widess equations separable beds were defined for this area as being 125 ft while visible beds were only 62.5 ft.

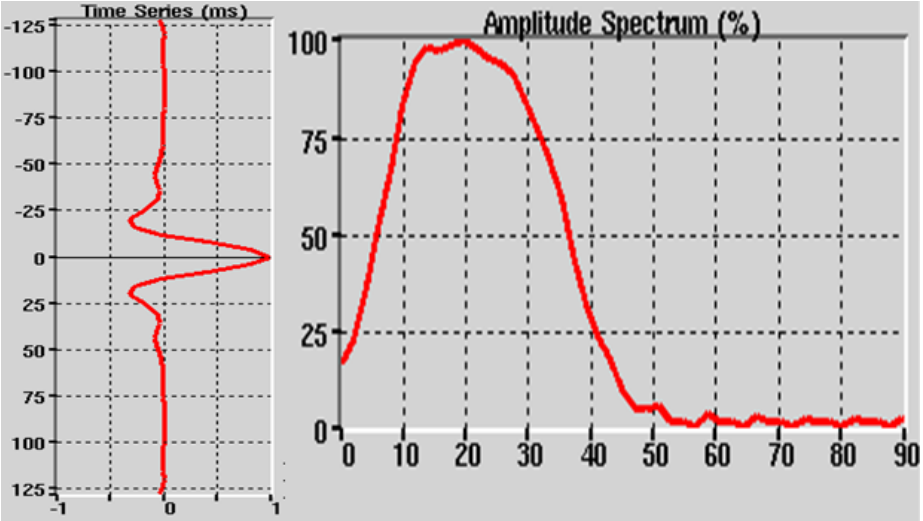

Figure 12: The source wavelet and amplitude spectrum for the seismic data. The wavelet is zero phase and the dominant frequency is around 20 Hz. Seismic data owned or controlled by Seismic Exchange, Inc.

Production Analysis

Production data is one of the key components to a detailed reservoir model. There are three main types of production data that this research utilizes: cumulative production, bottom hole pressure surveys, and completion periods. Produced reserves were used to calculate total cumulative production by reservoir compartment. This was used when analyzing the reservoir for remaining reserves. If the produced reserves are less than the original calculated reserves there may be potential for zones of bypassed hydrocarbons. Bottom hole pressure surveys were used to interpret whether or not reservoir compartments were in communication with each other. If pressure readings from one fault block corresponded to similar pressure readings in another fault block it was determined that the two compartments were in communication. Another indication of leaking faults could be interpreted from the cumulative production. If wells from the

same fault block produced more than the original calculated recoverable reserves, then the trapping fault(s) could be interpreted as leaky. Completion periods were taken into account when interpreting gas water contacts in order to make sure contacts were corrected when previous production altered the original contacts.

Subsurface Integration

The integration of data is imperative to create a series of subsurface maps leading to detailed reservoir models. Analog models, well logs, core, production, and seismic data all were used for the subsurface model generation. The first series of subsurface maps generated were the gross sand isopachs. Gross sand isopachs were interpreted from wireline logs and did not contain any porosity cut-offs. Sand thicknesses were posted on base maps and contoured to follow the interpreted depositional environment. The sand isopachs helped further understand the depositional process; these isopachs also revealed possible sediment source directions. Next, structure maps were created on all of the sand units. These maps display the formation tops as determined by well-log correlation, and they show hydrocarbon and water contacts. Contouring of the formation tops was done by overlaying a base maps with posted formation tops over the seismic time structure map. The contours were driven by the seismic time data but also honored the well control. The process led to the creation of structure maps. There are three different types of hydrocarbon contacts displayed on the structure maps. Gas-water contacts were displayed when the contact was observed in the well log. Lowest known gas was displayed when the formation was full to base with hydrocarbons and there was not a highest known water found in any of the well logs. Assumed gas-water contacts were

displayed when there was a lowest known gas and a highest known water. Assumed gas water contacts were just the difference between the lowest known gas and the highest known water. Next, net sand isopachs were created; these isopachs were created the same way as the gross sand isopach except with a porosity and shale volume cut-off of 20% and 30% respectively. The porosity and shale volume cut-off was previously defined as the limit for commercial production of hydrocarbons (Personal communication Harris 2010). The last set of subsurface maps created were the net pay isopachs. The net pay isopachs integrated the net sand and depth structure maps. The net pay isopachs defined the area of the reservoir as well as the reservoir thickness. Reservoir volumes were then calculated as acre feet. The reservoir volumes then were used in order to calculated reserves.

Seismic Amplitudes

Seismic amplitude anomalies play an important role in de-risking potential drilling prospects. Seismic amplitude anomalies often indicate the presence of hydrocarbons. Amplitude anomalies are caused by changes in seismic reflections. In unconsolidated Tertiary sediments of the Gulf of Mexico, seismic amplitude anomalies are considered one of the best Direct Hydrocarbon Indicators (DHI's) (O'Brien 2004). Seismic anomalies can indicate the presence of hydrocarbons due to the physical rock properties of hydrocarbon bearing zones. The most notable change that hydrocarbons have on rock properties are their respective densities and velocities. The density of unconsolidated sandstone is 2.65 g/cm^3, saltwater 1.15 g/cm^3, oil .75 g/cm^3, and gas .02-.15 g/cm^3 (Asquith and Krygowski 2004, and Domenico 1974). The density of gas is

much lower than oil and saltwater; this lower density effects the rocks impedance contrast more than oil or a brine filled rock. There is a positive correlation between a rocks density and velocity. As rock density decrease, the rock velocity will decrease as well. As observed from the synthetic seismogram model, gas saturated sands have a velocity of 9,500 ft/s water saturated sands have a velocity of 10,000 ft/s and the shale of 10,900 ft/s. Gas saturated rocks have the lowest densities and velocities when compared to the other rocks. This large contrast of parameters is what gives gas bearing zones such a different impedance and reflection coefficient when compared to other intervals which can lead to seismic amplitude anomalies.

The most notable feature that can help confirm DHI amplitude anomalies is the amplitudes conformance to down dip depth structure (O'Brien 2004). Also, proven nearby analogs that exhibit similar amplitude characteristics that are linked to production, can help confirm the amplitude response as a DHI. Amplitude vs. Offset (AVO) is another useful way to confirm DHI amplitude anomalies when angle stack data is available. Most of the Tertiary sediments of the GOM are considered to be unconsolidated, Class 3, low-impedance sands, which would indicate increasing amplitude with offset (Rutherford and Williams 1989).

There are many pitfalls when using amplitude anomalies as DHI's. The most notable pitfall when using amplitude anomalies is identifying low gas saturated reservoirs (Domenico 1974). Low saturations of gas in a reservoir can have velocities similar to those of high saturations of gas in the reservoir (Figure 13).

Table 1: Density and compressibility values for water and gas at selected subsurface depths (Modified from Domenico 1974).

		Depth (ft)	
	2000	6000	10000
Densities			
Water (g/cc)	1.097	1.089	1.083
Gas (g/cc)	0.023	0.103	0.156
Compressibility's			
Water (Gpa)	0.4587	0.42016	0.41529
Gas (Gpa)	159.2357	47.984	26.143

The factors which most effect on velocity with respect to water saturation in the compressibility and density of the fluid. Gas has a much larger compressibility factor than water (Table 1).

The velocities of low and high gas saturations reservoirs produce similar seismic amplitude anomalies. Strong lithologic variation in the reservoir can also give false amplitude anomalies. This is due to changing velocities and densities associated with the lithology (Forrest et al. 2010). Also, anomalously high pressure can affect the rock velocity. Overpressured reservoirs have high pore pressure, which slows the velocity when compared to normal pressured reservoirs (Sheriff 1980). Tuning effect can give false amplitude as well. Tuning refers to the interference of closely spaced intervals, in which the beds are changing thickness in proximity to each other (Sheriff 1980).

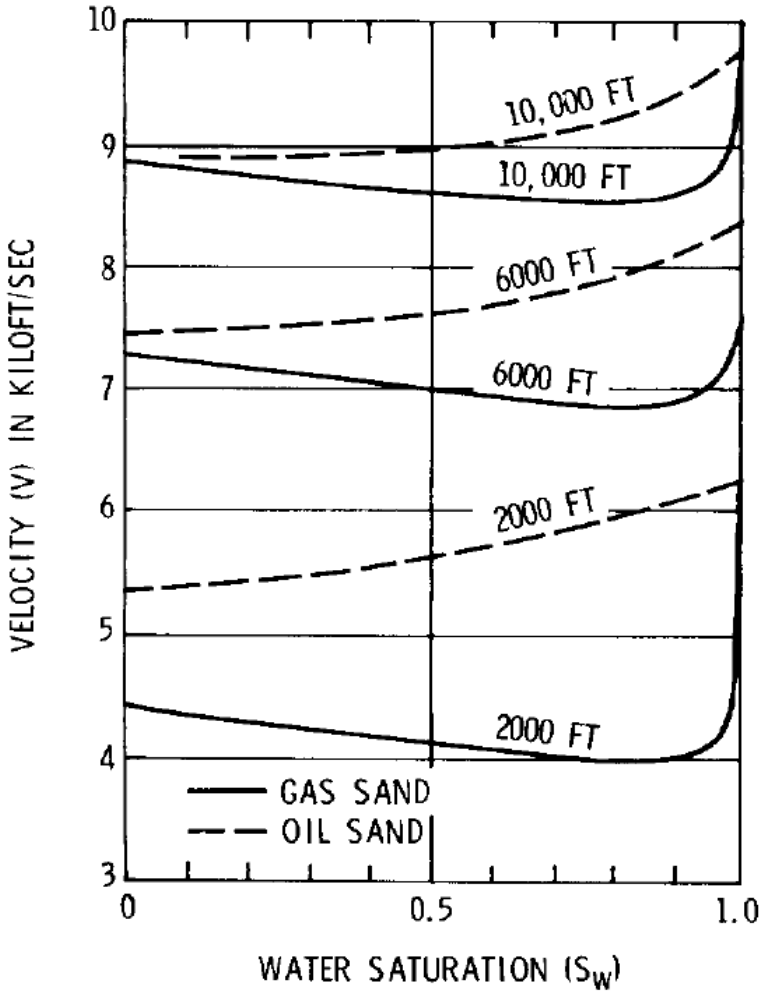

Figure 13: Effects of water saturation on velocities of gas and oil reservoirs at depth. Similar rock velocities can be seen in reservoirs with 5-10% and 90-95% water saturations (Domenico 1974).

Volumetrics

The volumetric calculations performed in this research were used to identify zones of bypassed hydrocarbons and possible infill-drilling prospects. This was done by using structure and isopach maps porosity and water saturations, to interpret reservoir volumes. By using the parameters rock volume (*V*), recovery factor (*Rf*), and the formation volume factor (*Bg*) along with reservoir parameters for porosity and water saturation. The equation used for the volumetric calculation follows (Hyne 2001):

$$Recoverable\ Gas = \frac{V \times 43{,}560 \times \emptyset \times (1 - S_W)Rf}{B_g}$$

After the volumetric calculations were performed they were used to identify areas that had been completely depleted, bypassed zones, or areas for future infill drilling locations. The volumetrics were compared to the cumulative production to see the relationship between the two different values.

CHAPTER IV

LATE MIOCENE MIDDLE (QH) SAND CHARACTERIZATION

Introduction

Geological, geophysical, and petroleum engineering data was used to create a detailed reservoir model for the Late Miocene middle (QH) sand. This sand provided a baseline understanding and interpretation of the field. The QH reservoir is the most abundant source of data within the field. Available data on the QH consists of wireline logs, paleo, core, petro-physical data, drilling data, production information, and seismic. The QH, is laterally continuous and has slight variations in overall thickness. The seismic reflector used to map the QH sand is a very strong continuous trough (Figure 14).

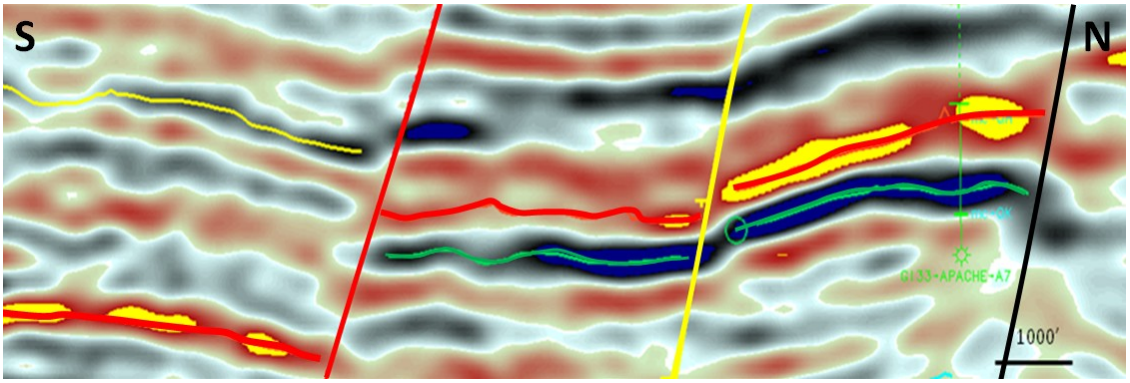

Figure 14: A north-south seismic line through the study area showing the strong seismic reflector used to map the QH sand, shown in red. Seismic data owned or controlled by Seismic Exchange, Inc.

The QH reservoir was the main exploration and development target in Grand Isle 33 and 43 fields. The first well that encountered commercial quantities of hydrocarbons was the GI-32 Conoco W-1 in 1972. After its discovery in the W-1, the QH remained a

development target until 2001. During that time the QH was produced from 13 wells in the two fields. The reservoir ranges in depth from -12,076 to -12,525ft subsea.

Depositional Setting

The QH sand was penetrated by twenty-five well-bores in the study area. Overall sand thickness varies from about one hundred to one hundred and fifty feet. Sand was deposited in a marginal marine environment. Paleontological samples from the GI-33 A-1 wellbore indicate *Cyclammina 3* shales buried the QH. *Discorbis 12* sediments underlie the QH. These sediments were deposited in middle to outer neritic paleo-environments, eight to nine million years ago (Paleo-Data 1983). Wireline logs in the GI-33 A-1 and the GI-32 W-1 wells indicate two main depositional processes: a transgressive marine shelf followed by a prograding delta (Figure 15). A fining upward sequence characterizes a transgressive marine shelf whereas a coarsening upward sequence characterizes the prograding delta.

Figure 14 is an analog for the two main depositional processes. The fining upward sequence in the well log is interpreted to be a transgressive marine shelf. The coarsening upward sequence in the well log is interpreted to be representative of delta border progradation (Ahr 2008).

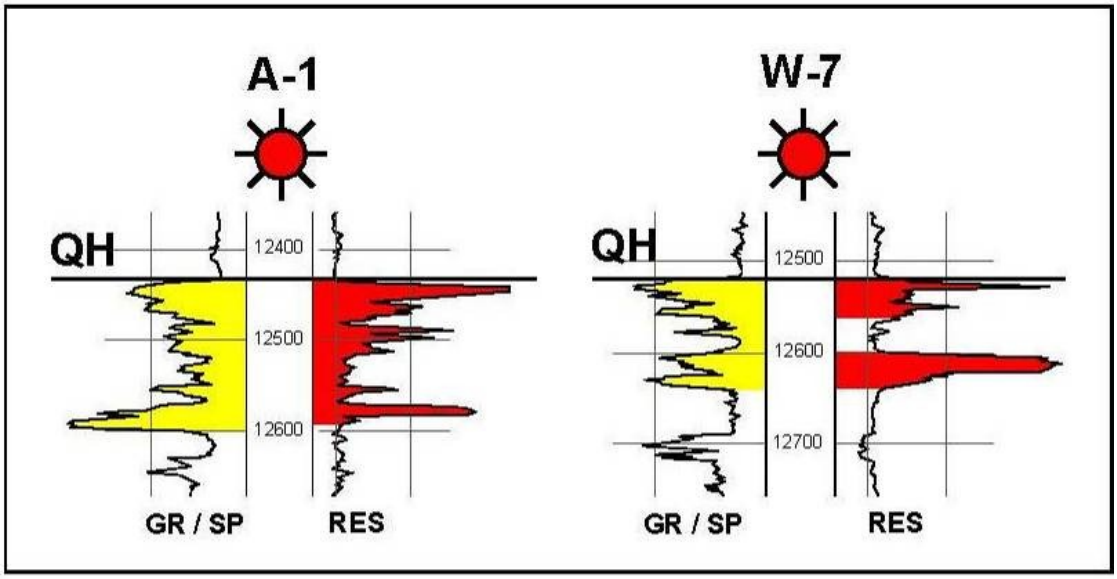

Figure 15: Well logs depicting the marine depositional environment for the QH sand. A fining upward trend followed by a coarsening upward trend from bottom to top. The logs are hung on the top of the QH sand. Wells A-1 and W-7.

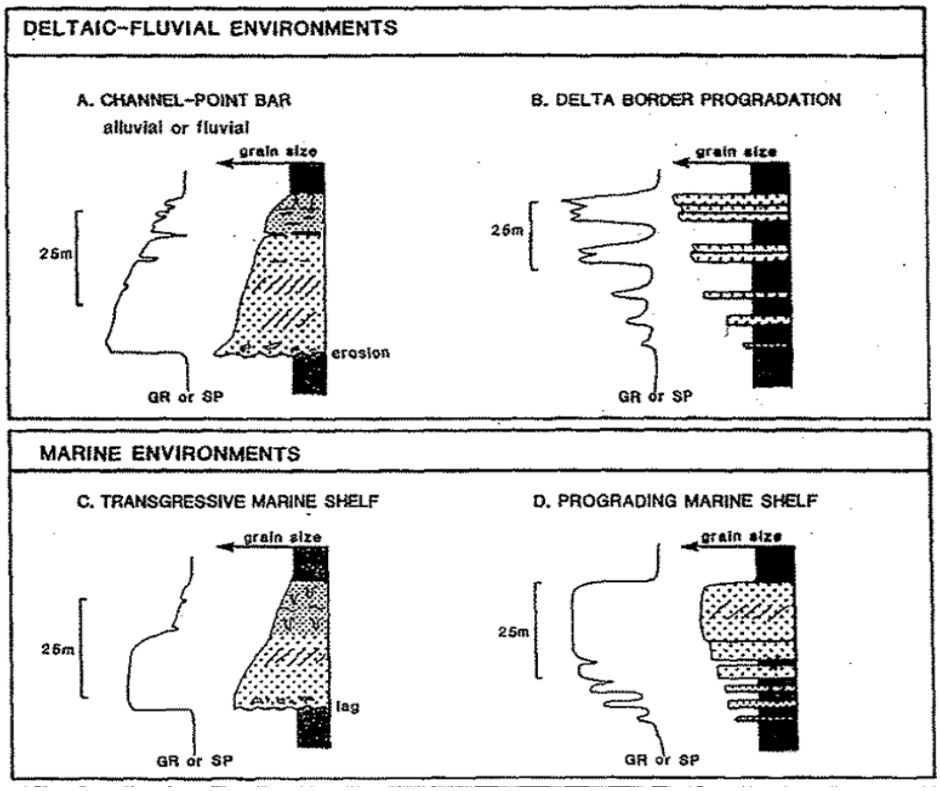

Figure 16: Wireline log signatures and there corresponding depositional environment (Modified from Ahr, 2008).

Although the QH is interpreted to be deposited in two separate environments, expanded 5 inch wireline logs suggest three individual sand packages. The middle QH sand lobe is interpreted to be a transition between the two main environments (Figure 18). The QH sand is sub-divided into three, distinct sand packages, QH-A, QH-B, and QH-C (Figure 18). An approximately east-west trending cross section through six wells has sands are interpreted to be pro-deltaic sands deposited in elongated and lobate

patterns (Figure 17). QH gross sand isopachs demonstrate elongate and lobate shapes (Figures 19, 20, & 21) following Walker's model (Figure 17) The QH gross sand isopachs indicate that the sediments were sourced from the north-northwest. The sediments display a thin basinward, with the thickest sediment interval in the middle of the lobes (Figures 19, 20, & 21).

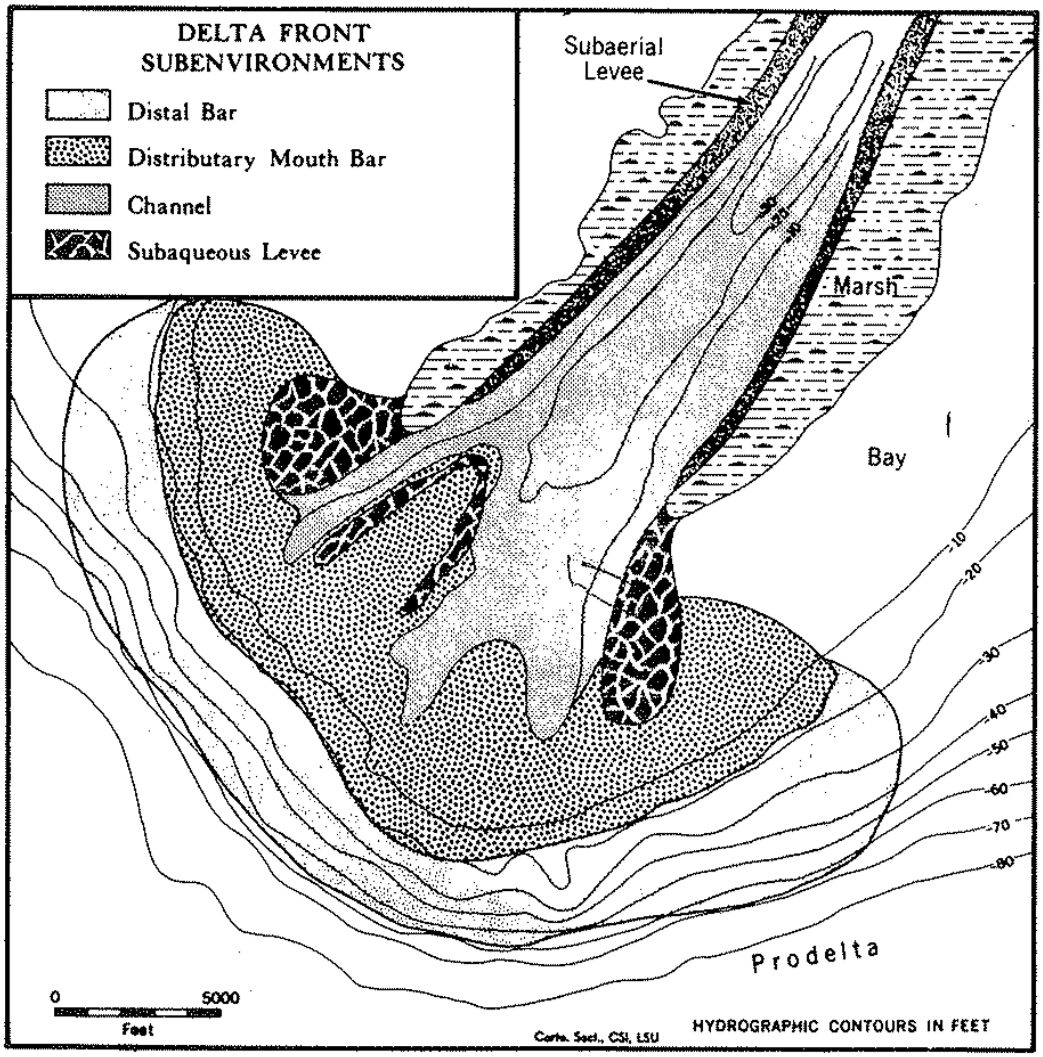

Figure 17: Depositional Environments of a fluvial dominated delta (Walker 1984). The QH sand is interpreted to be deposited in a distributary mouth bar system.

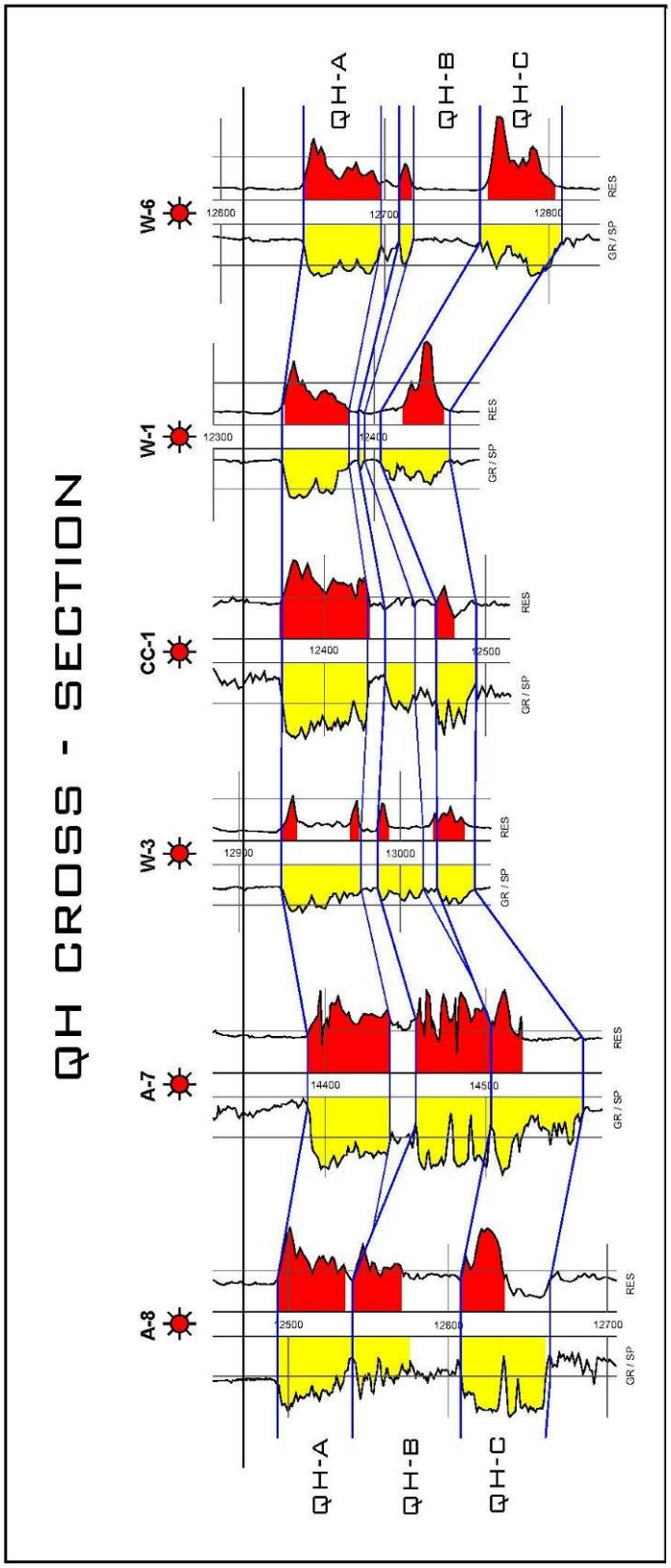

Figure 18: West-east trending QH sand cross section showing the three QH lobes. The cross section is hung on a resistivity marker just above the QH sand.

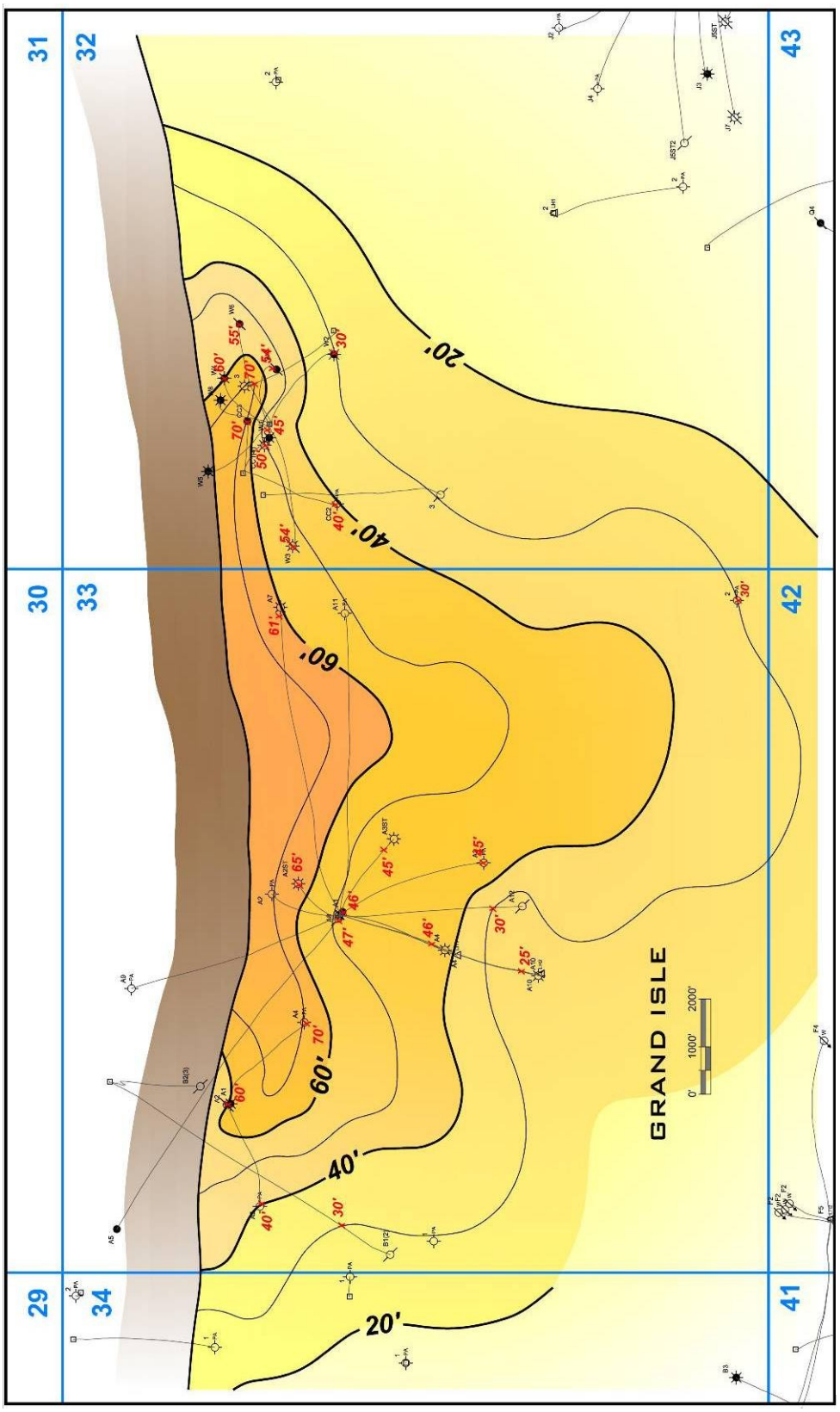

Figure 19: A gross sand isopach for the QH-A lobe indicating the depositional model. The sand are mapped against a large growth fault.

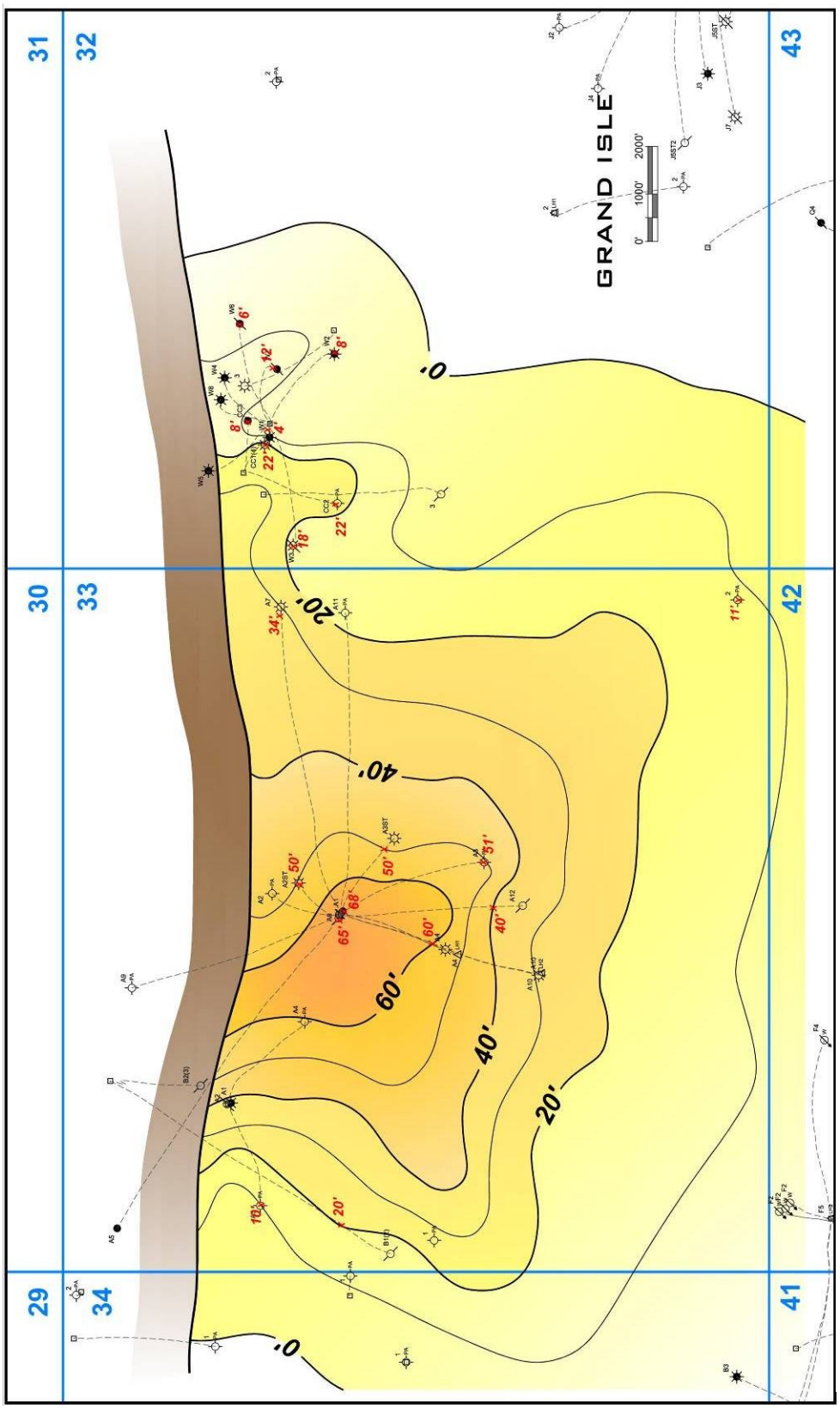

Figure 20: A gross sand isopach for the QH-B lobe indicating the depositional model. The sand are mapped against a large growth fault.

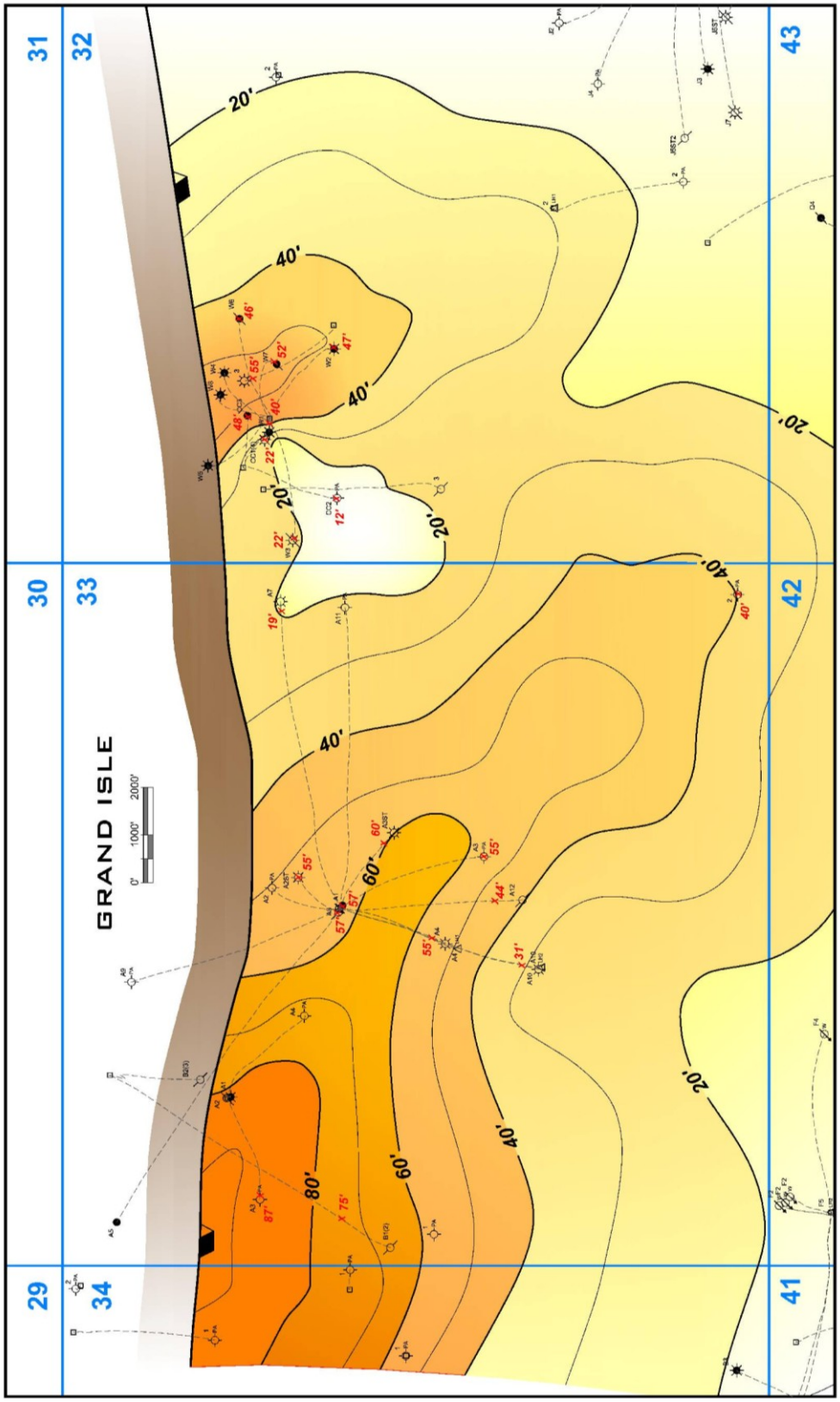

Figure 21: A gross sand isopach for the QH-C lobe indicating the depositional model. The sand are mapped against a large growth fault.

Local Structure

The local structure is controlled by a series of down-to-the-south growth faults (A, B, & C) and a two down-to-the-east faults, which are generally perpendicular to the regional growth faults. There are three main QH compartments in the study area, reservoir compartments QH-1, QH- 2, and QH- 3 (Figure 22) defined by faults A, B, C, & D.

The QH-1 compartment is an elongated, east-west trending, three-way closure on the down-thrown side of (fault A) and bounded to the west by fault D. The throw of fault A is between eight hundred and nine hundred feet based on fault cuts in the wellbores. There are two down-to-the-east faults (E & F). Throw on these faults range from fifty to seventy-five feet. The crest of the structure occurs at a depth of -12,197 ft in the GI-32 CC-3 well-bore. Dip of the QH-A is generally six degrees to the south.

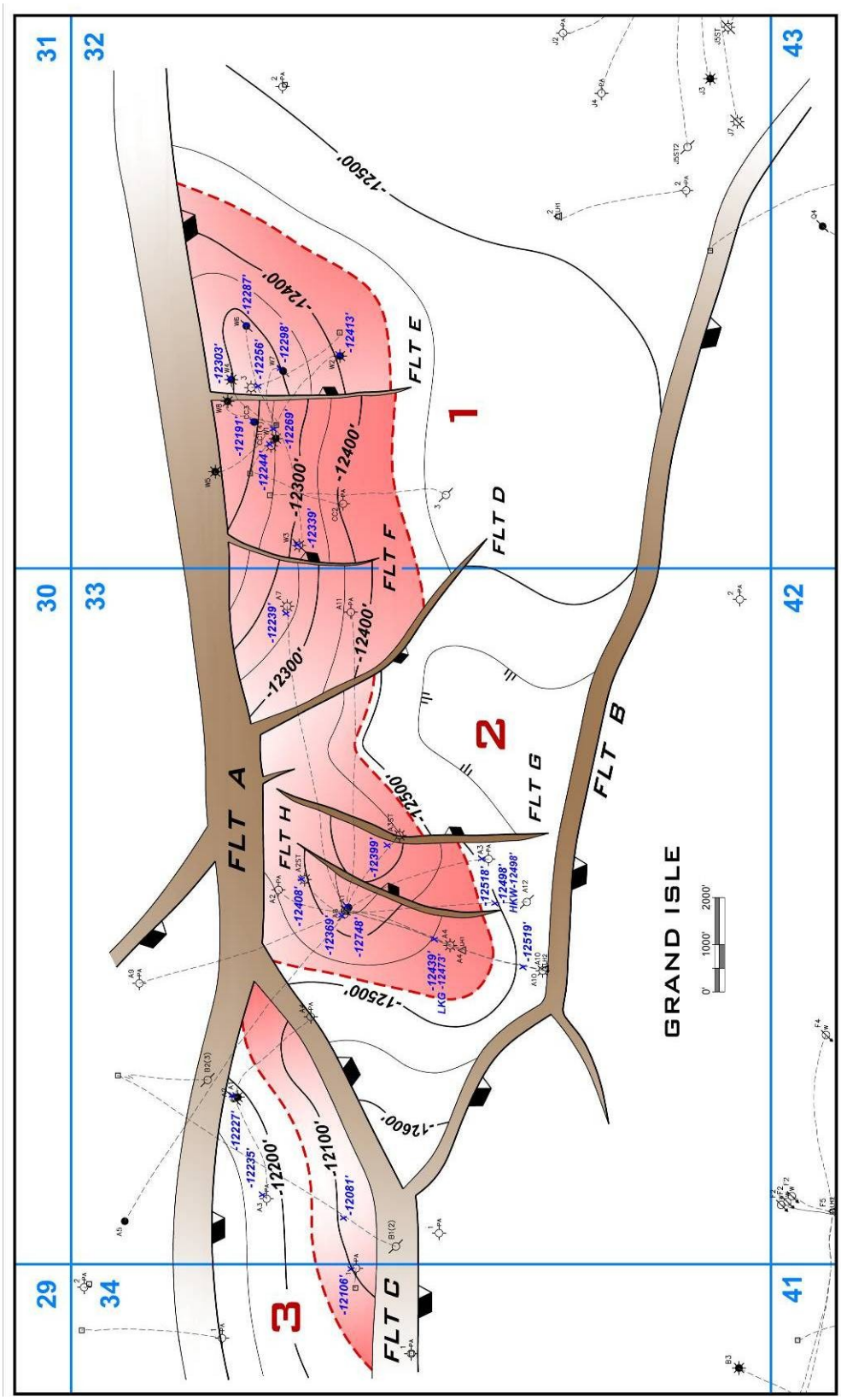

Figure 22: QH local depth structure map showing the three QH compartments (1, 2, and 3) and fault names.

The QH-2 compartment is an elongated, northeast-southwest trending, three-way closure on the down-thrown side of (fault A) and bounded by faults D and C laterally. There are two down-to-the-east faults (G & H), with throw ranging from fifty to seventy-five feet. The crest of the structure occurs at a depth of -12,348 ft in the GI-33 A-1 well-bore. Dip within the compartment varies both in magnitude and direction depending upon well location. Dip of the QH-B ranges from three to ten degrees, and dip direction is north west and south. Fault D has down-to-the-west throw of about one hundred and fifty feet.

The QH-3 compartment is an elongated, east-west trending, three-way closure (Figure 22) on the up-thrown side of (fault C), and is down-thrown to fault A. Throw on fault C varies from about three hundred to seven hundred feet. The crest of the structure is observed at a depth of -12,076 ft in the GI-33 B-1 well-bore. Dip of the QH-C is generally northwest at six degrees.

The local structure is well imaged in the seismic data displayed in time (Figures 23, 24, & 25). Figure 23 is a structural time map representing the QH sand. The seismic cross sections (figures 24 & 25) show the regional growth faults (blue, red, and green) as well as post depositional faults (yellow and pink).

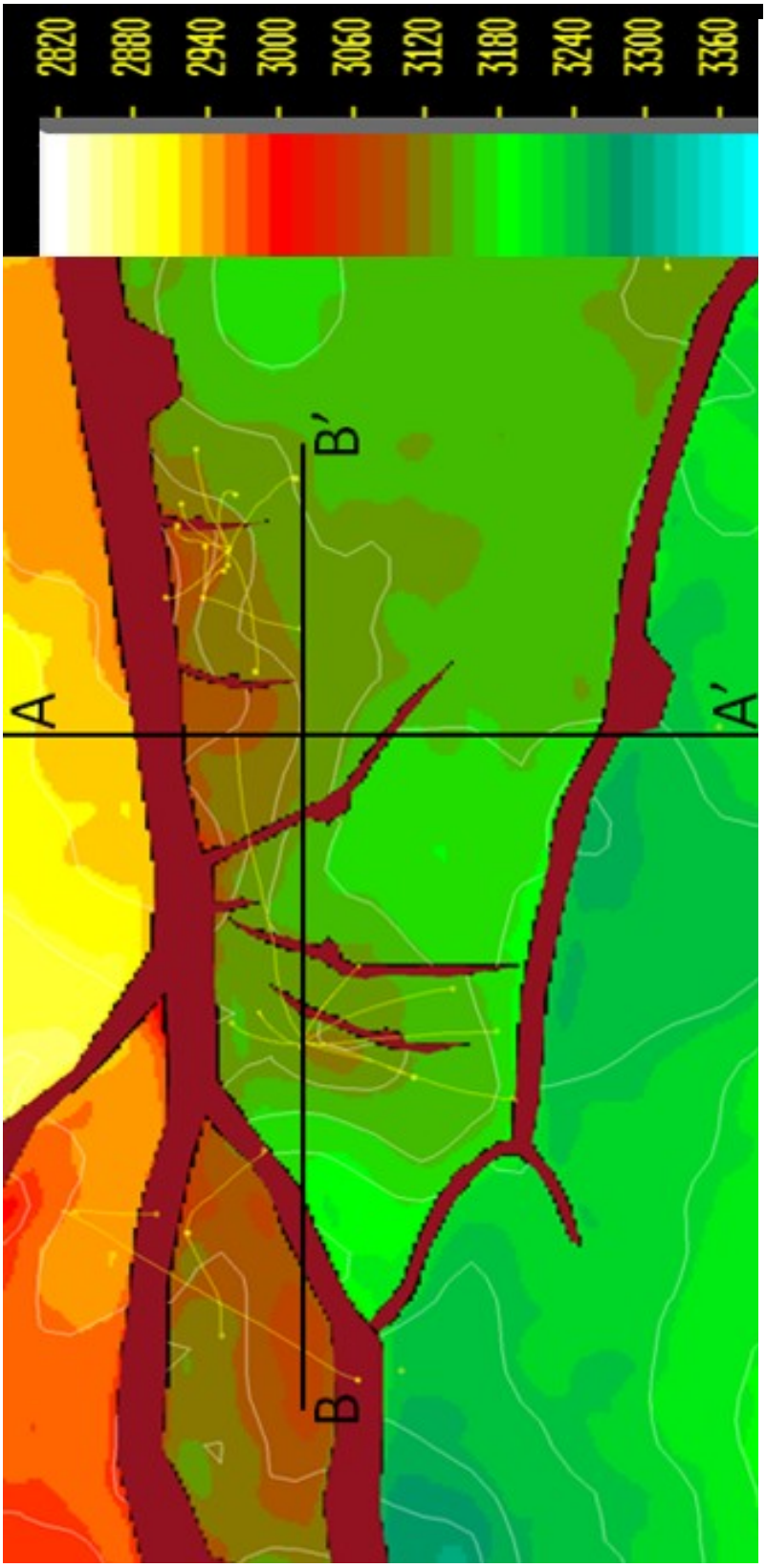

Figure 23: Top of QH structure, seismic time map. Color bar indicates that yellows and reds are structural highs and greens and blues and lows.

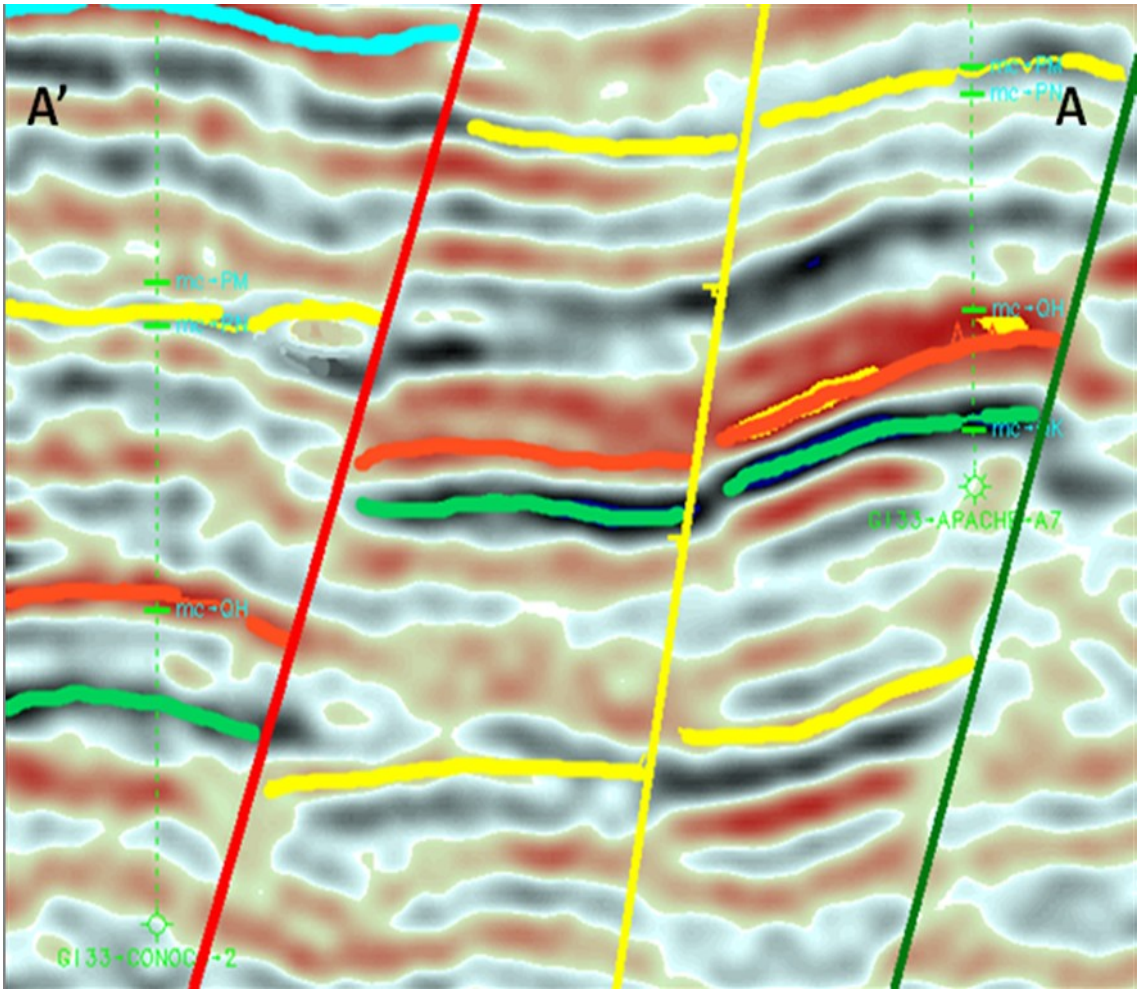

Figure 24: North-south trending seismic cross section from A to A' QH reflector is orange. Dotted green lines indicate wells. Seismic data owned or controlled by Seismic Exchange, Inc.

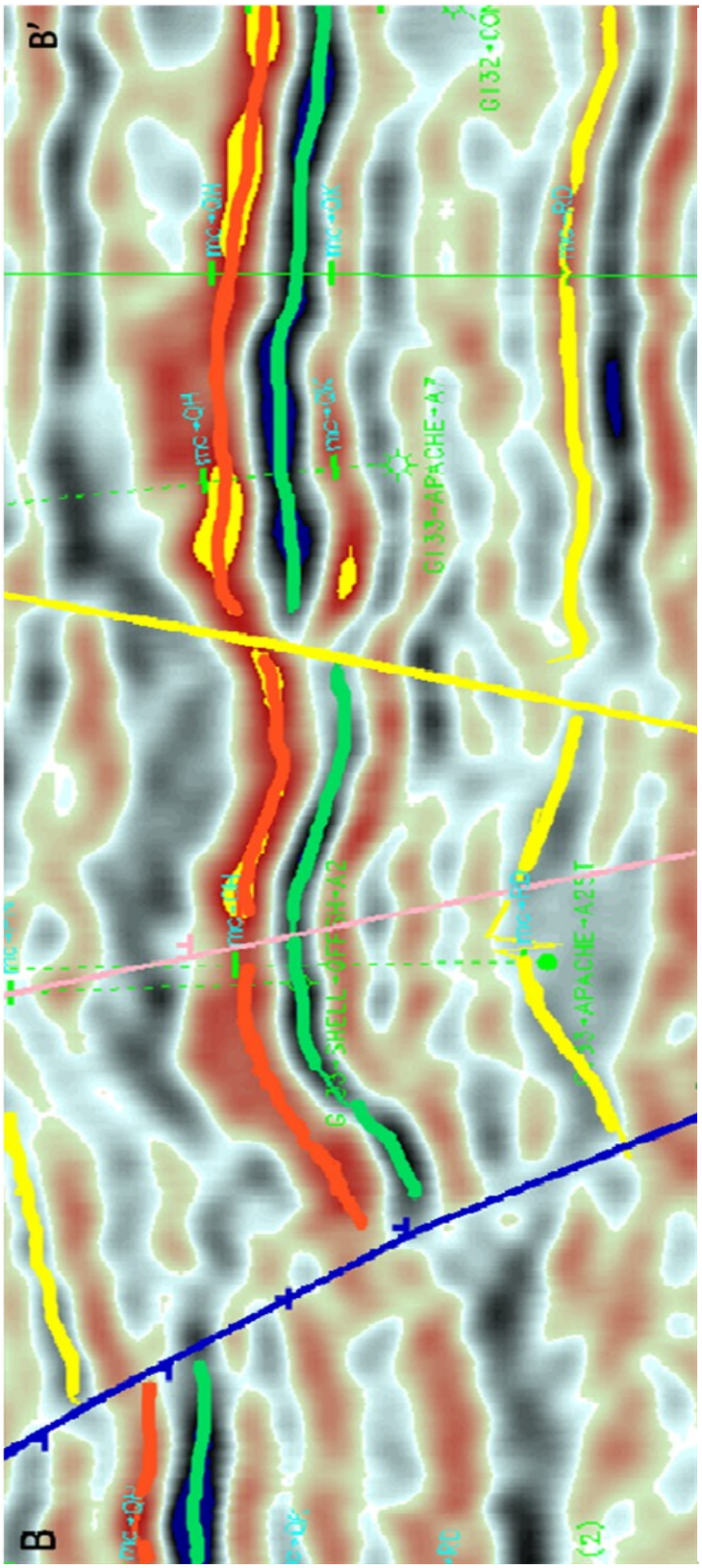

Figure 25: West-East trending seismic cross section from B to B'. The reflector used to map the QH sand is orange. Dotted green lines indicate wells, note the wells penetrating at the highs. Seismic data owned or controlled by Seismic Exchange, Inc.

Petrophysical Analysis

Petrophysical analysis was performed in all of the wells that penetrated the QH sand and contained viable log information. Porosity and water saturation were the main petrophysical calculations performed. Net pay was calculated from well logs using the previously defined methods in chapter 2. Net pay was defined as rock with porosities greater than 20%, water saturations less than 40%, and shale content less than 30%. These porosity and water saturation values were used in the volumetric calculations of the reservoir. The average porosity was 25% and the average water saturation was 24% with a hydrocarbon saturation of 76%. Previously interpreted core data suggest an average permeability of about 400-500 md (Everson 1989). Within the three QH zones (A, B, &, C), there are stringers of sand that contain very low porosity and permeability. These zones occur in the GI-33 A-3, GI-33 A-4, and GI-32 W-2 wells. These wells contain a tight zone at the top of the QH sand (Figure 26). This tight zone is interpreted to be a possible marine reworking zone with porosities from 15-18% Crossover of the neutron and density curves in all three well logs indicates the dominant hydrocarbon type is gas (Figure 26).

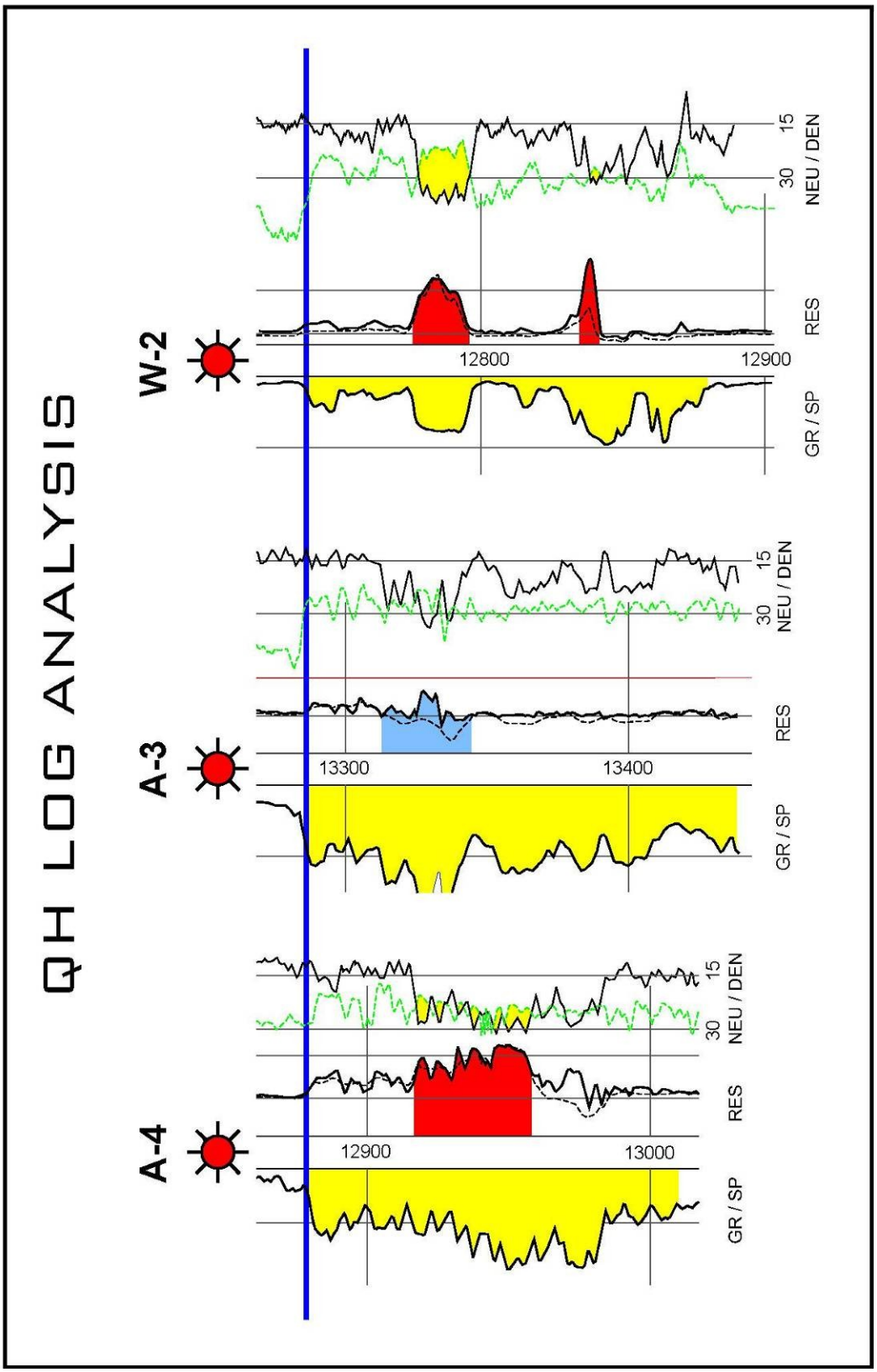

Figure 26: QH formation evaluation. Triple combo logs showing the tight zone at the top of the QH in the A-4, A-3, and W-2 wellbores which has porosity similar to the overlying shale. .

Production Analysis

The QH sand has the highest cumulative production in the Grand Isle 33 and 43 fields, producing from 13 of the 25 wells that penetrated this unit. Cumulative QH production to date is approximately 105 BCFG, 1895 MBO, and 2220 MBW from the three reservoirs (QH-1, QH-2, & QH-3) (OWL 2010). The average gas/oil ratios (GOR) for each reservoir are 59,000 cf/bbl, 43,000 cf/bbl, and 31,500 cf/bbl for the QH-1, 2, & 3 reservoirs. High GOR ratio indicate a strong gas reservoir. Individual QH production is presented for reservoirs or for individual wells (Table 2).

Table 2: Cumulative and individual well production for the QH sand.

QH Reservoirs Compartments		Gas Production	Oil Production	Water Production
QH-1	72-07	89 BCF	1500 MBO	500 MBW
QH-2	86-94	13 BCF	300 MBO	220 MBW
QH-3	01-10	3 BCF	95 MBO	1500 MBW
QH Total		105 BCF	1895 MBO	2220 MBW
Wells: (Completion Period)		Gas Production	Oil Production	Water Production
W-1	74-80	6 BCF	140 MBO	148 MBW
W-2	73-78	6 BCF	102 MBO	20 MBW
W-3	73-78	13 BCF	311 MBO	8 MBW
W-4	73-80	9 BCF	226 MBO	6 MBW
W-6	72-80	7 BCF	150 MBO	55 MBW
W-7	73-80	8 BCF	202 MBO	27 MBW
CC-1	81-98	12 BCF	60 MBO	32 MBW
#3	80-97	14 BCF	56 MBO	5 MBW
A-2ST	86-90	5 BCF	166 MBO	35 MBW
A-3ST	87-90	5 BCF	94 MBO	49 MBW
A-7	87-07	14 BCF	130 MBO	195 MBW
A-8	89-94	3 BCF	36 MBO	135 MBW
B-1	01-10	3 BCF	95 MBO	1500 MBW

Production from the wells completed in the QH-1 compartment is significantly higher than the production from the wells completed in the QH-2. The lack of production from the QH-2 suggests that some of the faults (B,C,D,G & H) that compartmentalize this reservoir are not sealing faults. Bottom hole pressure surveys were available for a few of the wells in both the QH-1 and QH-2 compartments. Bottom hole pressure graphs, records the pressure drawdown over the production period, indicate that QH-1 and QH-2 reservoir compartments are in communication with each other. Wells that were drilled and produced in the 1970s, which are primarily the W wells, have pressures from 7000 psi initially to about 4000 psi at abandonment. While wells that were drilled and produced in the 1980s and 1990s comprising of the A wells, came online with pressure around 4000 psi (Figure 27). These data indicate that fault D (Figure 9 or 22) has QH sand juxtaposed on either side of the fault that is in communication. The consistent decline in reservoir pressure (Figure 25) suggests that the reservoir drive mechanism is pressure depletion. Assumed recovery factors for a pressure depletion reservoir is 65% (J. Harris 2010 personal communication).

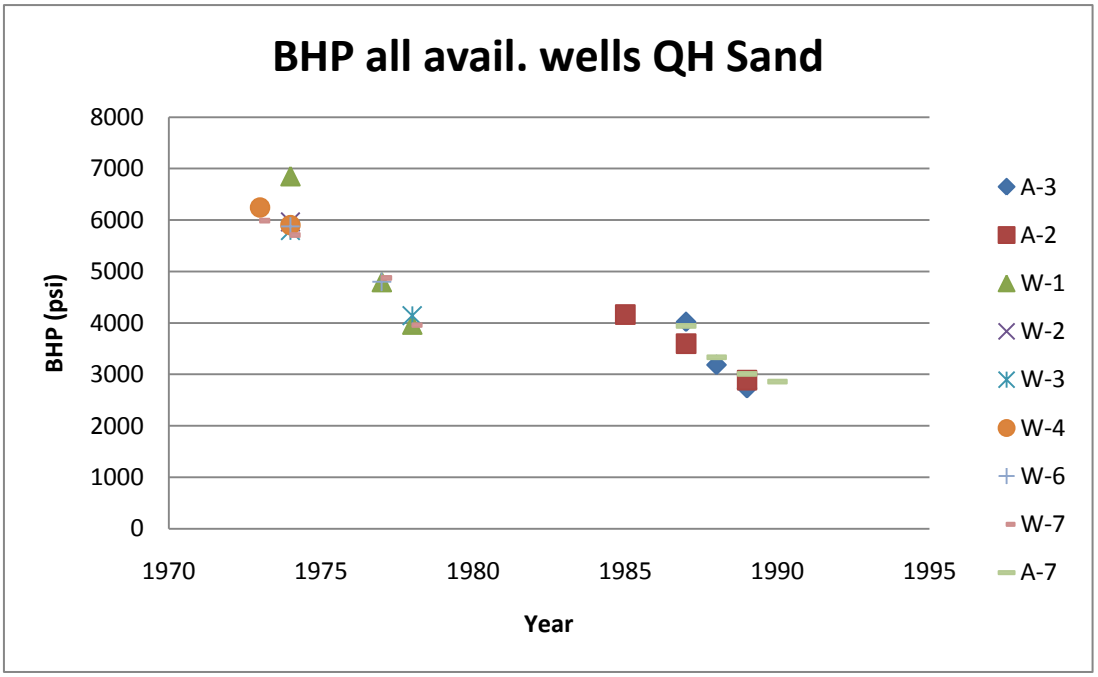

Figure 27: Bottom hole pressure graph showing the relationship between the QH-1 and QH-2 reservoir compartments. The occurrence of the abandonment pressure in the A wells and initial pressure in the W wells being the same indicates Fault D is not a sealing fault between the two compartments

Subsurface Maps

A series of subsurface structure, sand isopach, and net pay isopach maps were generated by integrating the well log, seismic, and production data used to create a reservoir model. The first set of maps created were structure maps (Figures 28, 29, & 30) for the three different QH lobes (A, B, & C). Three QH structure maps were required because varying gas water contacts occur throughout the wells in GI-32. The differing gas water contacts imply that the three different QH lobes are not always in contact with each other (Figures 28, 29, &, 30). Because the lobes are so close vertically, the structural picture remains consistent. However, the QH-3 Compartment acts as one connected sand this is observed from the gas water contact levels from the two wells that penetrate the sand. Also, the QH-C lobe has a much smaller reservoir area in the QH-2 compartment when compared to the A and B lobes.

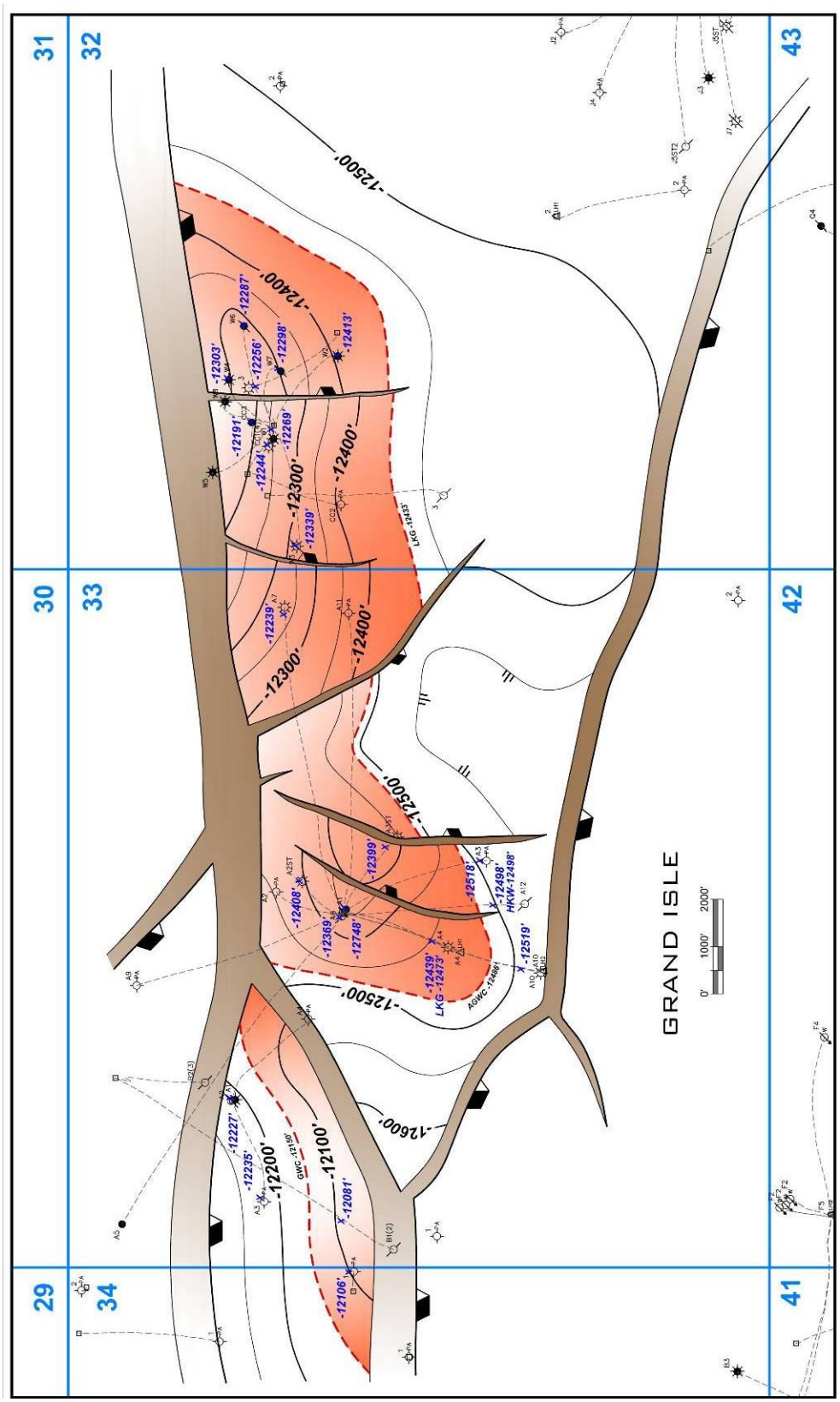

Figure 28: QH-A depth structure map with gas contacts (dashed red lines).

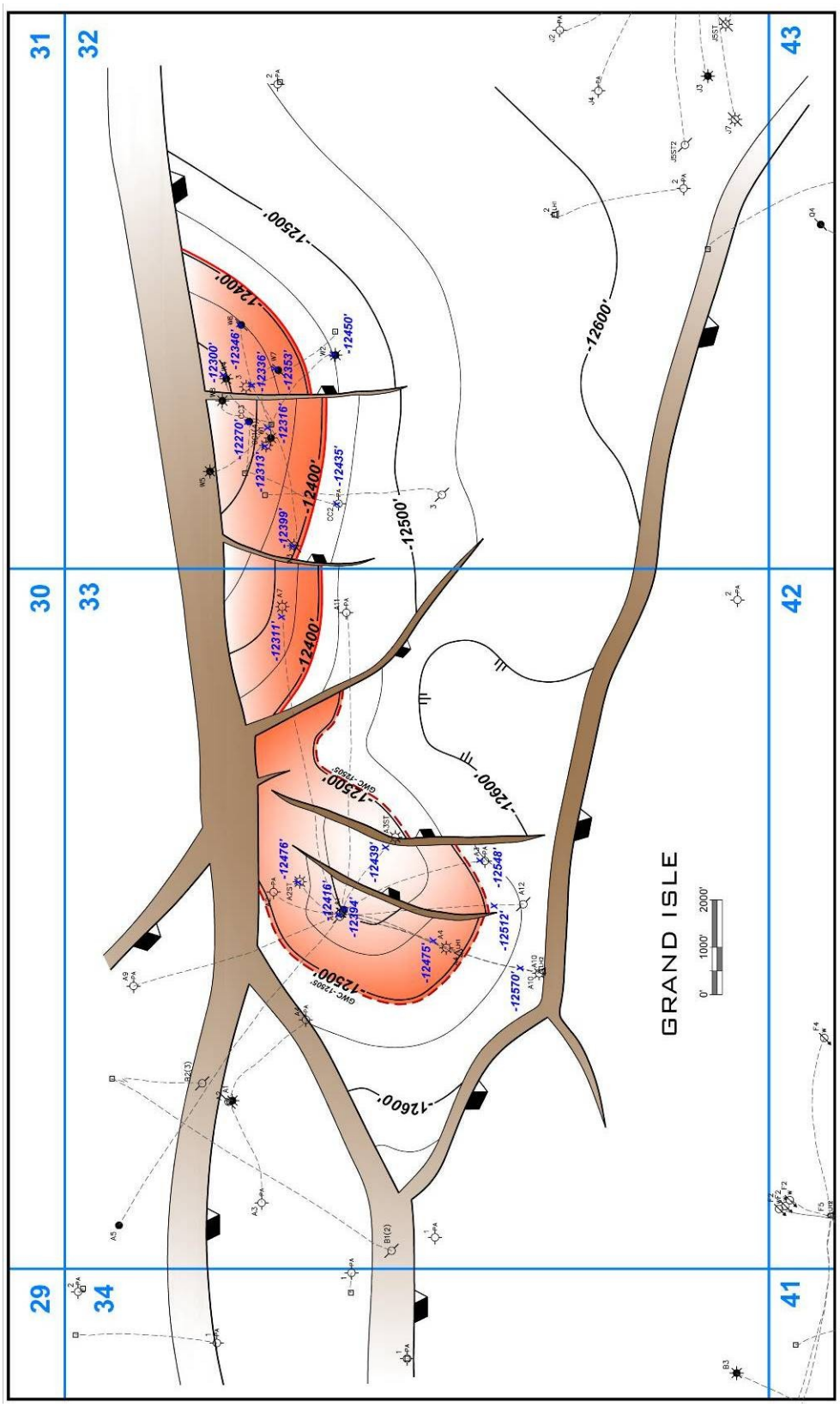

Figure 29: QH-B depth structure map with gas contacts (dashed red lines) no pay sand were observed in the QH-3 compartment at this level.

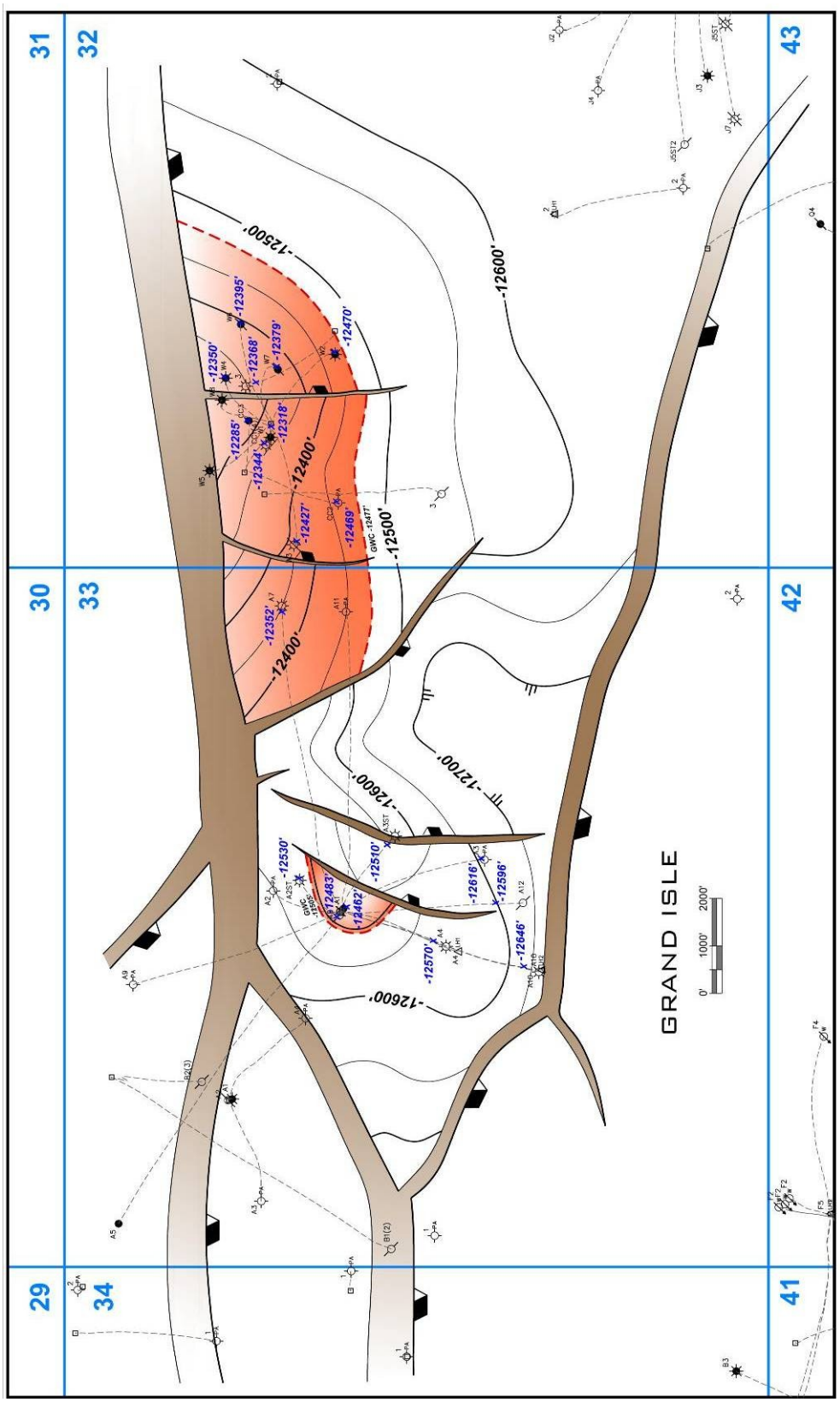

Figure 30: QH-C depth structure map with gas contacts (dashed red lines) no pay sands were observed in the QH-3 compartment at this level.

The next series of maps (Figures 31, 32, & 33) are net sand isopachs (Net/Gross). These isopachs were created using a porosity cutoff of 20%. Three different isopach maps were created for the different QH lobes (Figures 31, 32, & 33). The net sand isopach maps do not record the same depositional picture as the gross sand maps. This difference is likely produced by a marine reworking. The net porosity maps indicate the stratigraphic nature of the QH is very complex.

Finally, net pay isopachs (Net/ Gross Pay) were created for each of the QH lobes using both the structure and net sand isopachs (Figures 34, 35, & 36). These net pay isopachs represent the reservoirs thickness and aerial distribution (Reservoir Volume). The QH-1 reservoir area is 1,728 ac with an average thickness of 24 ft, the reservoir volume is 41,950 ac-ft. The QH-2 reservoir area is 449 ac with an average thickness of 22 ft, and a reservoir volume of 10,015 ac-ft. The QH-3 reservoir area is 187 ac. with an average thickness of 15 ft, and a reservoir volume of 2,885 ac-ft. These reservoir volumes will be used in the volumetric calculations.

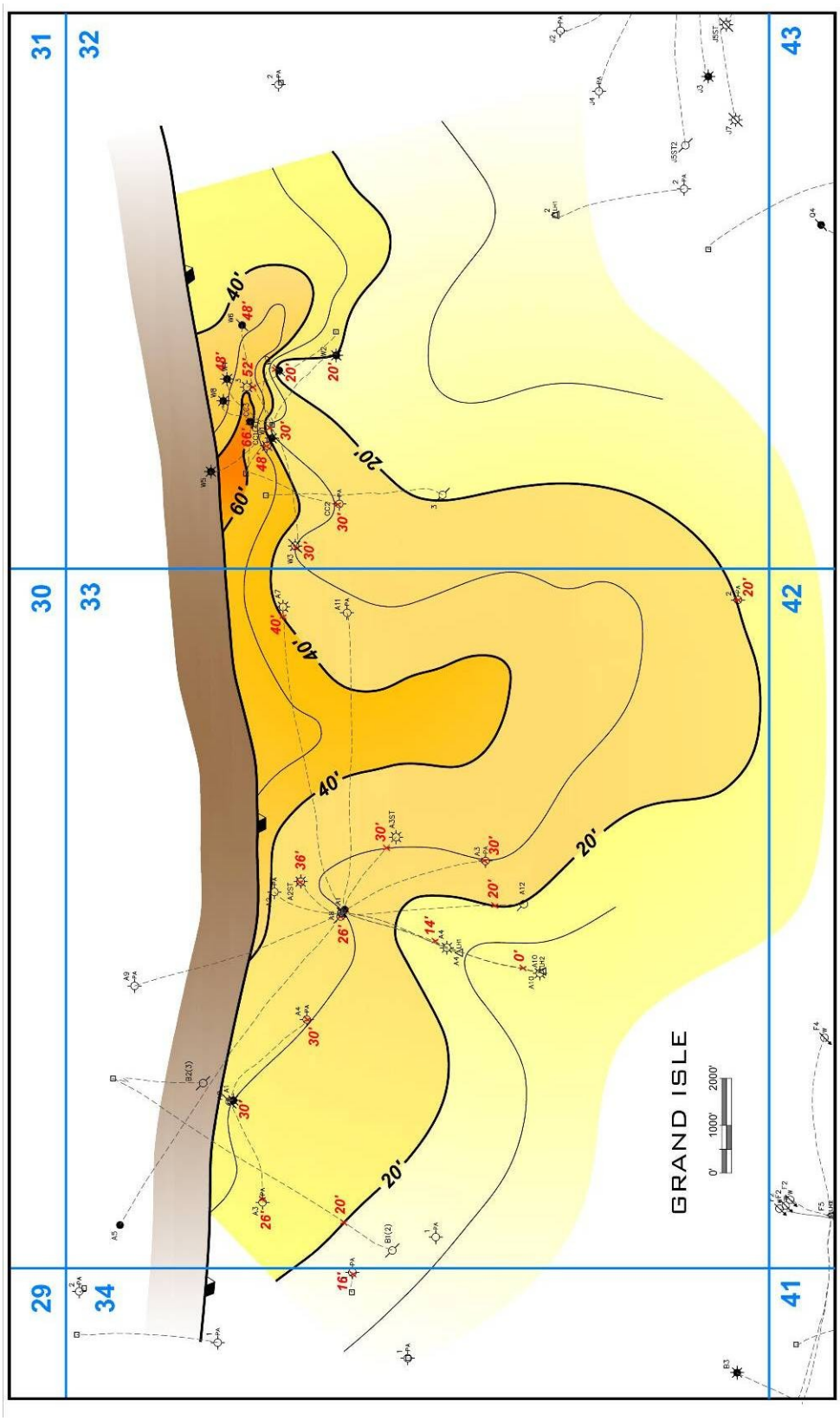

Figure 31: QH-A net sand isopach.

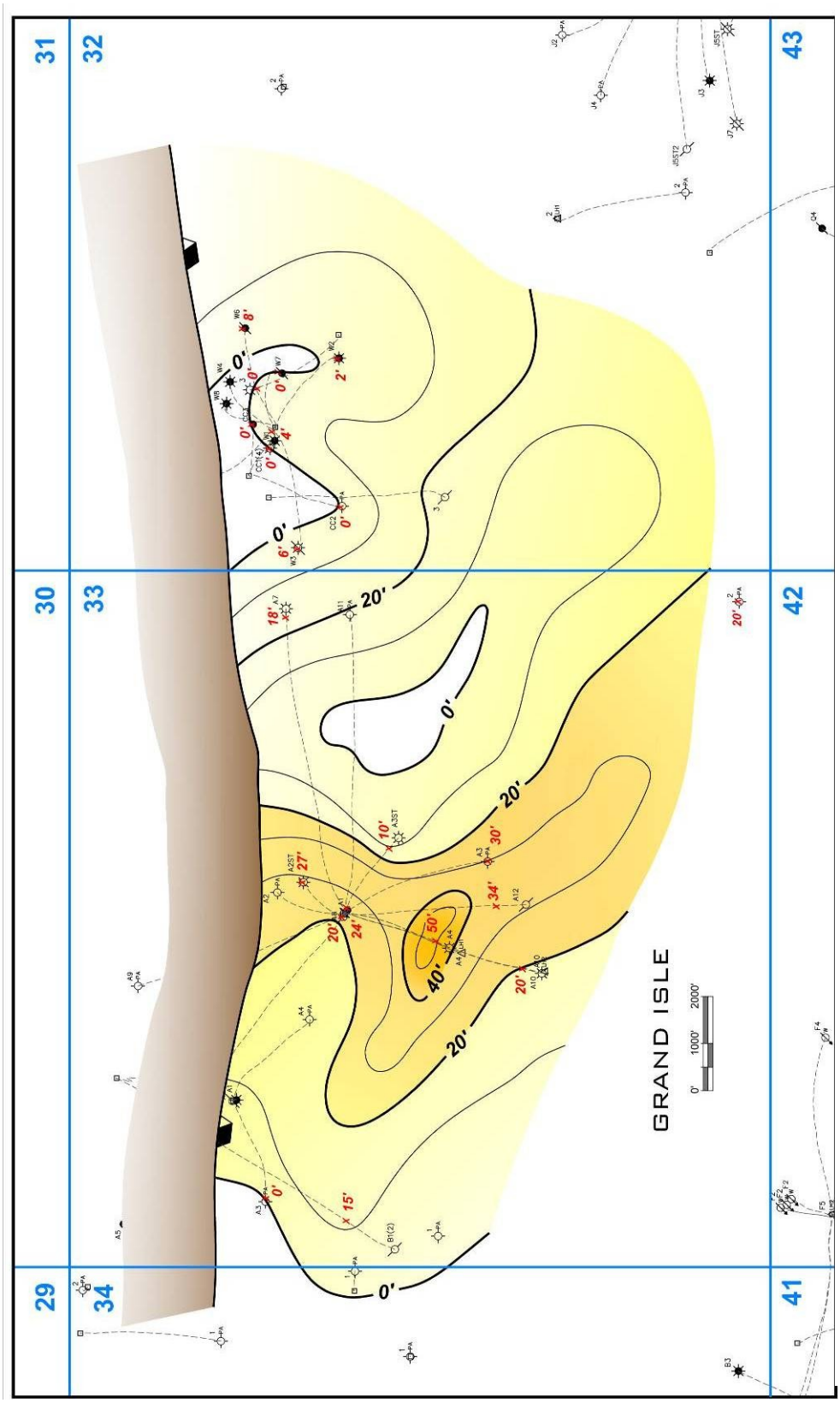

Figure 32: QH-B net sand isopach.

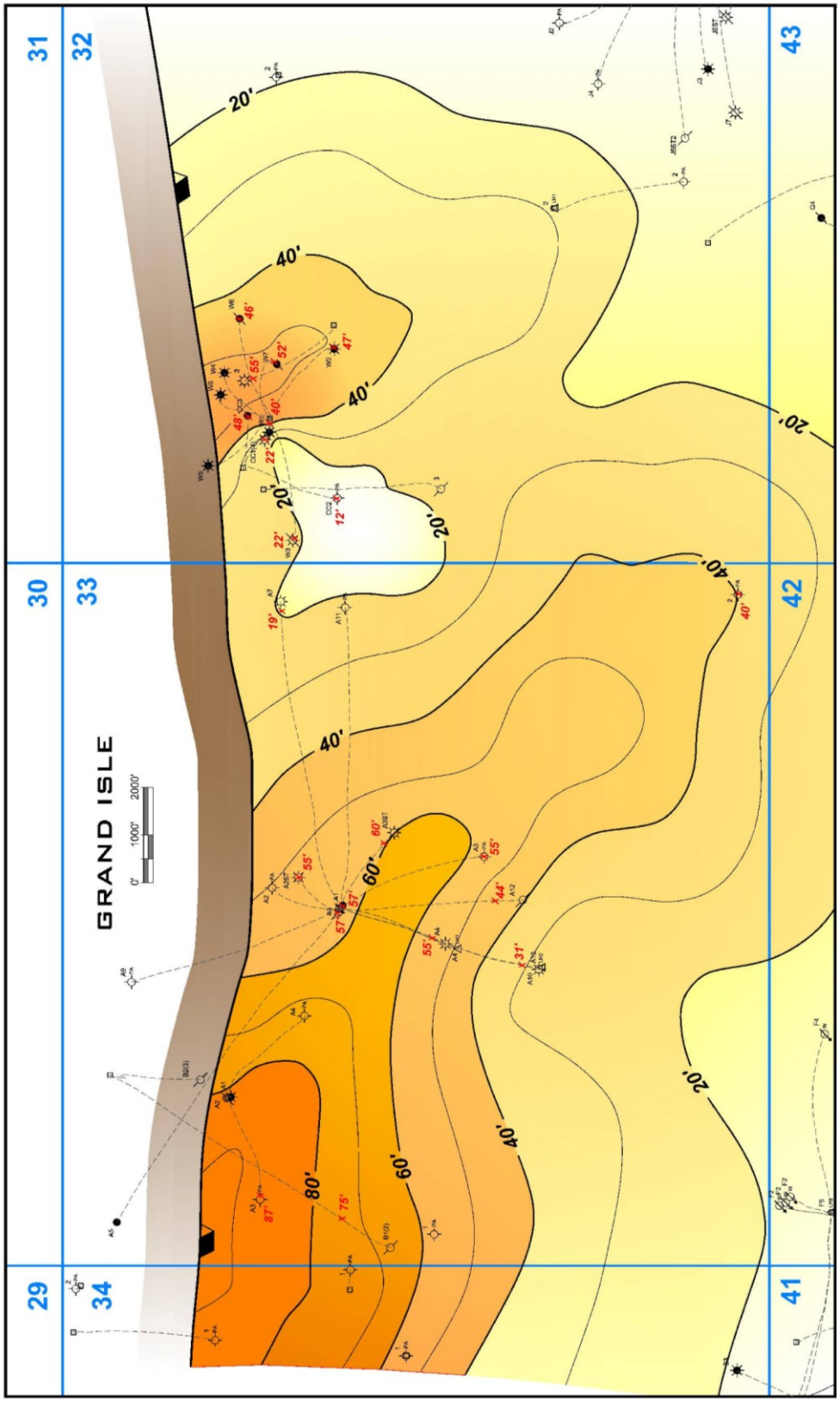

Figure 33: QH-C net sand isopach

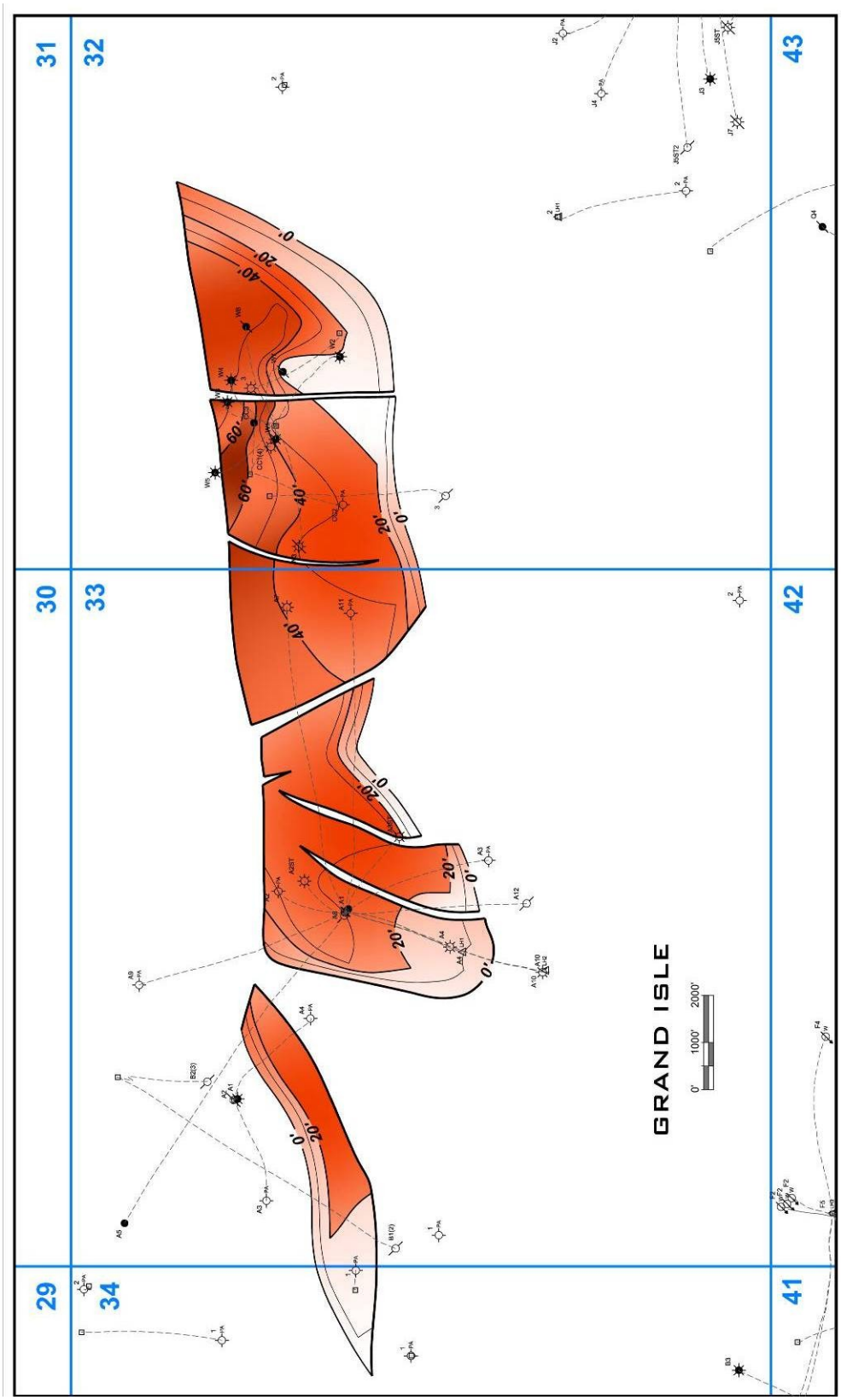

Figure 34: QH-A net pay isopach used for volumetrics.

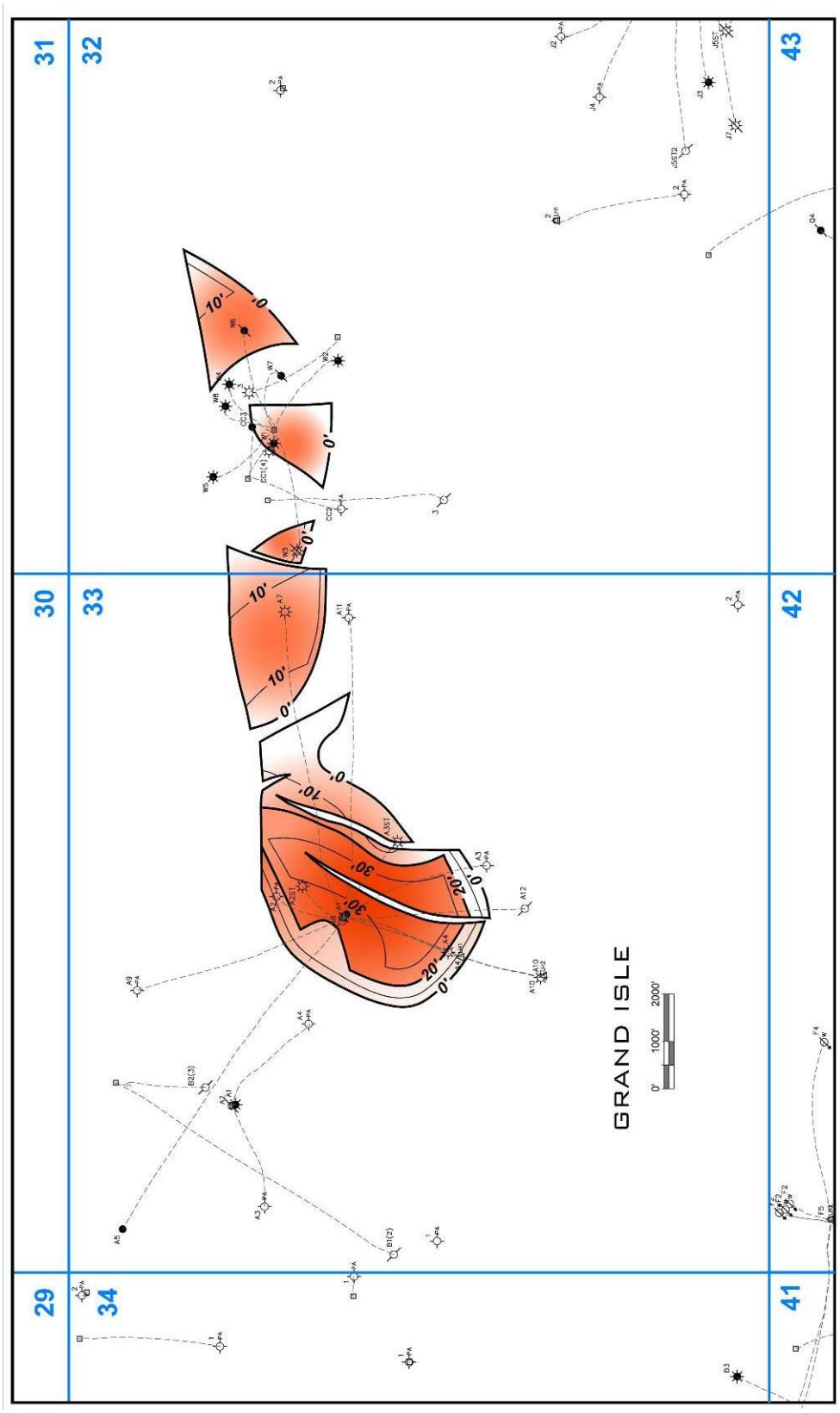

Figure 35: QH-B net pay isopach used for volumetrics.

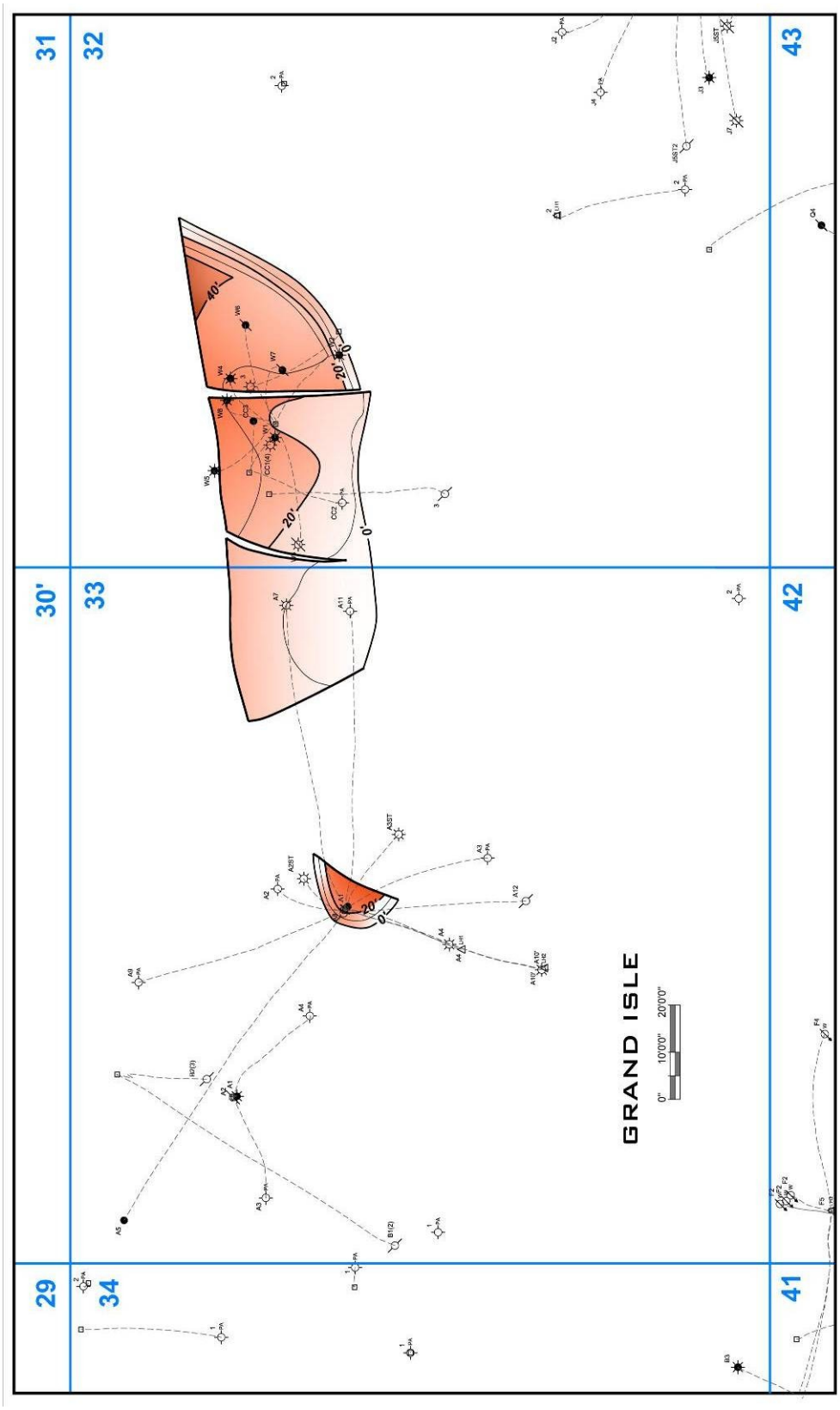

Figure 36: QH-C net pay isopach used for volumetrics.

Seismic Amplitude Extractions

Amplitude was the dominant seismic attribute used to delineate the QH reservoir (Figure 37). Amplitudes were extracted from an auto tracked and smoothed, seismic time horizon corresponding to the QH reflection. The extraction consisted of maximum absolute amplitude, maximum negative amplitude, and root mean square amplitude. The maximum negative amplitude extraction was the main amplitude map that was interpreted (Figure 37). The maximum absolute and root mean square amplitude extraction response was very similar to the maximum negative amplitude extraction.

The amplitude response from the QH sand does not seem to be a hydrocarbon indicator (Figure 37). Downdip conformance to depth structure maps is a significant indicator of hydrocarbons presence (Forrest et al. 2010). Amplitude at the QH level fills virtually the entire fault block without regard to structural position, with amplitude that extends well past the downdip limit of the reservoir, as previously defined in Figures 26, 27, 28.

Amplitude response of the QH is interpreted to be a lithologic indicator and possibly the presence of the underlying over-pressured zone (O'Brien 2004). There is only slight lithologic variation among the wells drilled into the area of greatest amplitude. Thus, amplitude is considered to be indicative of the presence of sand, not the thickness.

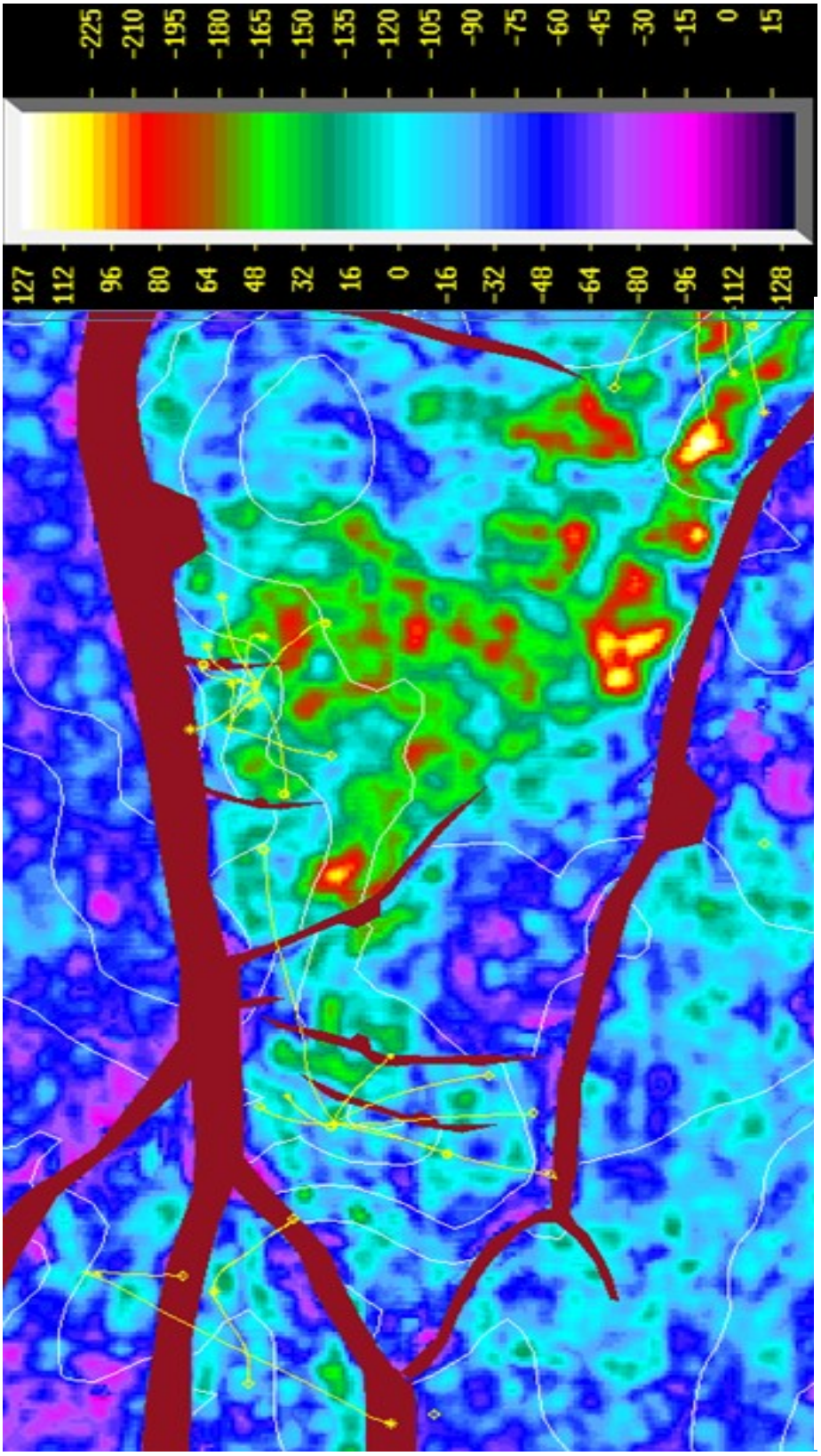

Figure 37: Maximum negative amplitude extraction taken from the QH horizon. The amplitude at this levels fills virtually the entire fault block, indicating that the amplitude response is more of a lithologic indicator rather than hydrocarbon.

Volumetrics

Volumetric calculations for the QH reservoir compartments were performed to look for remaining potential. Volumetric calculations are based on reservoir parameters defined in earlier chapters. Original recoverable reserves were calculated for comparison with the total produced reserves to see if remaining reserves exist (Table 3).

Table 3: Calculated original reserves and produced reserves for the QH reservoirs.

Reservoir	Original Calculated Recoverable Reserves	Produced reserves
QH-1	70 BCF	89 BCF
QH-2	18 BCF	13 BCF
QH-3	4 BCF	3 BCF

The QH-1 significantly over produced from the calculated value, while the QH-2 reservoir under-produced. This relationship is connected to the bottom hole pressure data which indicates that the two reservoir compartments are connected and act as one large tank. There is still a 14 BCF difference between the produced reserves and original calculated reserves. The differing reserves could be from the pay cut-offs that were established for the petrophysical calculations, even though there was a cut-off these zones could still contribute to the overall production. Also the presence of sand and complex faulting can lead to juxtaposed sands on each other leading to breached reservoirs, and unaccounted production. The QH-3 reservoir has not yet reached the original calculated recoverable reserves, but production is still ongoing in the GI-33 B-1 well. From these volumetric calculations it is concluded that there is little to no remaining reserves left within the QH reservoir in the Grand Isle 33 & 43 fields (Figure 38). The QH-1 wells were able to drain the reserves from across a fault and partially deplete the QH-2 compartment.

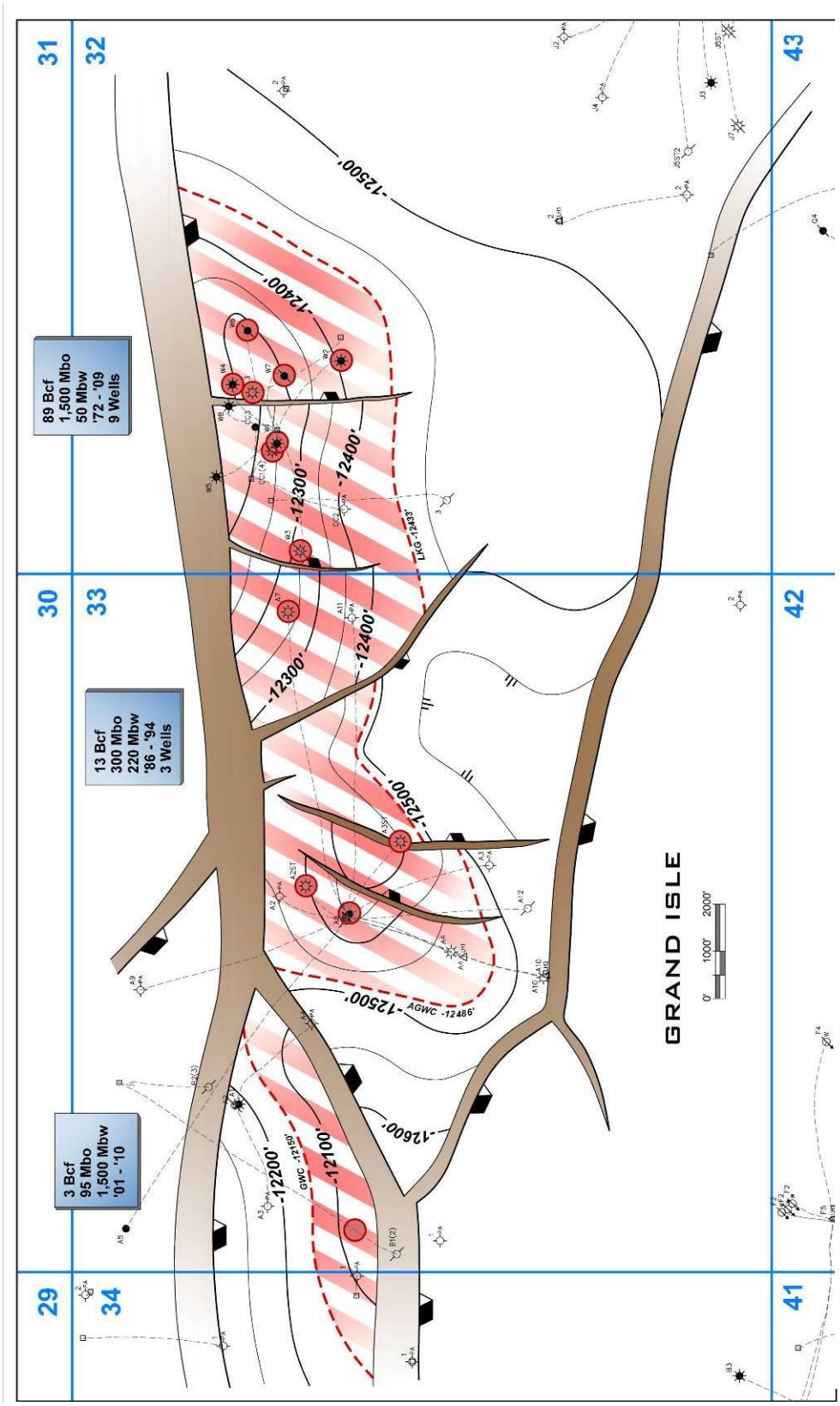

Figure 38: QH pay structure map showing the QH completely depleted. The calculated recoverable reserves matching very closely with the actual produced reserves.

Conclusion

The detailed reservoir model created for the QH sand delineate reservoir features that were not apparent when previous field evaluations were conducted. Although the QH sand appeared to be a single large connected sand package it is actually three distinct and separate sand packages. Pressure data reveals communication between the QH-1 and QH-2 reservoir compartments. This enabled wells from the QH-1 compartment to recover reserves from the QH-2 compartment. There is a large seismic amplitude anomaly associated with the QH sand which encompasses nearly all of the fault block. This seismic amplitude anomaly associated with the QH is interpreted to be a lithologic indicator rather than a hydrocarbon indicator. Volumetric calculations show that the QH over-produced the original recoverable reserves. The over anticipated production in the QH-1 it is assumed that the QH reservoir has been completely depleted.

CHAPTER V

LATE MIOCENE LOWER (RD) SAND CHARACTERIZATION

Introduction

The Late Miocene lower RD sand is stratigraphically the lowest producing sand in Grand Isle 33 & 43 fields. The RD reservoir ranges in depth from -13,117 to 13,340 ft. The well and production data is extremely limited in this interval with only eight wells penetrating the RD. The RD was only produced from three wells the A-4, A-10, & A-12. The RD sand is not as laterally continuous as the QH and is mapped on a weaker trough reflector (Figure 39).

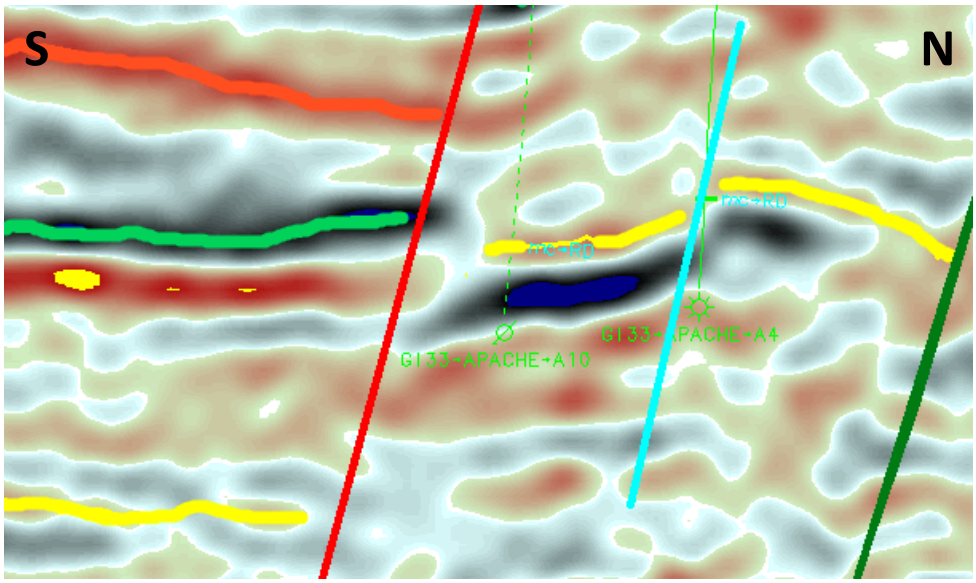

Figure 39: A north-south seismic line showing the weak trough reflector used to map the RD sand, (yellow). Seismic data owned or controlled by Seismic Exchange, Inc.

Depositional Setting

The RD sand is penetrated by five well bores in the study area. Overall thickness varies from one hundred to one hundred of fifty feet. The RD sand was deposited in a marine shelf deposition environment. Paleontological studies of the samples taken from the GI-33 A-1 wellbore indicate *Discorbis 12* shales buried the RD. *Textularia L* sediments underlie the RD. These sediments indicate outer neritic to upper bathyal paleo environments, that formed about nine to nine and a half million years (Paleo-Data 1983). Wireline log signatures in the GI-33 A-10 and the GI-33 W-7 wells demonstrate a outer shelf depositional environment (Figure 40). Figure 41 was used as an analog model. A laminated channel like facies is observed in the wireline logs.

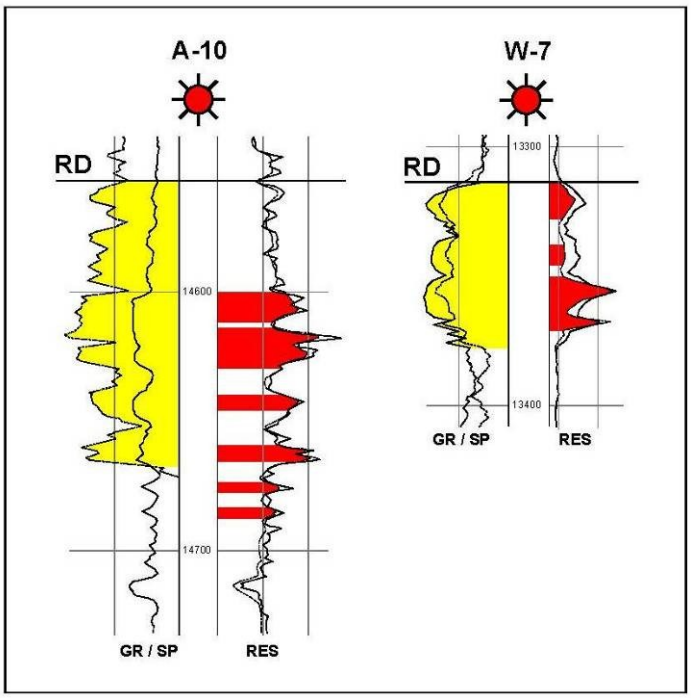

Figure 40: Well log signatures depicting the marine depositional environment for the RD sand. A overall blocky shape can be seen with some thin shale laminations.

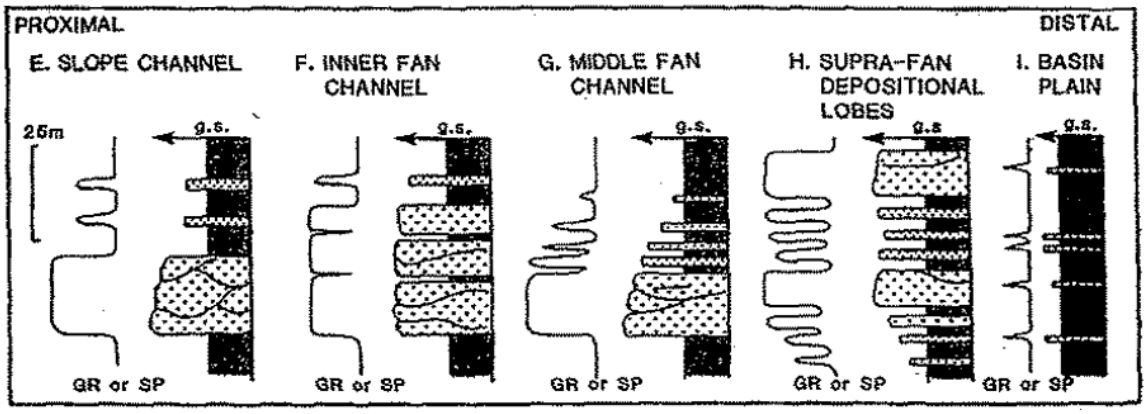

Figure 41: Wireline log signatures and their corresponding depositional environment (Modified from Ahr, 2008).

Figure 41 is an analog for the slope channel depositional process. The RD sands are interpreted to be deposited in an outer shelf to upper slope feeder channel fan system. A gross sand isopach was created to further understand the depositional process of the RD sand. Figure 42 shows two thick intervals that suggest a sediment transport direction from the northwest. Also from the gross sand isopach there is evidence for two separate sand bodies. These sand bodies are wide broad features with sand thickness from fifty to one hundred feet.

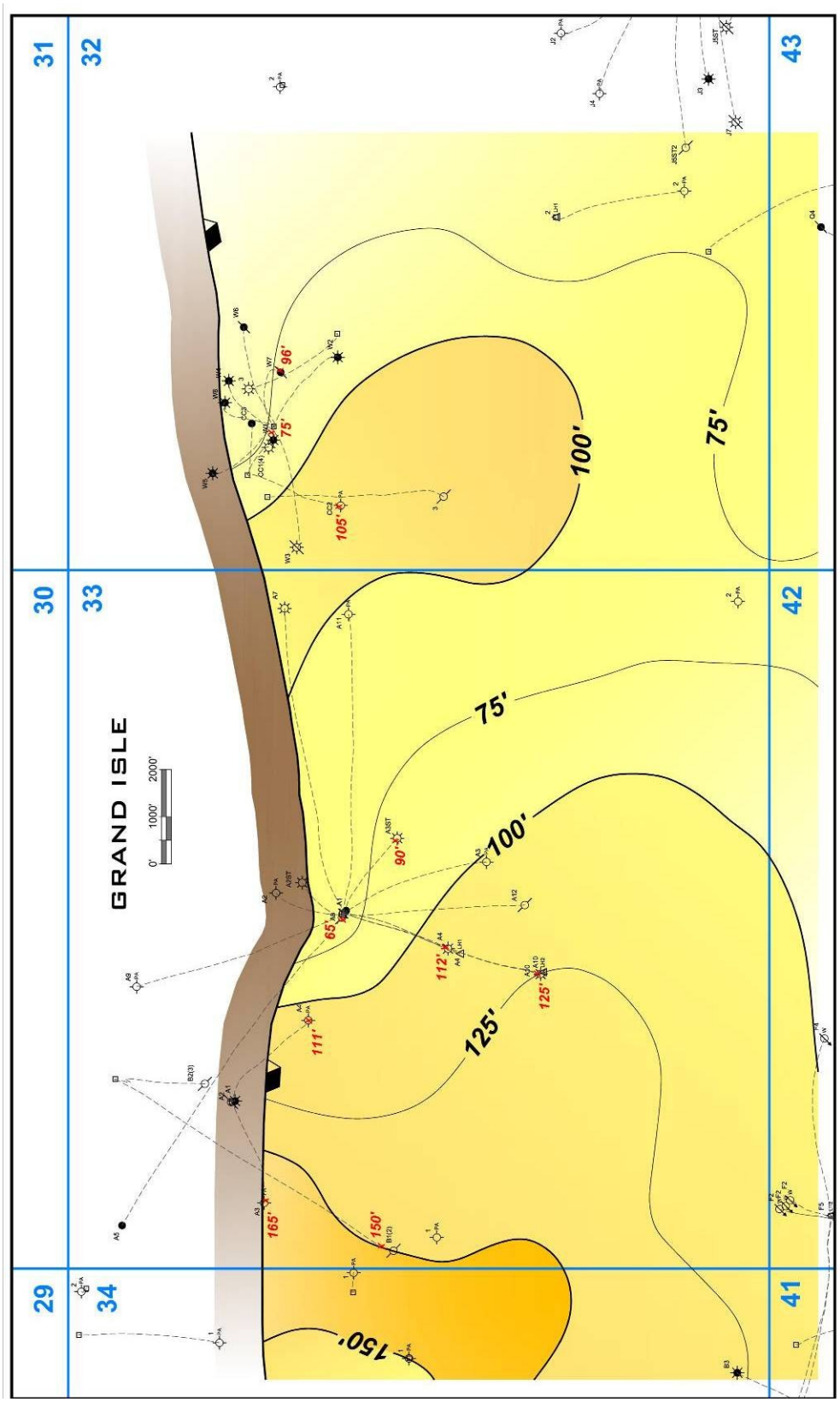

Figure 42: RD gross sand isopach showing the two thick separate sand bodies.

Local Structure

The local structure is controlled by a series of down-to-the-south growth faults, and a few faults that are generally perpendicular to the growth faults. There are two RD reservoirs compartments in the study area, the RD-1, and RD-2 (Figure 43).

The RD-1 compartment is an elongated, east-west trending, three way closure on the down-thrown side of the down-to-the-south fault (fault A). The throw of fault A is around one thousand feet. There are two down-to-the-east faults (faults E & F). The throw of these faults range from sixty to eighty feet. The crest of the structure is observed at a depth of -13,097 ft in the GI-32 W-1 well-bore. The dip is generally five degrees to the south.

Structure in the RD-2 compartment is elongated, north-south trending three-way closure on the down-thrown side of fault A. There are two down-to-the-east faults (faults G & H), with throw ranging from sixty to eighty feet. There is a down-to-the-south compensator fault (fault I), with throw around fifty feet. The crest of this structure is observed at a depth of -13,017 ft in the GI-33 A-8 well-bore. Within this compartment dip is ten degrees to the southwest and southeast depending on the location of the well. The time structure can also be seen from the seismic images (Figures 44, 45, & 46).

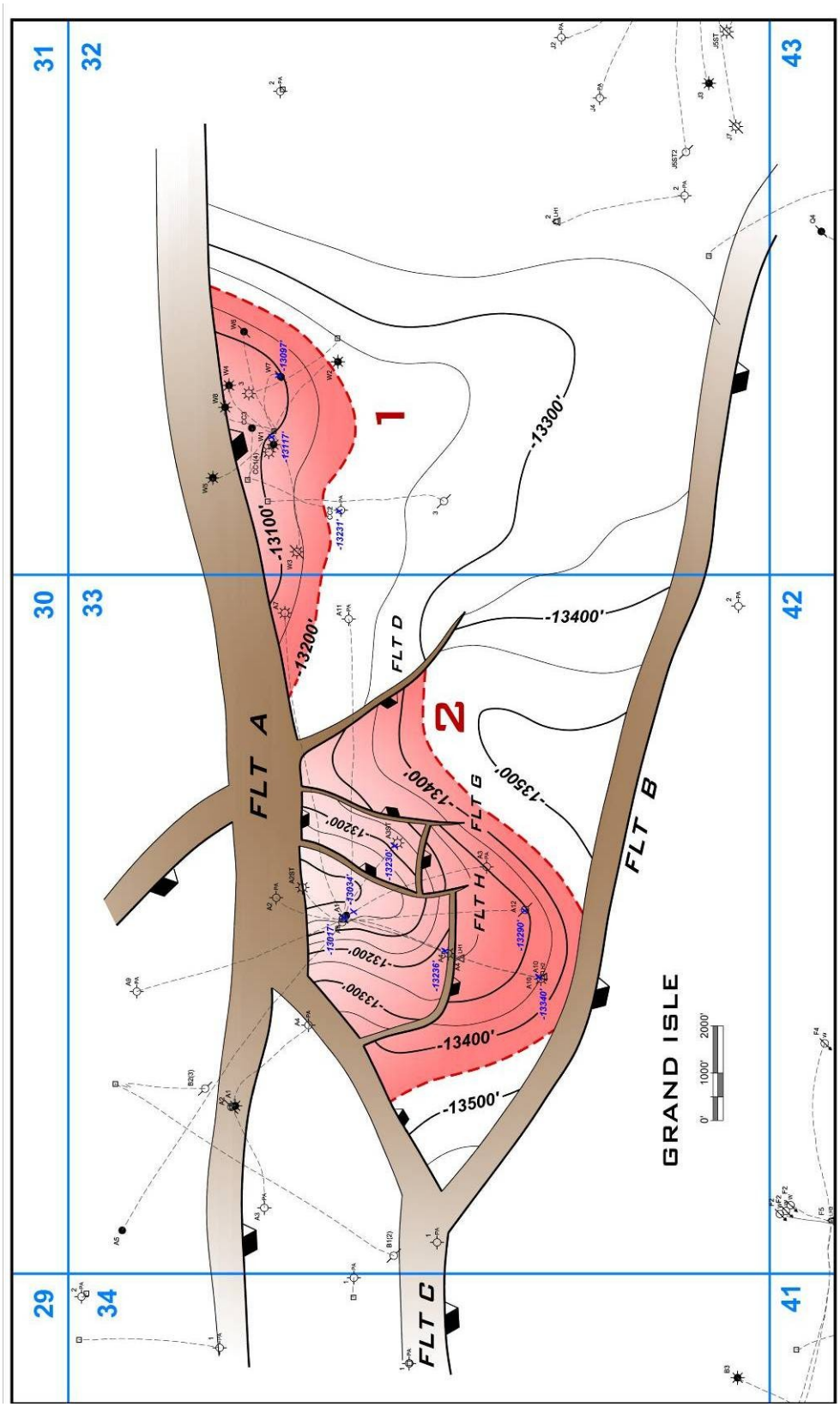

Figure 43: RD local structure map. Compartments 1 and 2 are separated by fault D.

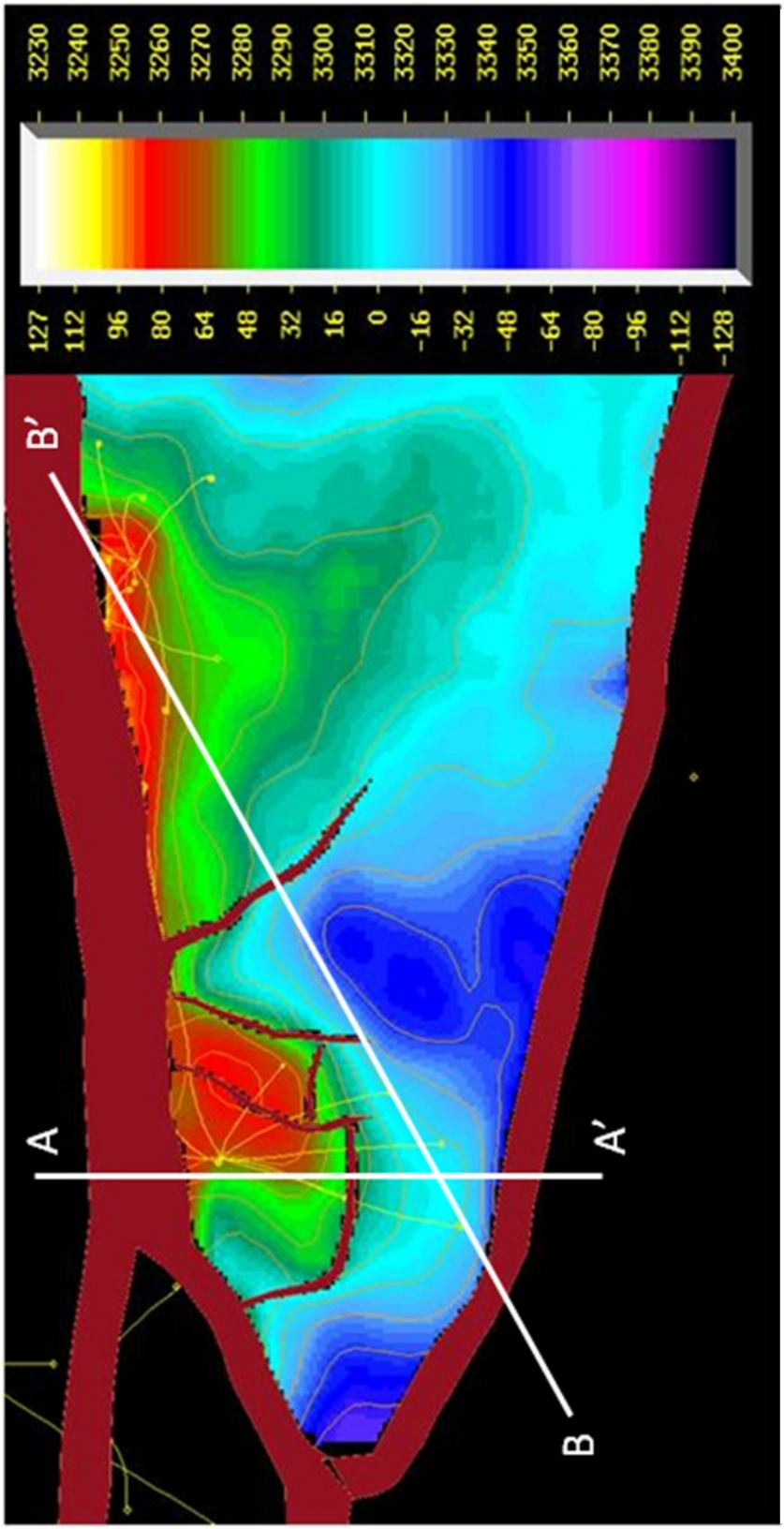

Figure 44: RD seismic structure map. Reds are the structural highs and the blues are the lows.

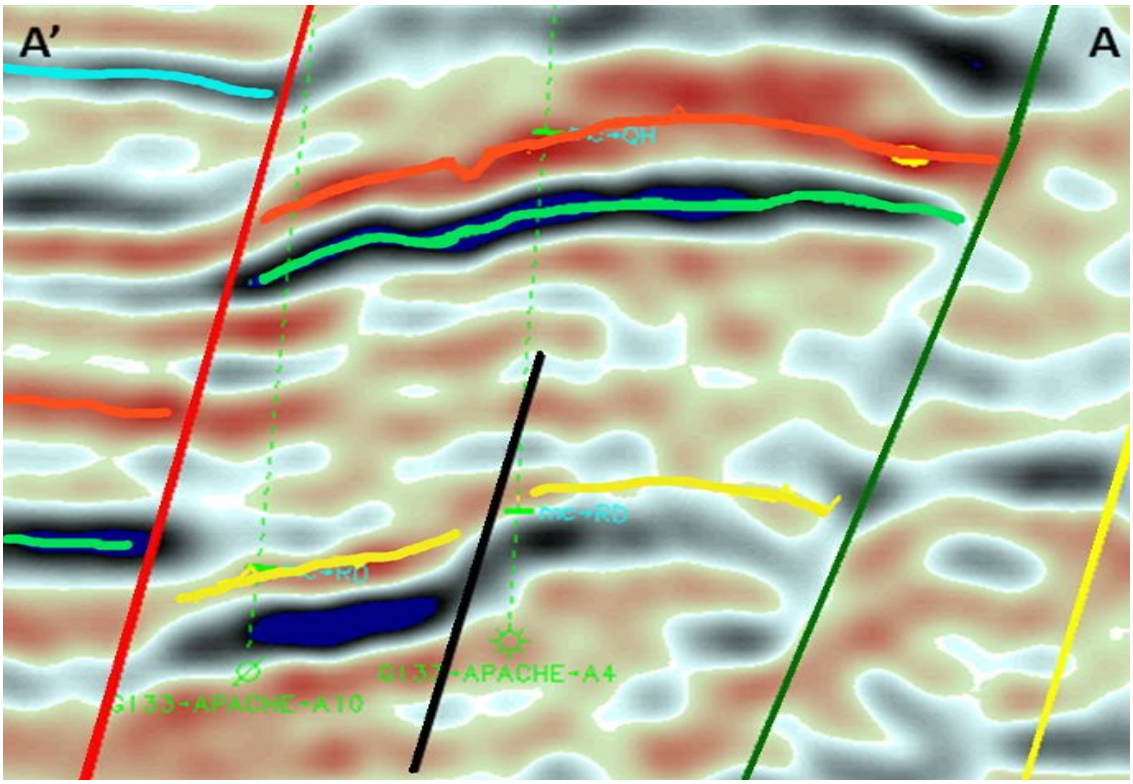

Figure 45: RD cross section from A to A'. The RD horizon is yellow, the reservoir is bound to the north by the green fault. Seismic data owned or controlled by Seismic Exchange, Inc.

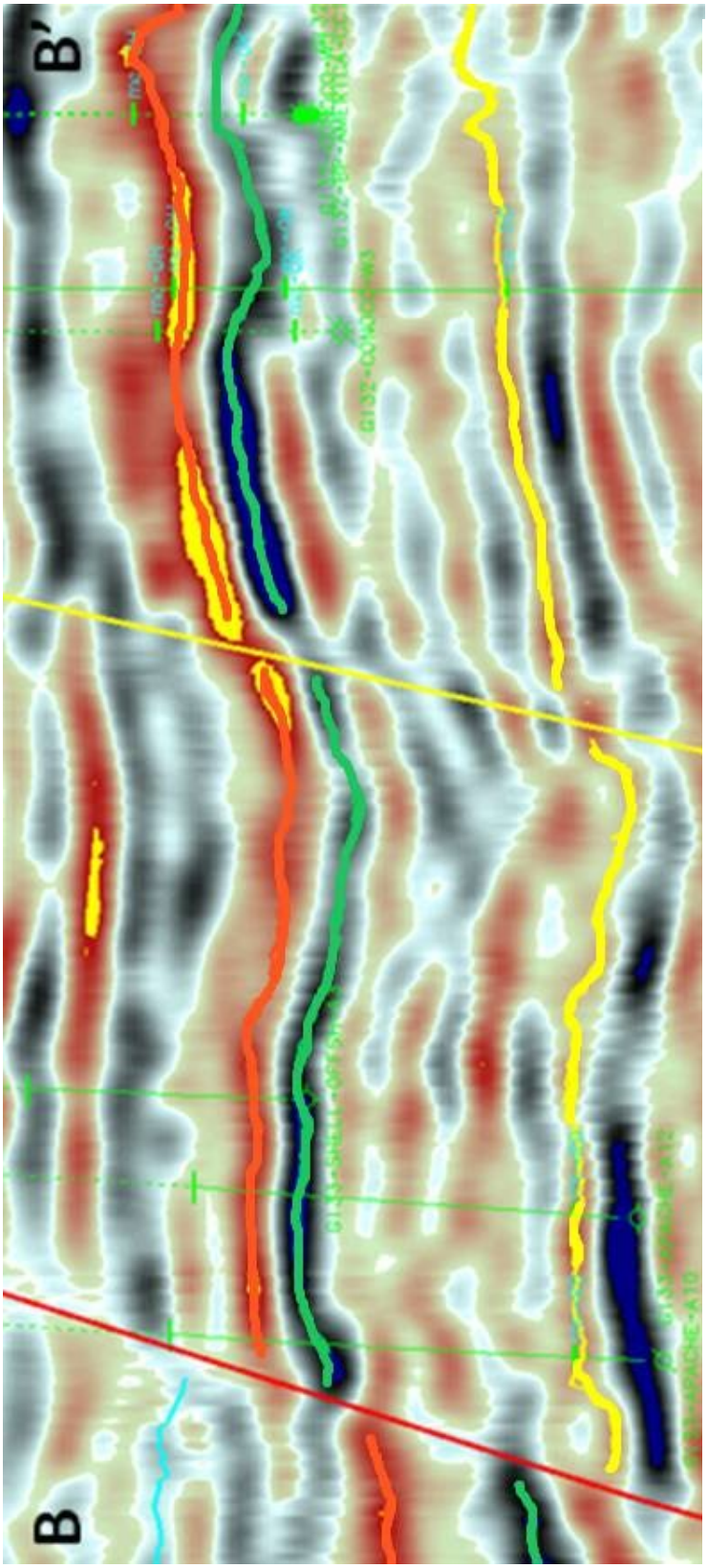

Figure 46: RD seismic cross section from B to B'. The RD horizon is yellow, the yellow fault separates the two reservoir compartments. Seismic data owned or controlled by Seismic Exchange, Inc.

Petrophysical Analysis

Petrophysical analysis was performed in all wells that penetrated the RD sand. Porosity and water saturation were the rock properties measured. Net pay was defined as rocks with porosities greater than 20%, water saturations less than 50% and shale content less than 30%. The average porosity was 23% and the average water saturation was 30% with a hydrocarbon saturation of 70%. There is no available core data on the RD reservoir. Within the RD sand there are sandstone stringers that contain very low porosity zones (15-20%), as observed in the A-10 and W-7 well bore. This tight top is interpreted to be a marine reworking event considering the depth during deposition. Cross over of the neutron and density curves in the well logs indicates the dominant hydrocarbon type is gas.

Production and Drilling Analysis

Production for the RD sand comes from three wells within the Grand Isle 33 field, the A-4, A-10, and A-12. Cumulative production from these wells is approximately 40.5 BCFG, 2049 MBO, and 570 MBW (OWL 2010). The GOR for this reservoir is about 20,000 cf/bbl. The high GOR indicates a strong gas reservoir. Individual RD production is presented in Table 4.

Table 4: Cumulative production for RD wells.

Wells: (Completion Period)		Gas Production	Oil Production	Water Production
A-4	87-02	19.4 BCF	868 MBO	106 MBW
A-10	87-00	21 BCF	1151 MBO	98 MBW
A-12	99-07	.34 BCF	28 MBO	363 MBW
Cumulative Prodution		**40.74 BCF**	**2047 MBO**	**567 MBW**

From the seismic data the A-4 well appears to be in a different fault block than the A-10 and A-12 wells. The bottom hole pressure surveys indicates that the RD reservoir is not affected by the faulting between the producing wells. Pressure from the A-4 and A-10 wells reads almost identical from 1992-1994 (Figure 45). In 2001 and 2002 the test from the A-12 and A-4 wells are somewhat different, this difference could be from the location on the structure that the well bores are produced. The A-4 well is structurally about 75 ft higher than the A-12 which could influence the slightly higher pressure reading. The RD reservoir is interpreted to be a pressure depletion reservoir as indicated by the constant decline in reservoir pressure throughout production. Assumed recovery factors used for the volumetric calculations were 65% (J. Harris, 2010, personal communication).

A drilling report for the A-12 well in the RD-2 compartment showed that upon drilling into the RD reservoir there was a series of drilling mud losses. Mud returns were never reestablished until a casing liner was set. Approximately 5,000 bbl of drilling fluid were lost into the reservoir. This data suggest that the RD reservoir was under-pressured at the time of drilling and the reserves that were being drilled for might have already been depleted by other wells.

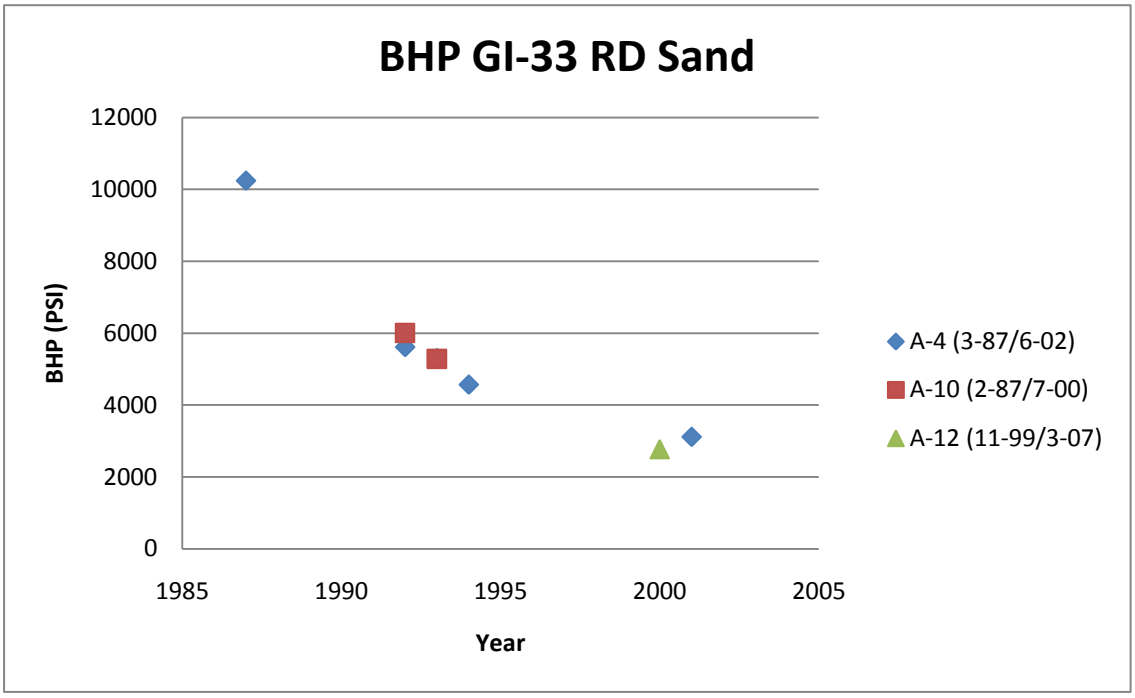

Figure 47: Bottom hole pressure surveys readings from the A-4, A-10, and A-12 wells. From these constant declining pressure readings it is interpreted that the RD reservoir in this compartment is connected.

Subsurface Maps

A series of subsurface structure, sand isopach, and net pay isopach maps were created to produce a detailed reservoir model. The first subsurface map created was the depth structure map with the corresponding gas-water contacts (Figure 48). The RD sand is mapped as one connected lobe because of the matching gas-water contacts. Comparing the time structure (Figure 44) to the depth structure they are very similar. The next subsurface map created was the net sand isopach. The net sand isopach used the 20% porosity cutoff that was one of the parameters that defines pay. The net sand isopach shows a thickening of the sand as you move away from the large down-to-the-south growth fault. The last subsurface map generated was the net pay isopach, this is created from both the depth structure map and net sand isopach. The net pay isopach represents the reservoir's thickness and aerial distribution (reservoir volume). The RD-1 reservoir compartment has an area of 300 ac and an average thickness of 14 ft, the reservoir volume is 4,051 ac-ft. The RD-2 compartment has an area of 773 ac and an average height of 24 ft, the reservoir volume is 18,539 ac-ft. The reservoir volumes are used in the volumetric calculations.

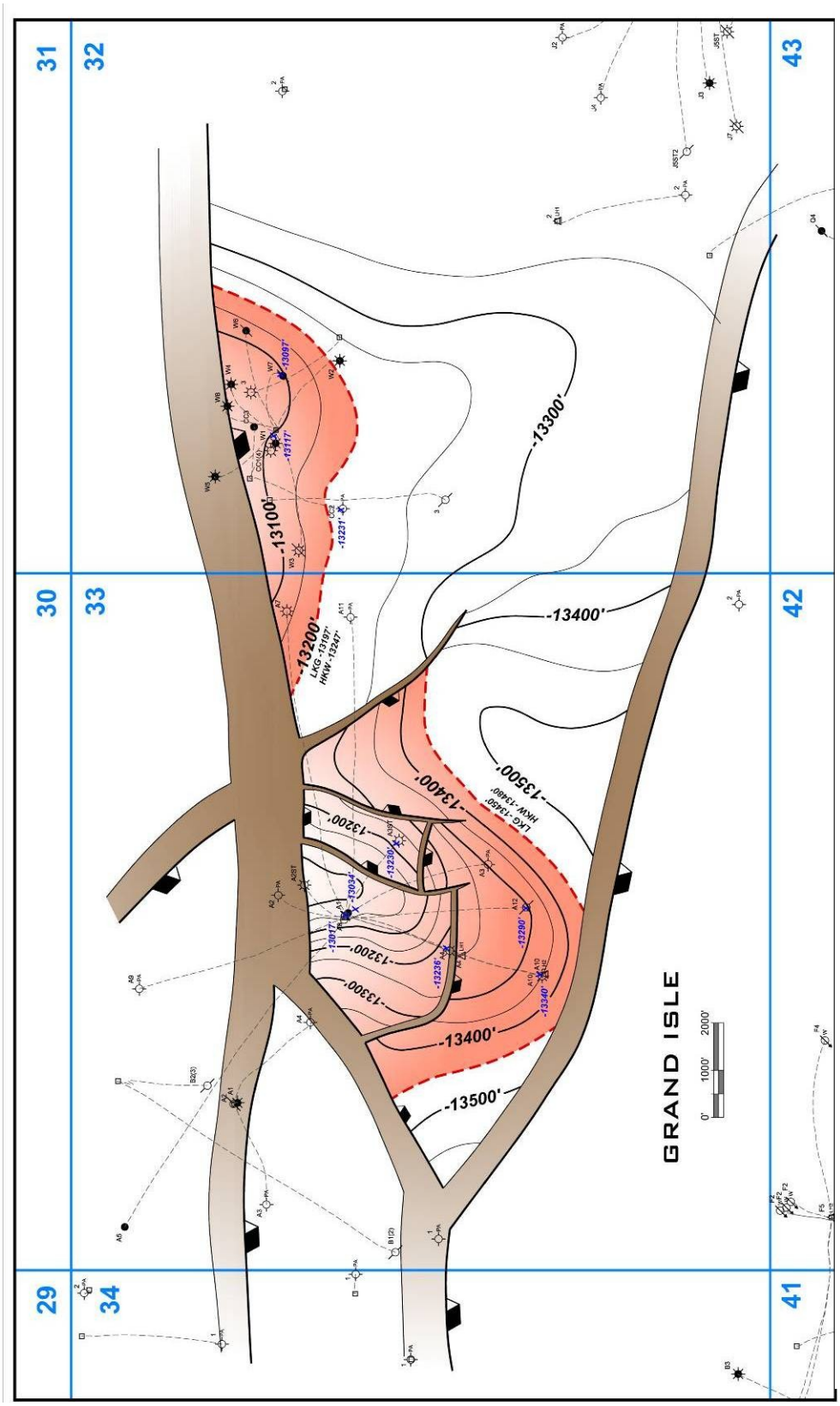

Figure 48: RD structure map with the gas contacts posted by the dashed red line.

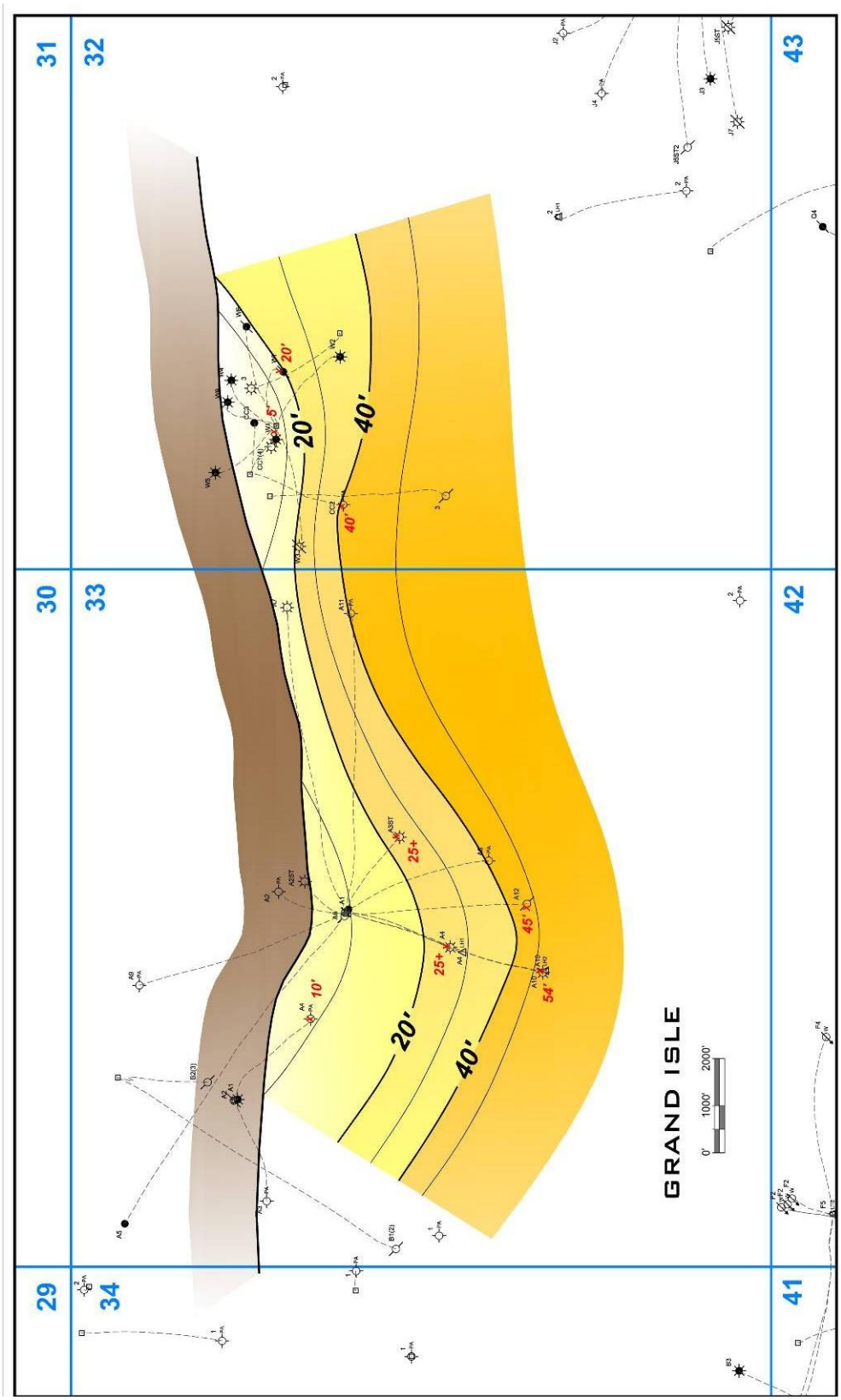

Figure 49: RD net sand isopach. The sand thickens away from the fault.

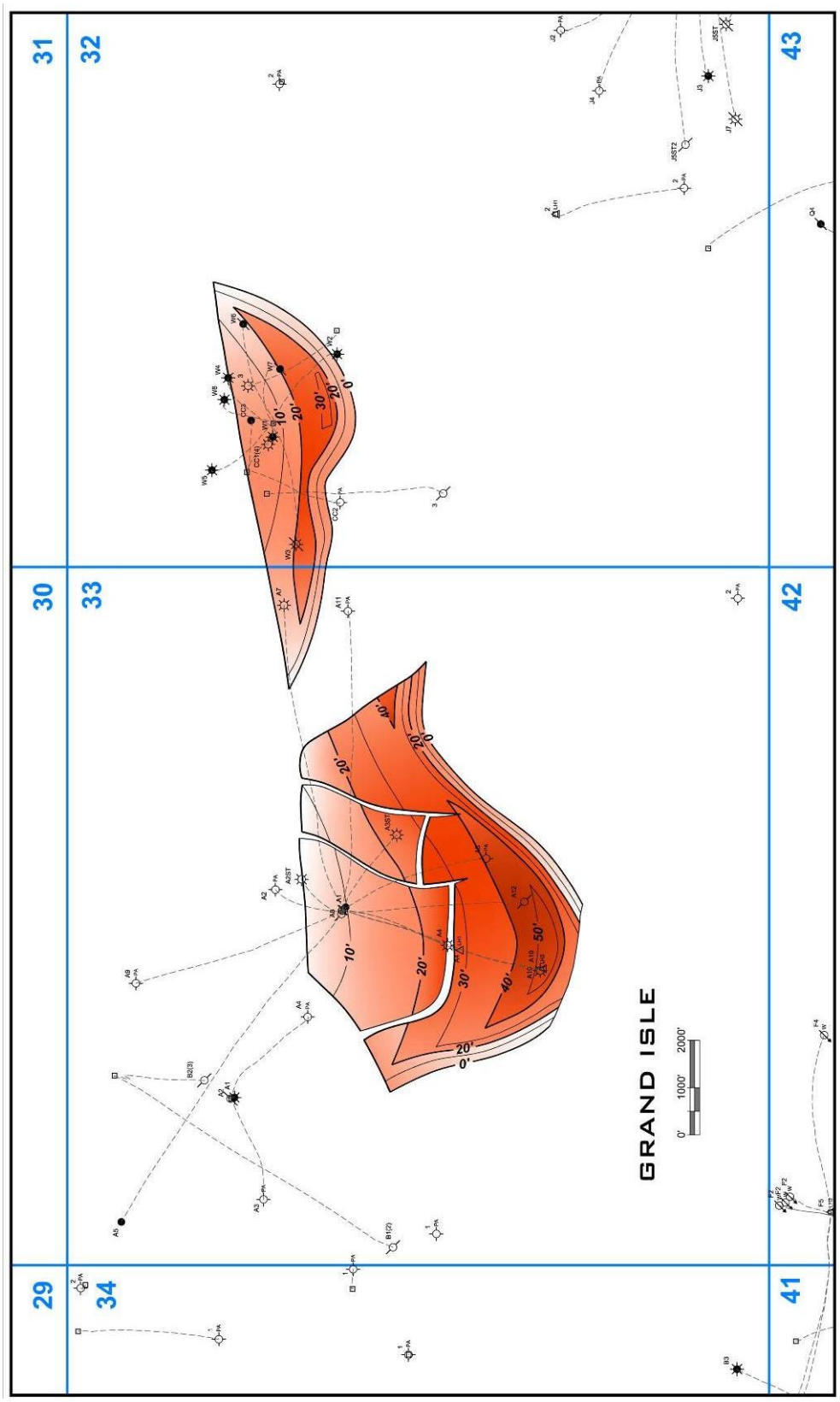

Figure 50: RD net pay isopach used for volumetrics.

Seismic Amplitude Extractions

Amplitude was the dominant seismic attribute used to try to further delineate the RD reservoir. The amplitude map was extracted from an auto tracked and smoothed, seismic time horizon corresponding to the RD reflection. The amplitude map was then interpreted to see if it could be used as a DHI.

The amplitude response from the RD sand does not seem to be a hydrocarbon indicator (Figure 51). The amplitude at the RD level fills virtually the entire fault block without regard to structural position, with amplitude that extends well past the down dip limit of the previous defined reservoir (Figure 48).

Amplitude response at the RD level is interpreted to be a lithologic indicator. The RD sand is within the over-pressured zone. The presence of over-pressure could also have an negative impact on the overall amplitude response (O'Brien 2004). There is only slight lithologic variation among the wells drilled into the greatest amplitude. The amplitude at the RD is not interpreted to be an indicator of sand thickness.

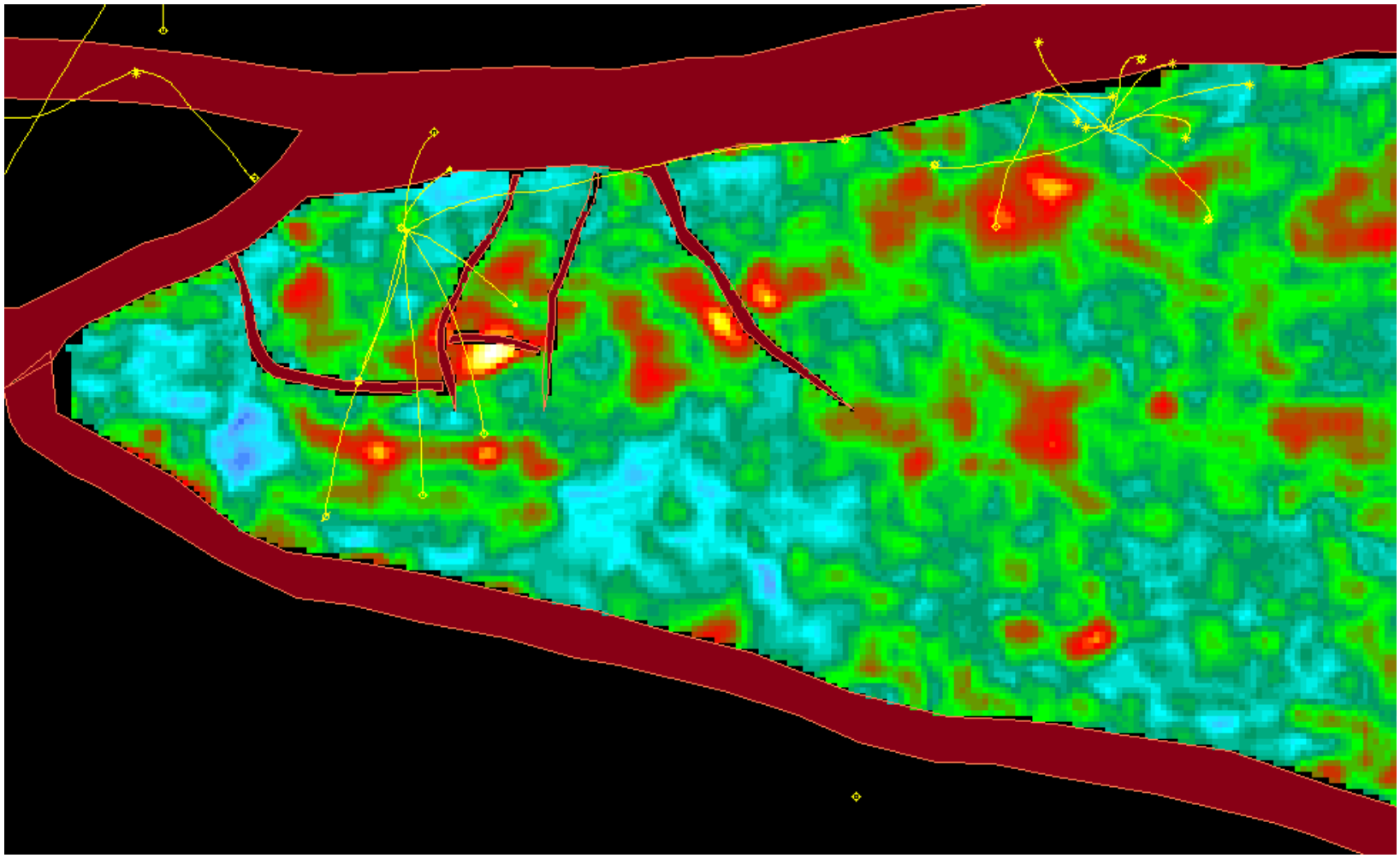

Figure 51: Maximum negative amplitude extraction taken from the RD horizon. The amplitude response at this level fills virtually the entire fault block without regard to structural position extending well past the downdip limit of the reservoir. The amplitude response at this level is interpreted to be a lithologic indicator, indicating the presence of sand.

Volumetrics

Volumetric calculations were performed to further evaluate the RD reservoir for further exploitation. The volumetric calculations were based on the previously defined reservoir parameters. Original recoverable reserves were calculated for comparison with the total produced reserves to see if there is any remaining potential (Table 5). The RD has produced just over 40 BCF from three wells in the RD-2 compartment. The calculated original recoverable reserves is 38.4 BCF. With the produced reserves almost equaling the original calculated reserves the RD-2 is interpreted to be completely depleted. However there was no production in the W-7 well, which encountered 40 ft of pay in the RD-1 compartment. Since this interval was never produced, reserves are stilling remaining. Estimated recoverable reserves for this compartment are 6.7 BCF (Figure 52).

Table 5: Calculated original recoverable reserves, produced reserves, and remaining recoverable reserves.

Reservoir Compartment	Original Calculated Recoverable Reserves	Produced Reserves	Remaining Recoverable Reserves
RD-1	6.7 BCF	0	6.7 BCF
RD-2	38.4 BCF	40 BCF	0

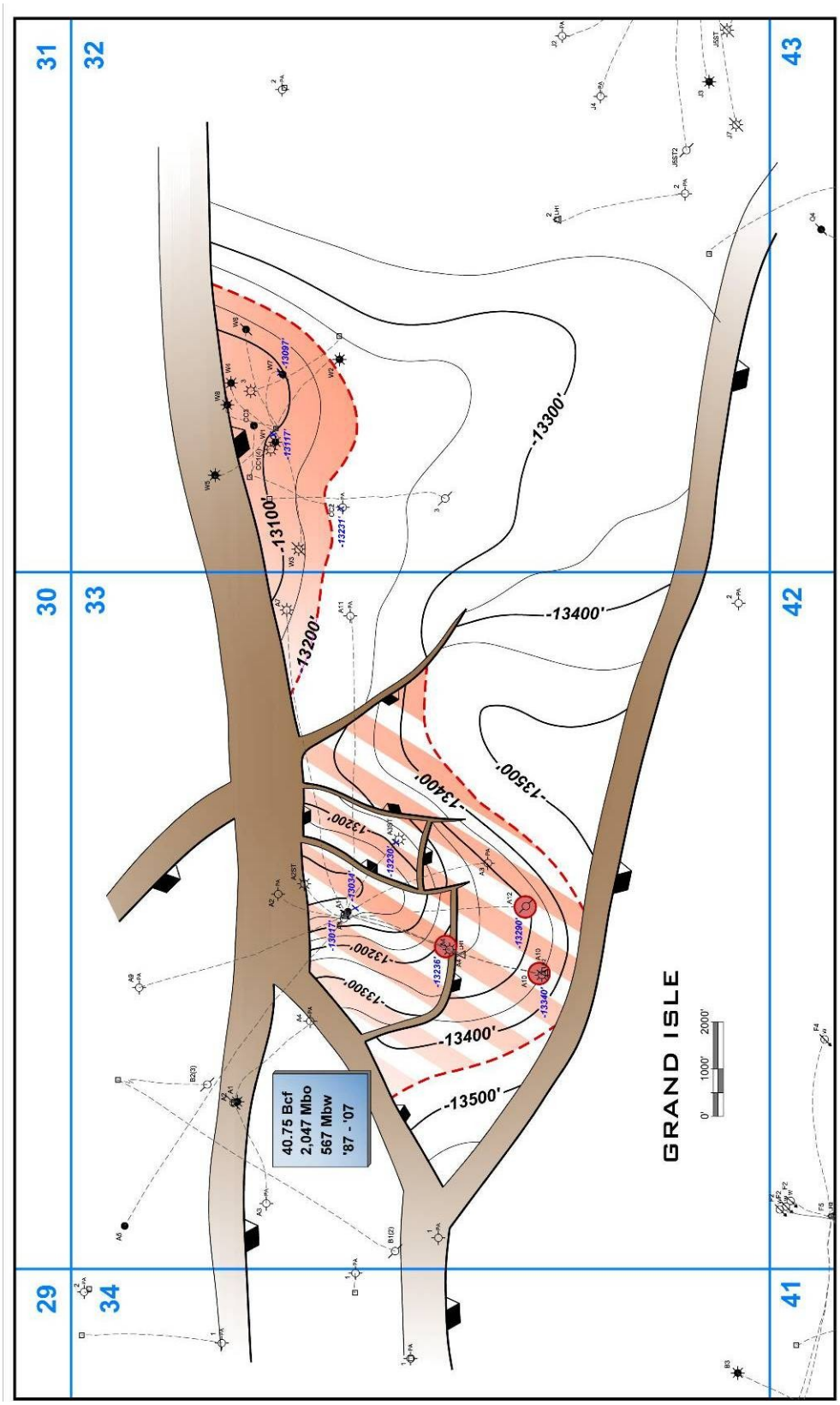

Figure 52: RD pay structure map showing the remaining reserves in the RD-1 compartment.

Conclusion

A detailed reservoir model was generated on the RD sand from the integration of geology, geophysics, and engineering data. This enhanced and detailed model revealed some key finding about the RD reservoir. Pressure data reveal that the wells in the RD-2 compartment are all in communication with each other despite minor faulting within and between the compartment. This model indicates that when the A-12 well was drilled and completed in the RD sand in 1999 that the original recoverable reserves might have already been produced. The RD sand would have been depleted when the A-12 well was drilled. This integrated modeled suggest that the A-12 well might should have never been drilled. Most importantly the RD has remaining potential in the RD-1 compartment. It was calculated that there is approximately 6.7 BCF of recoverable reserves remaining. Given the substantial amount of reserves remaining the RD sand has some significant economic potential in this field.

CHAPTER VI

LATE MIOCENE UPPER (PM) SAND CHARACTERIZATION

Introduction

The PM sand is stratigraphically the highest producing unit within the studied interval. The PM reservoir ranges in depth from -11,494 to -11,979 ft. The PM sand was produced from all three reservoir compartments PM-1, PM-2, and PM-3 The PM sand was only produced from 4 wells. The PM sand is highly discontinuous and has large variation in stratigraphic thickness. The seismic reflector used to map the PM is a trough (Figure 53).

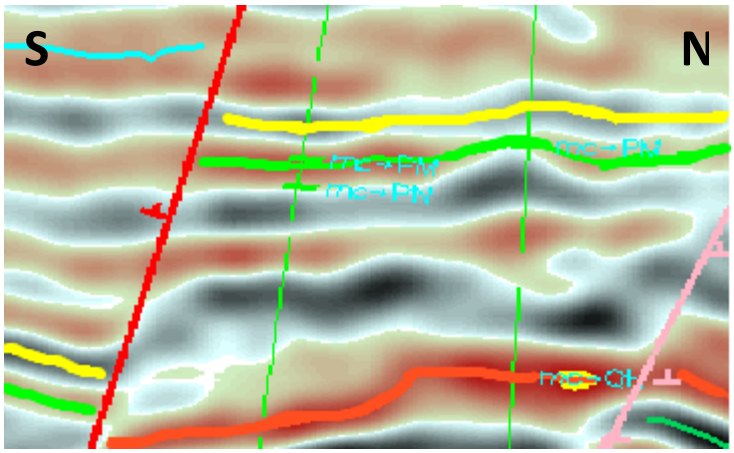

Figure 53: A north-south trending seismic line showing the seismic reflector used to map the PM sand, shown in lime green. Seismic data owned or controlled by Seismic Exchange, Inc.

Depositional Setting

The PM Sand is penetrated by 25wells in the study area. Overall sand thickness varies from completely shaled out to almost one hundred feet thick. Paleontological studies of samples from the GI-33 A-1 well indicate *Cyclammina 3* shales buried the PM. These sediments indicate inner to middle neritic paleo-environments about eight million years old (Paleo-Data 1983). Using Walkers delta front subenvironments as an analog, the PM sand is interpreted to be deposited in a distributary mouth bar system. The wireline log signatures seen in cross section demonstrate the highly variable log character of the PM sand (Figure 54). The wireline log signatures combined with the paleo data are interpreted that the PM sand was deposited in a distributary mouth bar system (Figure 15 Walker). Sand was deposited in a deltaic marine environment. A PM sand isopach shows clearly the highly stratigraphic nature of the sand (Figure 55). There are four interpreted shale outs that trend north-south. These shale out are interpreted to be a series of shale filled channels. The shale outs are extremely important when trying to determine the reservoirs connectivity, as they do provide a barrier between the sands.

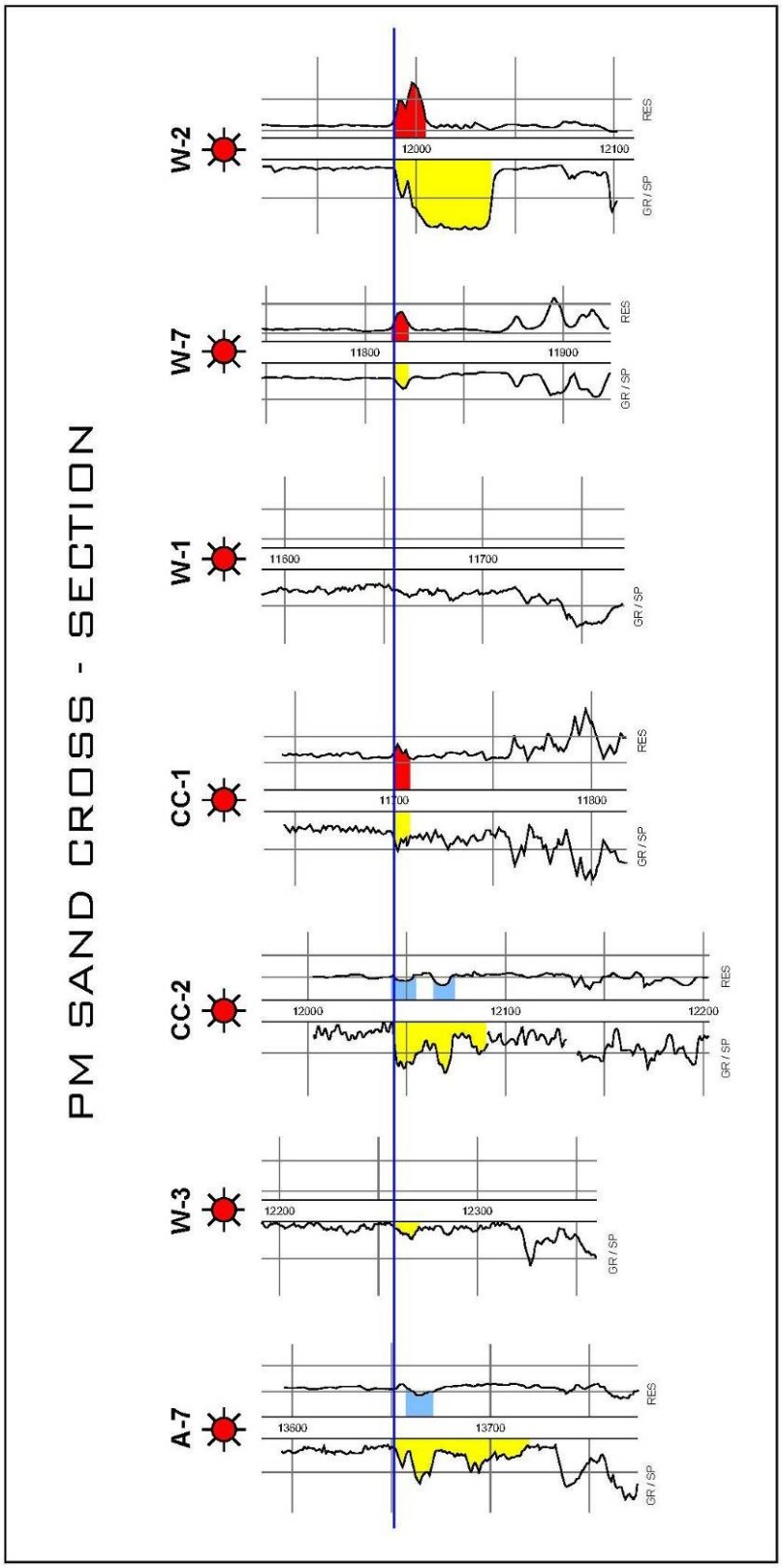

Figure 54: PM well log cross section depicting the variable log characters seen throughout the PM sand.

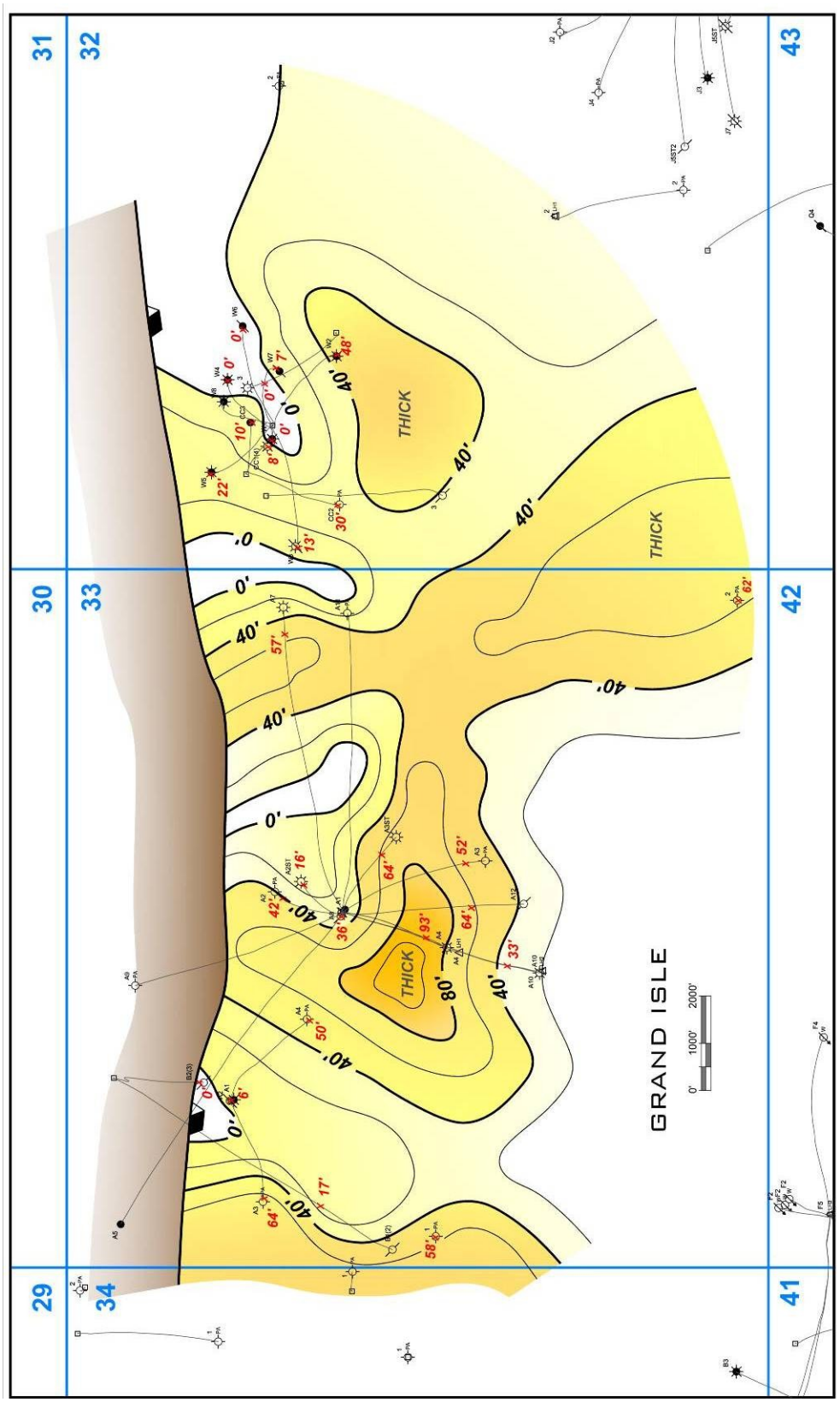

Figure 55 PM sand isopach showing the thick sand intervals in dark yellow and the thins in lighter colors.

Local Structure

The local structure is controlled by a series of down-to-the-south growth faults (faults A, B, & C), and a few faults, which are generally perpendicular to the regional growth faults. There are three productive PM reservoir compartments in the study area, reservoirs PM-1, PM-2, and PM-3 (Figure 56).

The PM-1 compartment, the largest of the three compartments, is an east-west trending, three-way closure on the down-thrown side of fault A. The throw of fault A is between seven hundred and eight hundred feet. There are two down-to-the-east faults (faults E & F). Throw on these faults die out as they propagate southward, the maximum throw observed is about seventy five feet. The crest of this structure is observed at a depth of -11,550 ft in the GI-32 CC-3 well. The dip is very flat at about one and a half degrees to the south.

The PM-2 compartment is a north-south trending, irregular anticlinal dome, between faults A and B. There are two faults that are down-to-the-east and have throw of about fifty to seventy five feet. These faults die out to the north, off the domal structure. The crest of this structure is at -11,766' in the GI-33 A-12 well. This structure dips in all direction and varies from three to seven degrees.

The PM-3 compartment is an east-west trending, three-way closure, on the up-thrown side of fault C. Throw of the fault varies from about two hundred and fifty to six hundred feet. The crest of this structure is observed at -11,494' in the GI-33 B-1 well. The dip is northwestern at about seven degrees.

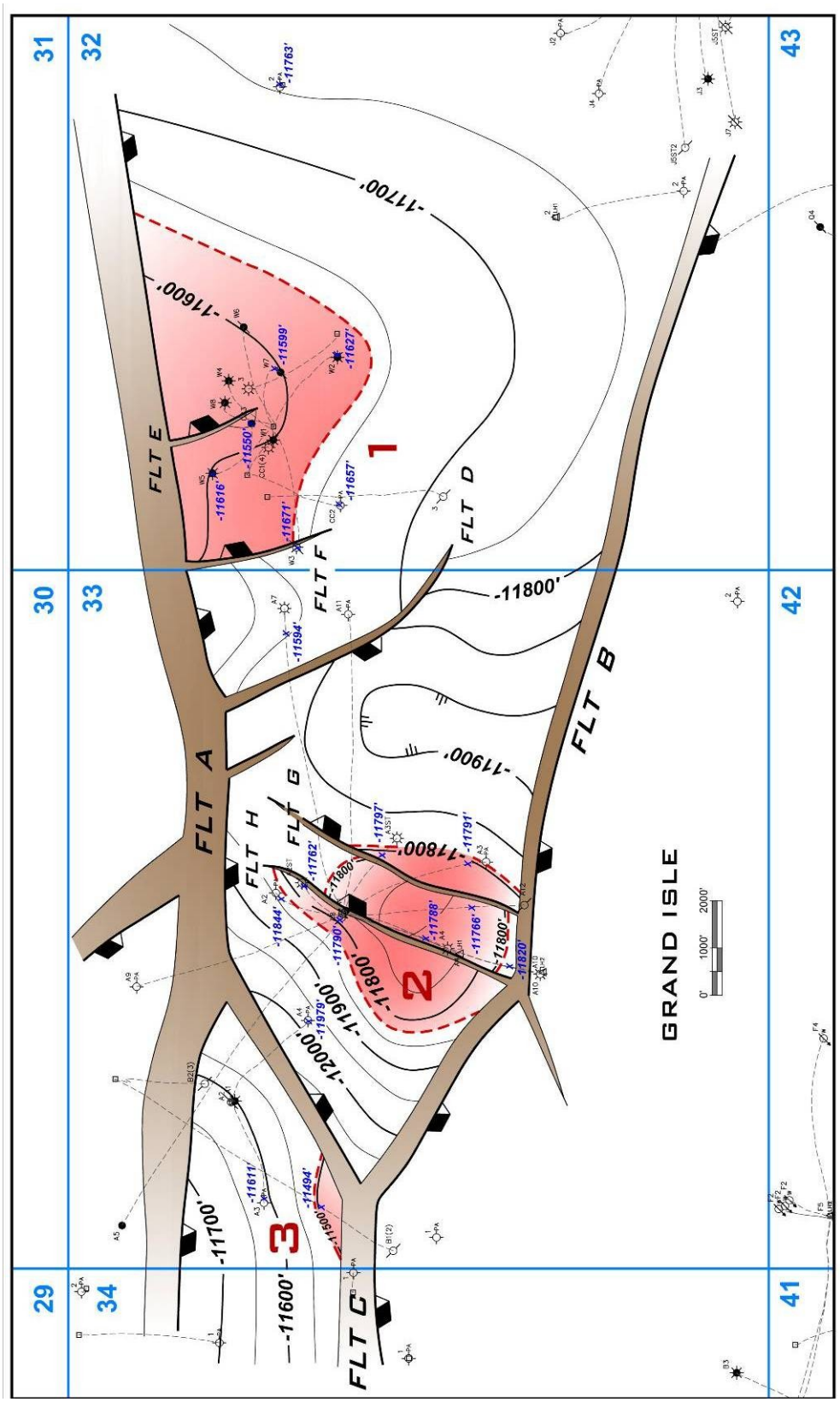

Figure 56: PM local structure showing the three different reservoir compartments.

Petrophysical Analysis

Petrophysical analysis was performed in all of the wells that penetrated the PM sand. Porosity and water saturation were the petrophysical values calculated. Net pay was calculated from the previously determined pay cutoffs, porosities greater than 20%, water saturations less than 40%, and shale content less than 30%. The porosity and saturation values were used in the volumetric calculations. The average porosity was 25% and the average water saturation was 15%. The PM sand does not contain any diagenetic alteration in it's well penetrations.

Production Analysis

The PM sand is only produced from 4 of the 25 well-bores that penetrate it in the study area. Cumulative production from the PM is approximately 6 BCFG, 281 MBO, and 441 MBW from the three PM reservoir compartments (OWL 2010). The average GOR for the PM-2 is 21,500 cf/bbl which indicates a strong gas reservoir. GOR were not calculated for the PM-1 and 3 because of the lack of production. Production for the PM can be seen by individual wells or by reservoirs (Table 6). The W-7 well encountered 10 ft of pay but was never completed in the PM sand. This is important because there might be remaining potential left in this reservoir. The PM sand was tested and flowed at a rate of about 1,700 MMCFG, 36 BO, and 30 BW a day, these rates are commercially producible rates.

Table 6: Cumulative and individual well production for the PM sand.

PM Reservoir Compartments		Gas Production	Oil Production	Water Production
PM-1	74	20,000 MCF	0	0
PM-2	92-09	5.85 BCF	280 MBO	438 MBW
PM-3	01-02	60,000 MCF	950 BO	2900 BW
PM Total		6 BCF	281 MBO	441 MBW
Wells: (Completion Period)				
W-5	74	20,000 MCF	0	0
A-2ST	92-02	.65 BCF	50 MBO	27 MBW
A-12	99-09	5.2 BCF	230 MBO	411 MBW
B-1	01-02	60,000 MCF	950 BO	2900 BW

Subsurface Maps

A series of subsurface structure, sand isopach, and net pay isopach maps were generated (Figures 57, 58, & 59). The PM structure map indicates the shale out in the PM-1 compartment separates the reservoir in two sub-compartments. There is a shale out on the western edge of the PM-1 compartment which isolates the A-7 well, that does not contain pay. The PM sand isopach used the porosity cutoff of 20% (Figure 58). From the sand isopach you can see there are four interpreted shale outs, these shale outs are interpreted to be levee complexes on the sides of the channels.

Finally net pay isopach maps were constructed for the PM compartments (Figure 59). The PM-1 compartment was divided into a southeastern and northwestern separated by the shale out. The southeastern compartment has an area of 123 ac and an average thickness of 7 ft, the reservoir volume is 855 ac-ft. The northeastern compartment has an area of 165 ac and an average thickness of 8 ft, the reservoir volume is 1,315 ac-ft. The PM-2 compartment has an area of 278 ac with an average thickness of 14.2 ft, the reservoir volume is 3,883 ac-ft. The PM-3 has an area of 18 ac with an average thickness of 13.3 ft, the reservoir volume is 238 ac-ft. These reservoir volumes are used in the volumetric calculations.

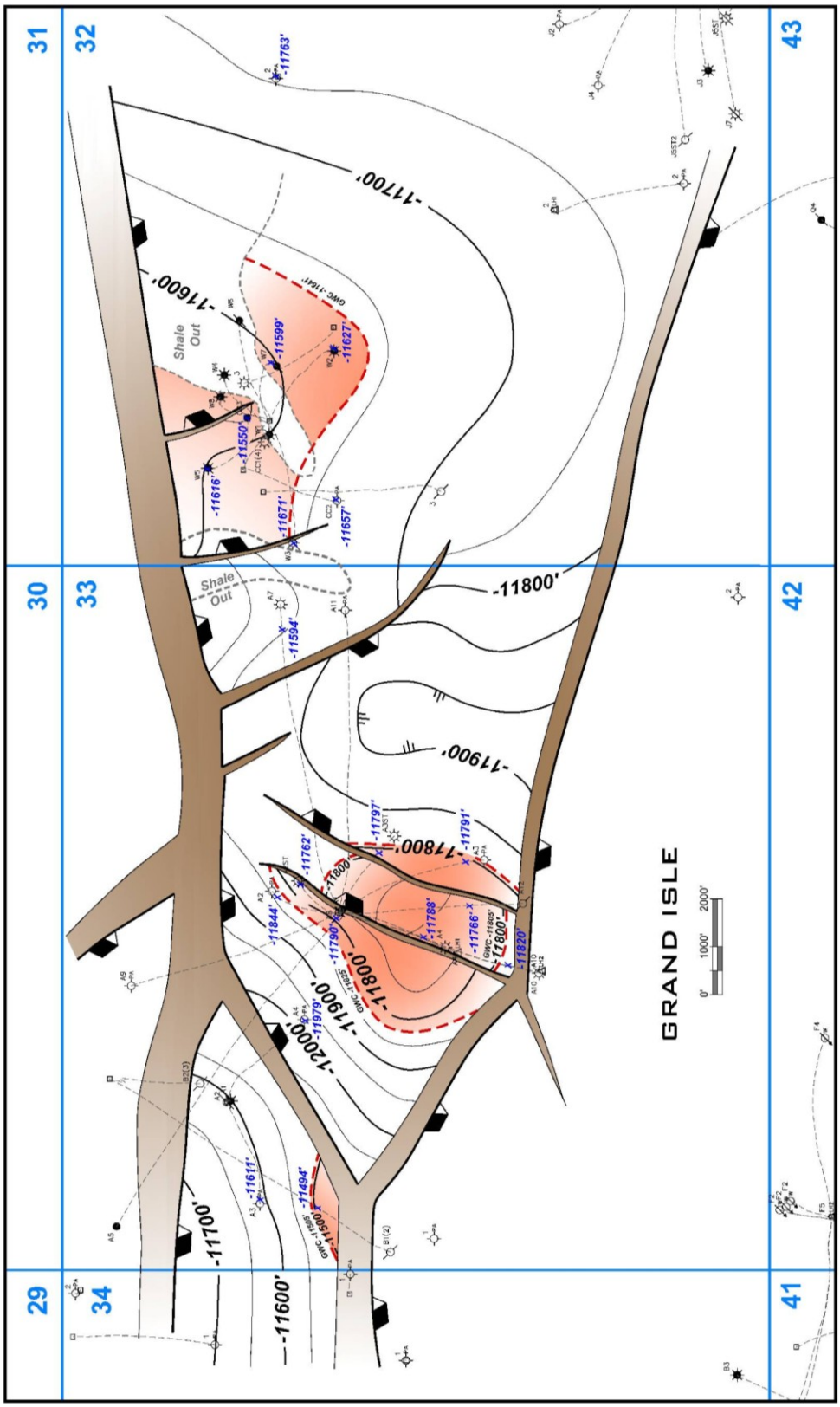

Figure 57: PM structure map with gas contacts posted as the dashed red lines.

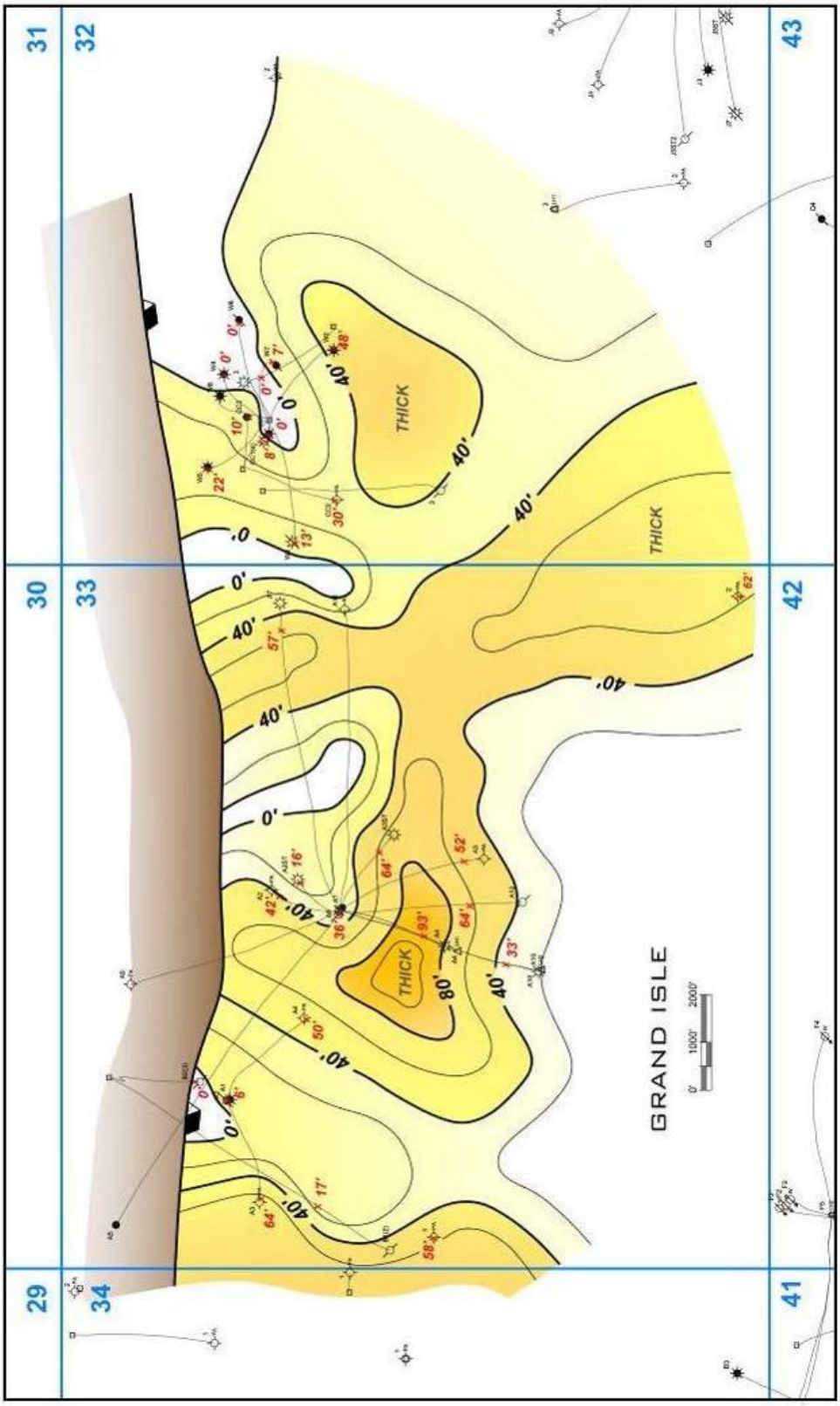

Figure 58: PM sand isopach showing the thick and thins.

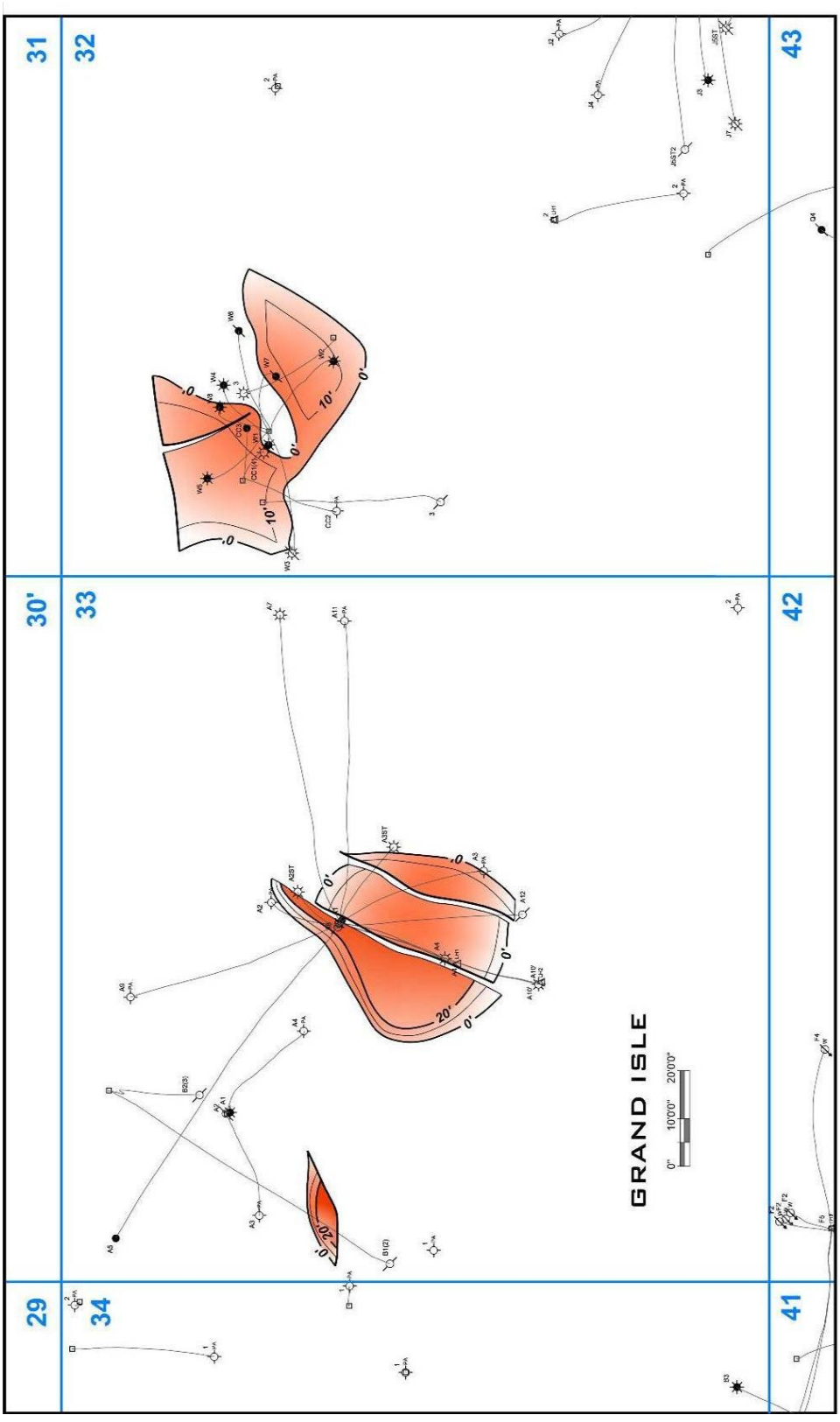

Figure 59: PM net pay isopach used for volumetrics.

Seismic Amplitude Extractions

Amplitude was the dominant seismic attribute used to try and further delineate the PM reservoir. Amplitudes were extracted from an auto tracked and smoothed seismic time horizon corresponding to the PM reflection. A maximum negative amplitude extraction was taken from the PM horizon.

The amplitude response from the PM sand does not seem to be a hydrocarbon indicator (Figure 60). The amplitude at the PM level fills most of the fault block without regard to structural position. Also, the amplitude response extends well past the down dip limit of the reservoir previously defined in Figure 57. The PM sand is in close proximity to two other sand packages the above PK and underlying PN. Both of these sand packages are within 50-75 ft of the PM sand. The amplitude at the PM level can be from interference from the sands on either side of this unit. A simple synthetic model was created to show the relationship of the three sands and the effect they have on the synthetic seismogram (Figure 61). The synthetic model was set up to resemble the PK, PM, and PN sands how they occur throughout the field. The PM sand is shown as an average thickness of 50 ft and the PN is right below it and it is a hundred ft thick sand filled with pay.

As seen in the figure 61 the three sands are displayed as one very weak trough although the impedance and reflection coefficient are all clearly visible the frequency of the data does not allow this to be resolvable. With a dominant frequency of 30 PK, PM, and PN sands can be resolved from each other (Figure 62).

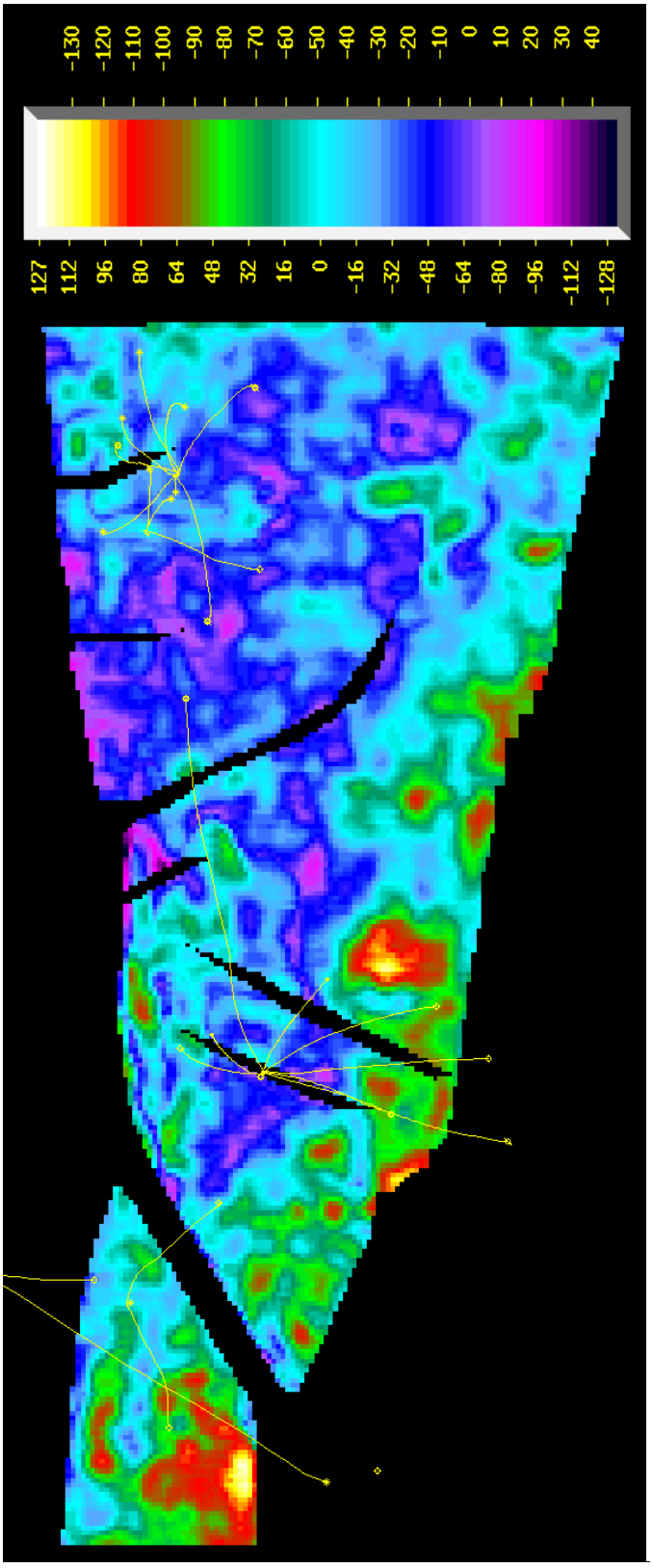

Figure 60: Maximum negative amplitude extraction taken from the PM time horizon. The amplitude at this response has no regard for structural position and extends outside the limits of the reservoir. This amplitude response in not interpreted to be a hydrocarbon indicator.

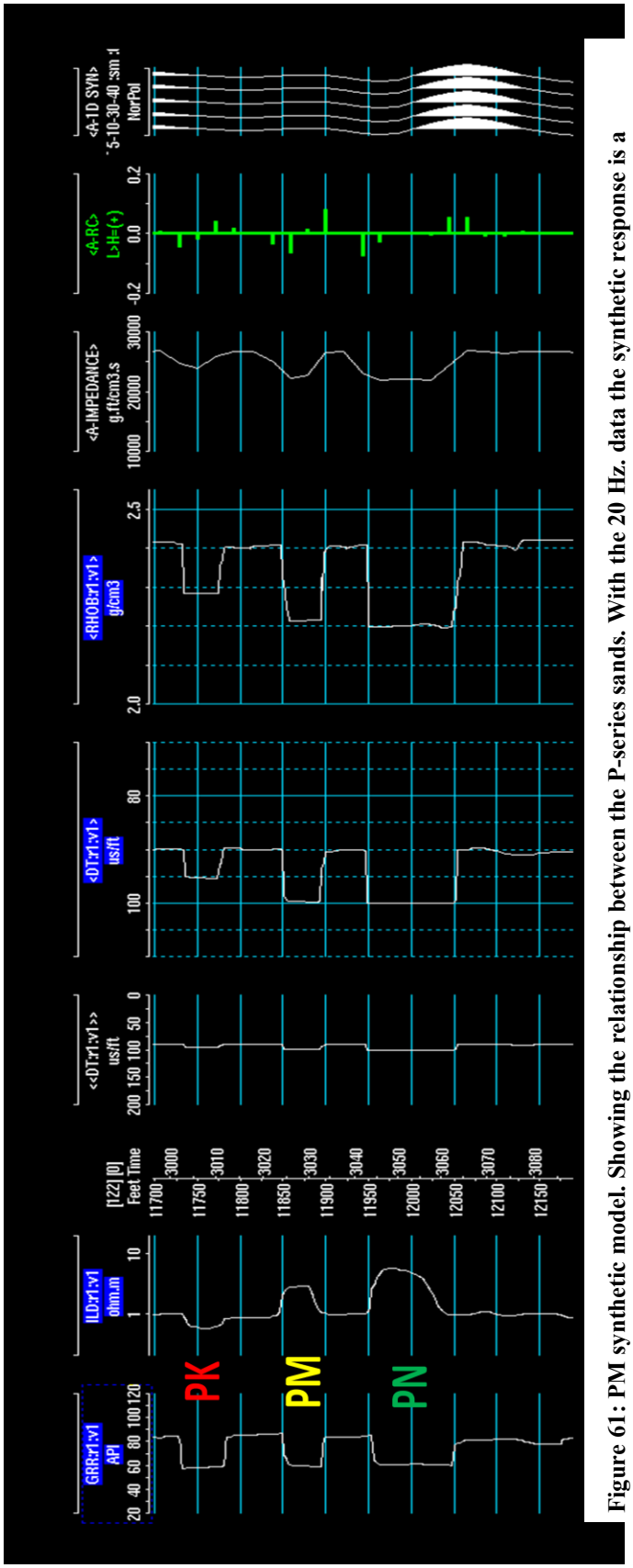

Figure 61: PM synthetic model. Showing the relationship between the P-series sands. With the 20 Hz. data the synthetic response is a washed out trough with no delineation between the sands.

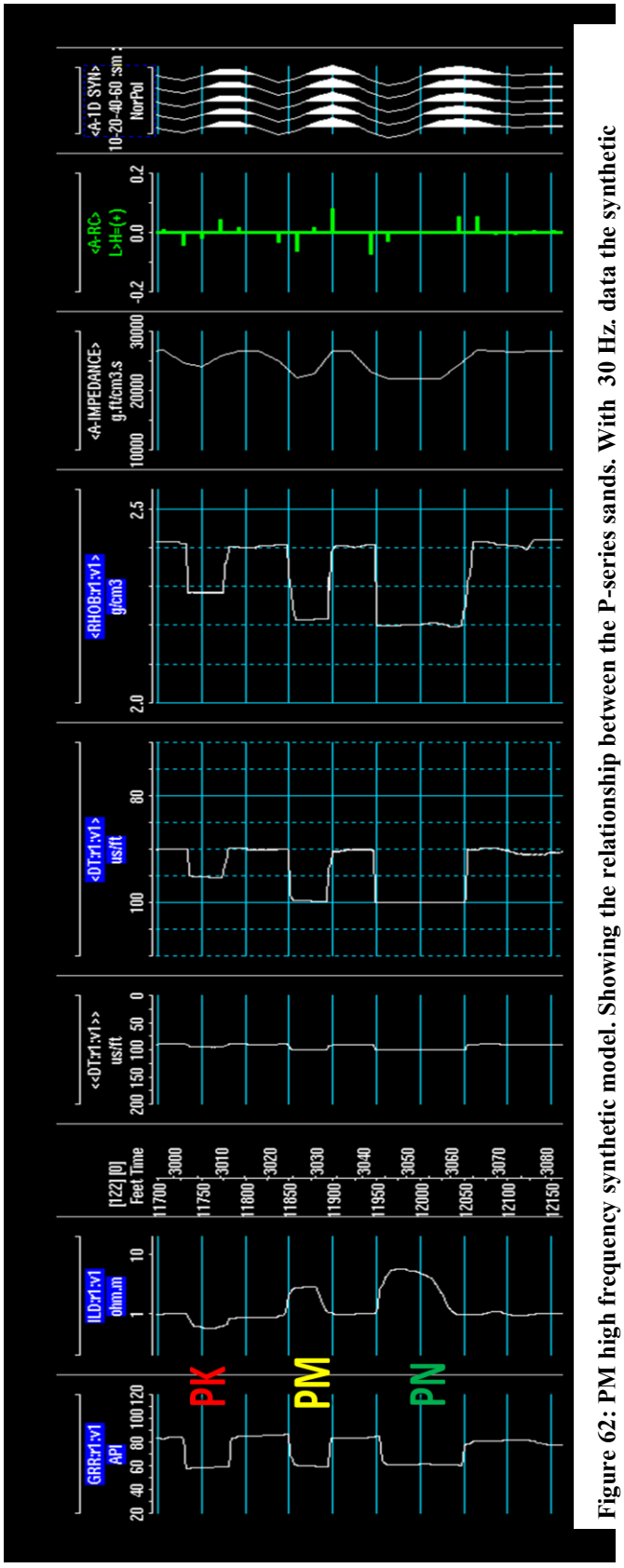

Figure 62: PM high frequency synthetic model. Showing the relationship between the P-series sands. With 30 Hz. data the synthetic response is much better being able to image both top and base of all of the sands.

Volumetrics

Volumetric calculations for the PM compartments were preformed to check for remaining potential within the reservoirs. The volumetric calculations are based on the reservoir volumes and the rock properties already defined. Original recoverable reserves will be check against the produced reserves in order to see if further exploitation is possible (Table 7).

Table 7: Calculated original recoverable reserves, produced reserves, and remaining recoverable reserves.

Reservoir	Original Calculated Recoverable Reserves	Produced Reserves	Remaining Recoverable Reserves
PM-1 (SE)	1.5 BCF	0	1.5 BCF
PM-1 (NW)	2.2 BCF	20,000 MCF	2.18 BCF
PM-2	5.8 BCF	5.85 BCF	0
PM-3	0.296 BCF	60,000 MCF	0.29 BCF

Production from the PM-2 compartment matches almost exactly with the original calculated recoverable reserves. However in the PM-1 (SE) compartment there is no production of the PM just a well test in the W-7 well-bore. There is 1.5 BCF of remaining recoverable reserves in this compartment. In the PM-1 (NW) compartment the W-5 well produced 20,000 MCF when calculated recoverable reserves were around 2.2 BCF. Also in the PM-3 the B-1 produced 60,000 MCF, original calculated recoverable reserves were about 0.3 BCF.

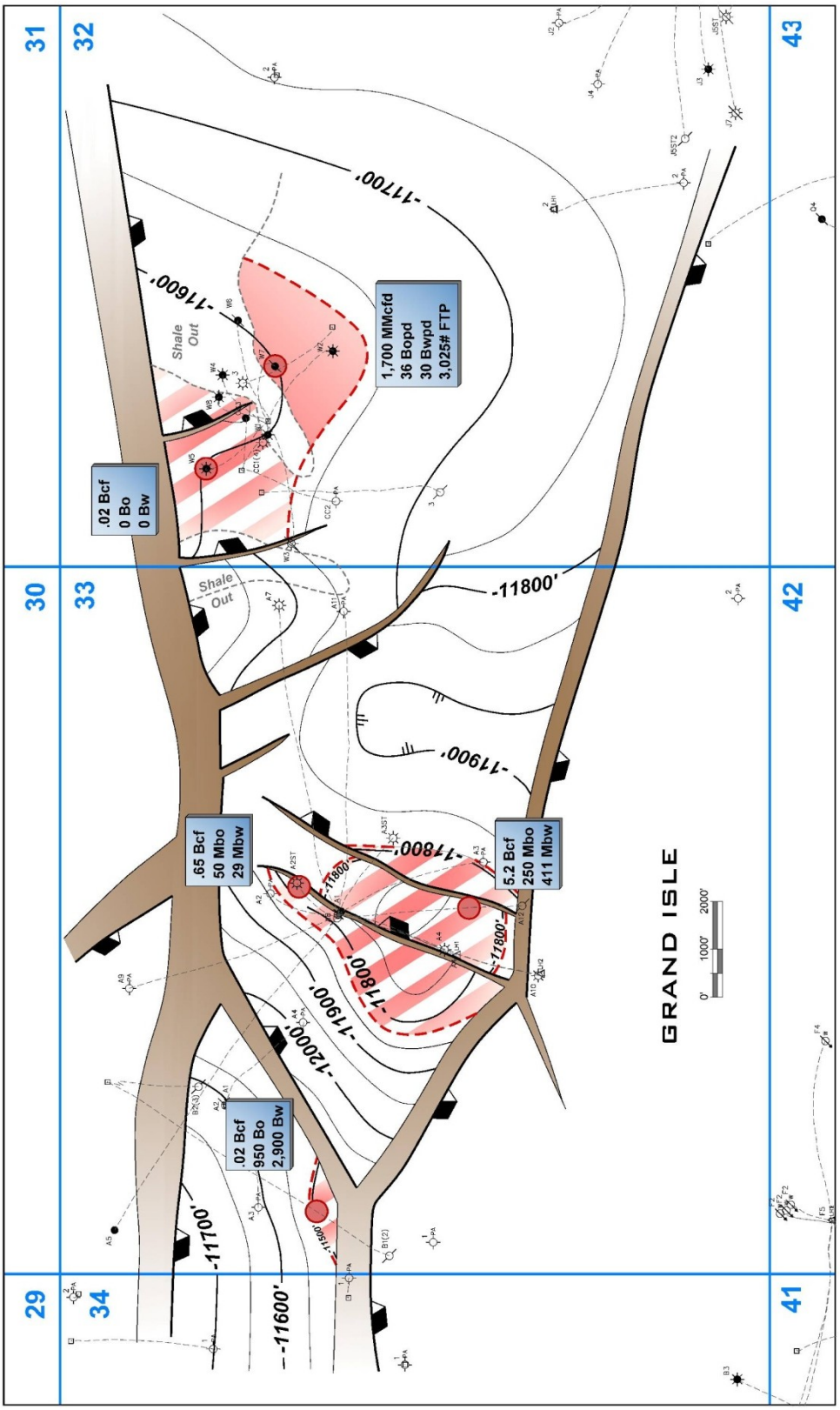

Figure 63: PM pay structure map. Potentially remaining PM reserves in the PM-1 compartment. Which is separated by a shaled out section.

Conclusion

The integrated reservoir model of the PM sand indicates the possibility for remaining hydrocarbons in Grand Isle 32. The PM sand was interpreted to be deposited in a distributary mouth bar setting which helps to explain the highly stratified nature of the sand. The amplitude response at the PM level is not considered to be a hydrocarbon indicator. Shale filled channels further divide the PM sand into small compartments, these channels can act like barriers in the reservoir. In the case of the PM-1 a shale out separates the reservoir into two smaller compartments. The northwestern compartment did have a well completed into the PM and had very poor production, producing only 20,000 MCF. Volumetric calculations have 2.18 BCF worth of reserves remaining in this compartment. These remaining reserves are subject to very limited well control, because of the poor initial production from the W-5 it is assumed that there might be another shale out that isolates the W-5 well. The PM sand does have some potential reserves in the southwestern compartment of PM-1. The W-7 well did test the PM sand and showed rates of 1,700 MMCFD, 36 BOPD, and 30BWPD. The W-7 well test indicates that economical rates are possible from the PM sand. Volumetric calculations estimate that there is about 1.5 BCF of recoverable gas remaining in the PM sand.

CHAPTER VII

DISCUSSION AND CONCLUSIONS

Integration of geological, geophysical, and engineering data creates a detailed reservoir model. This study focused on building a detailed reservoir model for a mature gas field in Grand Isle 32 and 33, offshore Louisiana. This study focused on using data integration to find bypassed zones of hydrocarbons. Specifically seismic amplitudes were used to try and further delineate the reservoirs and identify infill drilling opportunities.

The first reservoir model developed was for the Late Miocene middle (QH) sand. The QH sand was the single largest producer in the Grand Isle 33 and 43 fields (105 BCFG). Bottom hole pressure data helped to confirm that the QH-1 and 2 compartments were in communication with each other from a leaking fault (D). Pressures in the QH-1 compartment at abandonment directly corresponded to the initial pressures in the QH-2 compartment. The large amplitude anomaly associated with the QH sand filled the entire study area and extended well past the down dip limit of the reservoirs. The amplitude is interpreted to be a lithologic indicator. With the produced reserves matching to the original recoverable reserves the entire QH reservoir has been depleted in the fields.

The Late Miocene lower (RD) sand was the second reservoir model developed. The RD sand has limited production and well control making it more difficult to develop a detailed reservoir model. The RD reservoir model revealed that the faulting in the RD-2 compartment did not cut off communication of the RD. Volumetric calculation showed

that at the time the A-12 well was drilled that the reservoir had already produced more than the calculated original recoverable reserves. Upon drilling into the RD zone the A-12 well had a number of problems, including sticking of the drill pipe and losing mud into the formation. The drilling data and the volumetric data support the interpretation that the RD sand was already depleted upon the drilling of the A-12 well. Most importantly the RD sand has 6.7 BCF of potentially recoverable reserves remaining in the RD-1 compartment. The substantial amount of reserves remaining have tremendous economic significance for the Grand Isle 43 field.

The Late Miocene upper (PM) sand is the highest stratigraphic interval studied. The PM sand was deposited in a distributary mouth bar system. The PM sand has produced from four wells in the two fields, providing limited production data. The reservoir model indicates that the PM sand is separated into different compartments not only by structure but stratigraphy as well. The PM sand shales out completely in several locations in the field. In the PM-1 compartment the shale out is important because it further separates the compartment into smaller sub-compartments. This separation created a potential drilling prospects for 1.5 BCF of remaining recoverable reserves. The PM sand was tested in this compartment and tested at 1,700 MMCFD, 36 BOPD, and 30 BWPD. This test shows that the PM sand can flow at commercial quantities required for drilling.

Seismic amplitude anomalies are often used to identify the presence of hydrocarbons within the subsurface. For the purpose of this research amplitude anomalies were used to delineate reservoirs and understand the fields finer stratigraphic

characteristics of these units. However, in the case of the three intervals chosen for this study amplitude extractions did not provide results that would link seismic amplitude anomalies to hydrocarbon indicators. The amplitude responses in this area are hindered by the massive amounts of sands and their stratigraphic presence within close proximity to one another. Sands in this area are often very close to each other and are laterally discontinuous, making some of their features undetectable. It was shown that if the frequency of the seismic data was higher around 30 Hz. that maybe some of the finer features would be resolvable. All of the sands studied would benefit from higher resolution data, further allowing the models to break down the sands into the distinct lobes.

Although, most of the research results were not as expected the study still found some key features. Two of the three reservoirs sands in the study area have remaining recoverable reserves. The PM and RD sands have a combined total of an estimated 8.2 BCFG remaining in the Grand Isle 43 field. This amount of gas has serious economic potential remaining for the Grand Isle 43 field. The methods used in this research helped to outline the potential for finding bypassed hydrocarbons zones, and possible infill drilling.

REFERENCES CITED

Ahr, W. M., 2008, Geology of Carbonate Reservoirs: Hoboken, New Jersey, John Wiley & Sons, Inc., 277 p.

Asquith, G., and D. Krygowski, 2004, Basic Well Log Analysis, Tulsa, The American Association of Petroleum Geologists, 244 p.

Bird, D. E., K. Burke, S. A. Hall, and J. F. Casey, 2005 Gulf of Mexico tectonic history: Hotspots tracks, crustal boundaries, and early salt distribution: AAPG Bulletin, v.89, p. 311-328.

Bruce, C., 1973, Pressured shale and related sediment deformation: mechanism for development of regional contemporaneous faults: AAPG Bulletin, v. 57, p. 878-886.

Dewan, J., 1983, Essentials of Modern Open-Hole Log Interpretation, Tulsa, PennWell Publishing Company, 361 p.

Domenico, S., 1974, Effect of water saturation on seismic reflectivity of sand reservoirs encased in shale: Geophysics, v. 39, p. 759-769.

Everson, D., 1989, Geological Engineering Review of Grand Isle Block 33 Field: Shell Offshore, v. 1, 60 p.

Forrest, M., R. Roden, and R. Holeywell, 2010: Risking seismic amplitude anomaly prospects based on database trends: The Leading Edge, v. 29, no. 5, p. 570-574.

Hyne, N. J., 2001, Nontechnical Guide to Petroleum Geology, Exploration, Drilling, and Production: Tulsa, Penn Well Corporation, 578 p.

Kearey P., M. Brooks, and I. Hill, 2002, An Introduction to Geophysical Exploration, Oxford U.K., Blackwell Publishing, 262 p.

O'Brien, J., 2004, Seismic amplitudes from low gas saturation sands: The Leading Edge, v. 23, no. 12, p. 1236-1243.

Rutherford, S., and R. Williams, 1989, Amplitude-versus-offset variations in gas sands: Geophysics, v. 54, p. 680-688.

Salvador, A., 1991, Origin and Development of the Gulf of Mexico basin: The Geology of North America, v. J., p. 389-444.

Sheriff, R. E., 1980, Seismic Stratigraphy: Boston, International Human Resources Development Corporation, 227 p.

Steiner, R., 1974, Grand Isle Block 16 Field, Offshore Louisiana: New Orleans and Lafayette Geological Societies, p. 229-238.

U.S. Energy Information Administration, 2010, Gulf of Mexico Fact Sheet, <http://www.eia.doe.gov/dnav/ng/ng_prod_top.asp> Accessed May 15, 2010.

Walker, R. G., 1984, Facies Models: Kitchener, Ontario, Canada, Ainsworth Press Limited, 318 p.

Widess, M. B., 1973, How Thin Is a Thin Bed: Geophysics, v. 38, p 1176-1180.

Wu, X., W. E. Galloway, 2002, Upper Miocene Depositional History of the Central Gulf of Mexico Basin, Gulf Coast Association of Geological Societies Transactions, v. 52, p. 1019-1030.

VITA

Michael Chase Casey received his Bachelor of Science degree in geology from Texas A&M University in December 2008. He entered the Reservoir Geophysics Program at Texas A&M University in January 2009 and received his Master of Science degree in May 2011. His research interests include petroleum geology, petroleum geophysics, and reservoir engineering.

Mr. Casey can be reached at mcasey521@gmail.com or

Department of Geology and Geophysics

c/o Dr. Yuefeng Sun

Texas A&M University

College Station, Texas 77843-3115